JOHANNES GUTENBERG
UNIVERSITÄT MAINZ

Leishmania major parasites and their interaction with human macrophages

Dissertation

Zur Erlangung des Grades

Doktor der Naturwissenschaften

Am Fachbereich Biologie

der Johannes Gutenberg-Universität Mainz

Elena Bank

geb. am 07.06.1983 in Dshiginka

Mainz, 2012

Dissertation von Elena Bank

Leishmania major parasites and their interaction with human macrophages

Dekan:

1. Gutachter:

2. Gutachter:

Contents

1 Introduction **7**

1.1 Leishmaniasis 7
1.2 Life cycle of *L. major* parasites 8
1.3 Stage-specific characteristics of *L. major* 9
1.4 Apoptosis in *L. major* 11
1.4.1 Drug induced apoptosis 12
1.5 *Leishmania* and the adaptive immune system 14
1.6 The interaction with human MF 14
1.7 Defense of Leishmaniasis 16
1.8 Aim of the study 19

2 Material and Methods **23**

2.1 Material 23
2.1.1 Chemicals 23
2.1.2 Culture media and buffers 26
2.1.3 Westernblot buffers and solutions 28
2.1.4 *Leishmania* strains 31
2.1.5 Human leukocytes 32
2.1.6 Ready-to-use kits 32
2.1.7 Anti-Human antibodies 32
2.1.8 Anti-*Leishmania* antibodies 33
2.1.9 Oligonucleotides 34
2.1.10 Enzymes 35
2.1.11 Laboratory supplies 35
2.1.12 Instruments 36
2.1.13 Software 38

2.2 Methods . . . 39
2.2.1 Cell culture . . . 39
2.2.1.1 Cultivation of *L. major* promastigotes . . . 39
2.2.1.2 Isolation of metacyclic *L. major* promastigotes . . . 39
2.2.1.3 Generation and cultivation of *L. major* amastigotes *in vitro* . . . 40
2.2.1.4 Isolation of *L. major* amastigotes from infected MF . . . 41
2.2.1.5 Isolation of human peripheral blood mononuclear cells (PBMC) . . . 41
2.2.1.6 Generation of blood derived MF . . . 42
2.2.1.7 Co-incubation of macrophages with *L. major* parasites . 42
2.2.1.8 End-point titration . . . 43
2.2.1.9 Cytocentrifuging cells . . . 44
2.2.1.10 Diff QUIK staining . . . 44
2.2.2 FACS analysis . . . 44
2.2.2.1 Extracellular FACS analysis of (infected) MF . . . 44
2.2.2.2 Intracellular FACS analysis of (infected) MF . . . 45
2.2.2.3 Extracellular FACS analysis of *L. major* . . . 45
2.2.2.4 Intracellular FACS analysis of *L. major* . . . 45
2.2.3 ELISA analysis . . . 46
2.2.3.1 TNF alpha . . . 46
2.2.3.2 IL-12 . . . 46
2.2.3.3 IL-10 . . . 47
2.2.4 Arginase assay . . . 47
2.2.5 Molecular biology methods . . . 48
2.2.5.1 Transfection of primary cells with siRNA . . . 48
2.2.5.2 DNA isolation . . . 48
2.2.5.3 Amplification of the ribosomal internal transcribed spacer 1 (ITS1) . . . 49
2.2.5.4 Restriction digest . . . 50
2.2.5.5 RNA isolation . . . 50
2.2.5.6 Test-PCR . . . 51
2.2.5.7 cDNA synthesis . . . 52

2.2.5.8 Quantitative real-time PCR . . . 53
2.2.6 Transmission electron microscopy (EM) . . . 55
2.2.7 Westernblot analysis . . . 55
2.2.7.1 Sample preparation . . . 55
2.2.7.2 SDS-PAGE . . . 55
2.2.7.3 Band detection . . . 56
2.2.7.4 Coomassie staining . . . 56
2.2.8 Statistical analysis . . . 56

3 Results **57**
3.1 Confirmation of the *L. major* species . . . 57
3.2 Characterisation of *L. major* FEBNI parasites . . . 57
3.2.1 Morphological characteristics of *L. major* promastigotes . . . 58
3.2.2 Morphological characteristics of *L. major* amastigotes . . . 59
3.2.3 Annexin binding . . . 61
3.2.4 Stage-specific gene expression levels . . . 61
3.2.5 The surface marker lipophosphoglycan (LPG) . . . 63
3.2.6 Generation of axenic amastigotes in other *L. major* strains . . . 64
3.3 Detection of Apoptotic characteristics in *L. major* parasites . . . 68
3.3.1 Apoptosis mechanisms in promastigotes . . . 68
3.3.2 Apoptosis mechanisms in amastigotes . . . 70
3.3.3 FACS analysis of apoptotic parasites . . . 72
3.4 Interaction of *L. major* with human MF . . . 75
3.4.1 Infection of different phenotypes of MF with *L. major* . . . 75
3.4.2 Infection with eGFP expressing *L. major* . . . 78
3.4.2.1 *L. major* eGFP parasites . . . 78
3.4.2.2 Parasite development in infected MF . . . 78
3.5 Phenotype and parasites stage-specific MF surface marker expression . . . 81
3.5.1 CD163 . . . 81
3.5.2 CD206 . . . 82
3.5.3 MHC class II (MHC II) . . . 85
3.5.4 CD86 . . . 86
3.6 Phenotype and parasites stage-specific cytokine production . . . 87
3.6.1 TNF alpha . . . 87

3.6.2 IL-12 . . . 89
3.6.3 CCL3 and CCL4 . . . 89
3.6.4 IL-10 . . . 92
3.7 Phosphorylation of MAP kinases (MAPK) after *L. major* infection . . . 93
3.7.1 p38 MAP kinases . . . 95
3.7.2 ERK1/2 MAP kinases . . . 95
3.8 *L. major* parasite escape from phagolysosomes . . . 98
3.9 Arginase in infected MF . . . 100
3.10 Cathelicidin (LL-37) in infected MF . . . 100
3.10.1 Different LL-37 expression in MF I and MF II . . . 102
3.10.2 Killing effect of rhLL-37 on *L. major* promastigotes . . . 102
3.10.3 No effect of rhLL-37 on *L. major* amastigotes . . . 104
3.10.4 Knockdown of LL-37 in human MF . . . 106
3.10.4.1 Infection and parasite burden . . . 106
3.10.4.2 Survival of *L. major* parasites in knockdown MF . . . 108

4 Discussion **111**
4.1 Different life stages of the parasite *L. major* . . . 111
4.2 *In vitro* culture method for axenic *L. major* amastigotes . . . 113
4.3 Apoptosis in *L. major* parasites . . . 114
4.4 Interaction of *L. major* with human MF . . . 120
4.5 Clearance of *L. major* in human MF . . . 123
4.6 Concluding remarks . . . 127

5 Summary **129**

6 Zusammenfassung **131**

Abbreviations **163**

Acknowledgements **167**

1 Introduction

1.1 Leishmaniasis

Leishmaniasis is a parasitic infection with the protozoan genus *Leishmania* which is endemic in 88 countries, mainly prevalent in the tropical and subtropical regions of the world. Currently approximately 12 million people are suffering from Leishmaniasis, however about 350 million people are worldwide threatened and the estimated incidence of 2 million new cases arises each year [215, 4]. Up to date there are about 21 *Leishmania* species known to be pathogenic for humans [91]. According to the *Leishmania* species initiating infection and the immunologic status, humans can develop a large spectrum of symptoms ranging from self-healing lesions to a severe organ-infiltrating manifestation of the disease. Four major forms of human Leishmaniasis have been described: cutaneous, diffuse cutaneous, mucocutaneous and visceral Leishmaniasis. The localized cutaneous Leishmaniasis (LCL), which is primarily caused by *Leishmania major* (*L. major*) and *Leishmania tropica* (*L. tropica*) produces self-healing skin ulcers on exposed parts of the body, which is also known as "Aleppo boil". On the other hand, chronic diffuse cutaneous Leishmaniasis (DCL) caused by *Leishmania aethiopica* (*L. aethiopica*) and *Leishmania mexicana amazonensis* (*L. mexicana amazonensis*) produces widespread skin lesions all over the body which resemble leprosy [143]. Another more severe form is the mucocutaneous Leishmaniasis (MCL) characterized by the infiltration of the mucousal membranes, especially those of the nose and mouth leading to extensive tissue damage and disfiguration (Espundia). The causative agents of MCL are *Leishmania braziliensis* (L. braziliensis) and *Leishmania mexicana pifanoi* (*L. mexicana pifanoi*) [102]. The most severe and life threatening form is the visceral Leishmaniasis (VL) also named "Kala azar" caused by the *Leishmania donovani* complex, including *Leishmania*

donovani, *Leishmania infantum* and *Leishmania chagasi* (*L. donovani*, *L. infantum* and *L. chagasi*). This form affects internal organs such as the lymph nodes, the liver, the spleen and the bone marrow and is lethal if untreated [17].

1.2 Life cycle of *L. major* parasites

The *Leishmania* parasite is a dimorphic unicellular parasite belonging to the class of Kinetoplastida because of the prominent DNA-containing mitochondrion, the kinetoplast. The life cycle of *Leishmania* is characterized by the alteration between two hosts, a sand fly and numerous mammals [144]. The flagellated promastigote life stage of *Leishmania spp.* lives and replicates extracellular in the digestive tract of the female sand fly of the subgenera *Phlebotomus* and *Lutzomyia* [178]. In the midgut of the insect vector, the promastigotes mature through a differentiation process called metacyclogenesis [62] from a non-virulent procyclic form into the virulent metacyclic form. In contrast to gut epithelial attached procyclic parasites, metacyclic promastigotes detach and accumulate in the anterior parts of the digestive tract, like the glands from where they can be inoculated into the skin of a mammalia during a blood meal of the sand fly [159]. Inside the mammalian host, *Leishmania* parasites are only able to survive intracellular. Therefore the parasite attracts polymorphonuclear granulocytes (PMN) to the site of infection via a chemotactic factor termed *Leishmania* chemotactic factor (LCF) [197]. The virulent inoculum of *Leishmania* consists of viable and apoptotic promastigotes [198, 207] leading to a silent uptake of the promastigotes and to a higher intracellular survival rate inside the PMN by evading their antimicrobial killing mechanisms [210]. After engulfment by the recruited PMN, the parasites take advantage of the fact that aging neutrophils die by apoptosis and simultaneously recruit macrophages (MF) via MIP-1 beta (CCL4) release for their clearance. Hiding inside apoptotic PMN, the *Leishmania* promastigotes are transferred into their final host cells the MF, by using PMN as Trojan horses [94]. Inside MF the non-multiplying promastigotes are located within specialized compartments, called phagolysosomes, where they differentiate into the non-motile amastigote life stage, which is adapted to the acidic and hydrolase-rich environment within the phagolysosomes. Amastigotes are able to multiply inside MF and are responsible for the maintenance and propagation of the disease by infecting

surrounding phagocytes causing Leishmaniasis [22]. The life cycle is completed when a sand fly take a blood meal from an infected mammal. The free or in MF resident amastigotes are then able to rapidly differentiate into the promastigote life stage in the gut of the insect. The adaptation to both an arthropod vector and a mammalian host is a typical feature of the obligatory intracellular *Leishmania* parasite and is illustrated in fig. 1.

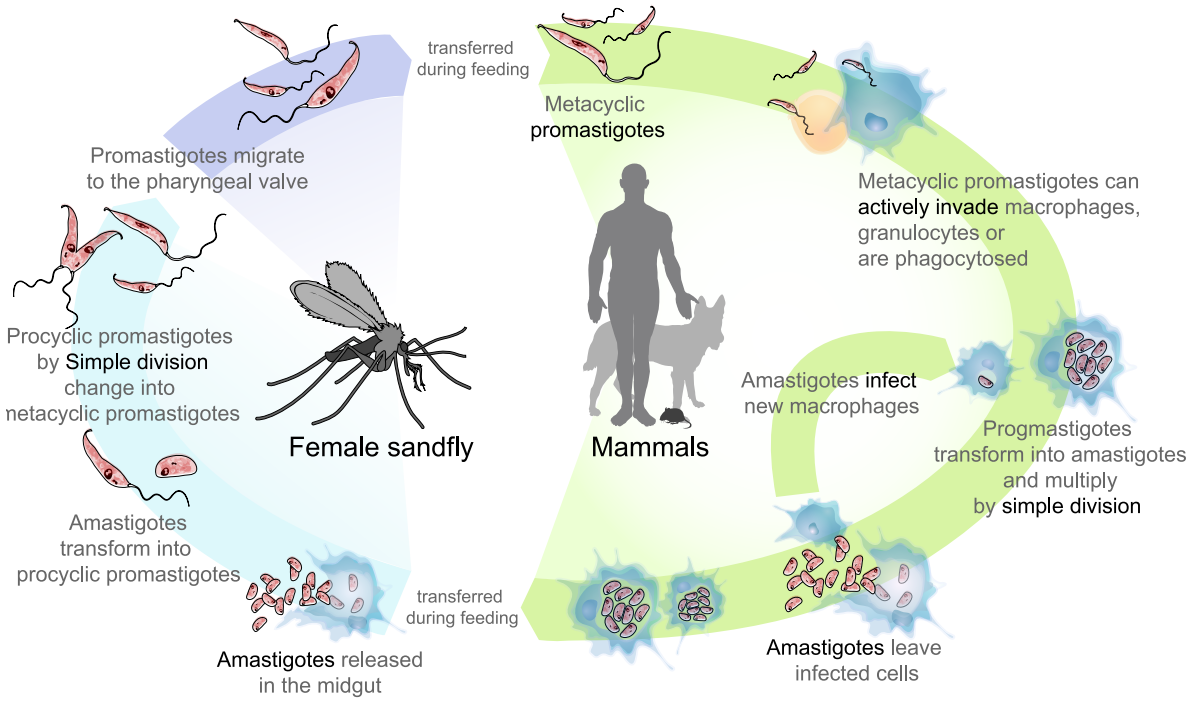

Figure 1: Life cycle of *Leishmania spp.*
[Source: `http://en.wikipedia.org/wiki/File:Leishmaniasis_life_cycle_diagram_en.svg`, accessed on 04/05/2012]

1.3 Stage-specific characteristics of *L. major*

Due to the alteration between two completely different hosts, *Leishmania* parasites had to evolve different strategies to survive in both environmental conditions. The two life stages of *Leishmania* display distinct morphologic and metabolic characteristics consistent with a stage-specific expression of parasitic genes and proteins of which some

are shown to be important for the survival and differentiation in the insect vector and a successful infection in the mammalian host. The lipophosphoglycan (LPG), which forms a dense glycocalyx around the parasitic body, is demonstrated to play an important role in the attachment of promastigotes in the digestive tract of the sand fly [147]. During metacyclogenesis the LPG molecules are modified by capping the galactosyl side chains of procyclic LPG with arabinosyl residues [164, 165]. Thus, metacyclic promastigotes lose their binding capacity to the midgut epithelium and are released for transmission [163, 113]. Inside the mammalian host LPG also inhibits the complement-mediated lysis of the parasites by blocking the insertion of the lytic C5b-9 complex into the promastigote membrane [149] and is involved in the mechanism to inhibit the protein kinase C (PKC) resulting in a delay of endosomal compartment fusion [134, 122, 185]. After the transformation of *Leishmania* parasites in the amastigote life stage they show a strongly reduced LPG expression compared to the infective metacyclic promastigotes, which correlates with the absence of a glycocalyx on the amastigote surface [112, 63, 194, 121, 11, 171, 146]. The major surface glycoprotein GP63 (GP63) is a metalloprotease on the surface of *Leishmania* promastigotes, which is known to cleave the C3b form of the complement system into the inactive C3bi form and thus block complement-mediated lysis inside the mammalian host [27, 39]. In addition, GP63 is able to directly interact with the macrophage surface receptor complement receptor type 3 (CR3, or CD11b/CD18). The opsonized parasites with C3bi are targeting for phagocytosis by MF via the corresponding CR3 [214, 183]. In the amastigote life stage of *L. major* the metalloprotease GP63 is found not to be expressed [170]. A well characterized marker for the *Leishmania* promastigote life stage is the gene expression of the small hydrophilic ER-associated protein (SHERP). SHERP is essential for the parasite development during the metacyclogenesis in the sand fly and may therefore be essential for transmission [86, 175]. Another stage-specific marker for *Leishmania* parasites is the structural protein gene alpha-tubulin which is up-regulated in the promastigote life stage [98]. The ABC-transporter homologue (ABC) belongs to a gene family coding for proteins involved in the ATP-dependent transport of a variety of molecules across biological membranes, including amino acids, sugars, peptides, lipids, ions, and chemotherapeutic drugs [68]. ABC is demonstrated to be specific up-regulated in the amastigote life stage of *L. major* [98]. Furthermore, quinonoid-dihydropteridine reductase (QDPR) is the key enzyme in *Leishmania* for the regeneration of H_4biopterin which is essential

for parasite growth and differentiation [40, 128]. QDPR is required for the reduction of quinonoid-dihydropteridine to restore the intracellular H_4biopterin pool [105]. The expression of QDPR in stat-phase promastigotes is reduced compared to both log-phase promastigotes and amastigotes [105]. An additional stage-specific marker is the cysteine protease b (Cbp) which is a multicopy gene family belonging to the cysteine proteases and is required for parasite replication and virulence [37, 114, 123]. Cpb is shown to be up-regulated in the amastigote life stage for several *Leishmania* species, including *L. tropica* and *L. mexicana* [129].

1.4 Apoptosis in *L. major*

Cell death is historically classified into regulated or programmed cell death (PCD), also termed apoptosis and the unregulated cell death often called necrosis. Apoptosis is a mechanism which is absolutely essential to remain homeostasis in multicellular organisms [188]. Apoptosis is a well-organized multi-step process with distinct events to occur. An early marker for apoptosis is the externalisation of phosphatidylserine (PS) from the inner to the outer leaflet of the cell membrane. The asymmetric distribution of phospholipids of the plasma membrane gets lost and PS is translocated to the outer leaflet of the plasma membrane via a flip-flop mechanism [110]. Simultaneously proteolytic enzymes termed caspases are sequentially activated which lead to the subsequent breakdown of the cell content. The mitochondria act as key players during this process releasing pro-apoptotic factors like cytochrome c into the cytoplasm accompanied by disruption of the mitochondrial membrane potential leading to caspase activation [219, 53]. Additionally, reactive oxygen species (ROS) which are highly reactive intermediates in the reduction of oxygen to water are generated and released [173]. As a result the cell rounds up followed by cell shrinkage while the integrity of the plasma membrane remains fully intact throughout the entire apoptotic process [82, 85, 127]. In the end the nucleus condensates and the DNA is degraded by fragmentation [216]. Since in the past apoptosis was claimed only for multicellular organisms, many researchers doubt the existence of a programmed cell death in unicellular life forms. But during the last years, there have been reports for different phyla of protists demonstrating several markers of apoptosis [44, 199, 95]. Many characteristics of metazoan apopto-

sis have been described to occur in *Leishmania* parasites when apoptotic death was induced by diverse stimuli. The externalization of PS was demonstrated for several different species, including *L. major*. Furthermore, the loss of mitochondrial membrane potential as well as the formation of ROS and the release of cytochrome c was observed after apoptosis induction. Although no proteolytic caspases were found in *Leishmania*, several caspase-like proteases were shown to be present [96, 43, 131]. Moreover, the maintenance of the plasma membrane integrity, cell shrinkage and nuclear chromatin condensation and fragmentation of the DNA were observed [9, 42, 176, 130, 117, 5]. These findings demonstrate the existence of all characteristics of an apoptosis program in *Leishmania*. However the exact mechanisms responsible for apoptosis regulation are still not known.

1.4.1 Drug induced apoptosis

The above mentioned apoptotic characteristics were also found after the treatment of *Leishmania* parasites with different drugs to induce apoptosis, including staurosporine, camptothecin and the anti-leishmanial drug miltefosine.

Staurosporine:
Staurosporine was originally isolated in 1977 from the bacterium *Streptomyces staurosporeus* and was found to strongly induce apoptosis. The main biological activity of this compound in mammalian cells is the inhibition of protein kinases through the prevention of ATP binding to the kinase. This is achieved through the stronger affinity of staurosporine to the ATP-binding site on the kinases, though with little selectivity [80]. The underlying mechanism of apoptosis induction via staurosporine is reported to be the mitochondrial apoptotic pathway [190, 191]. For *Leishmania spp.* staurosporine was demonstrated to induce cell death with several cytoplasmic and nuclear characteristics of apoptosis, including cell shrinkage, PS externalisation, cytochrome c release and DNA fragmentation [13, 9].

Camptothecin:
Camptothecin is a cytotoxic alkaloid isolated from the bark and stem of *Camptotheca acuminata* (Happy tree) in 1966. It is a potent inhibitor of both DNA as well as

RNA synthesis and a strong inducer of immediate and reversible strand breakings in chromosomal DNA by the inhibition of the DNA enzyme topoisomerase I in mammalian cells [72]. Camptothecin binds to the covalent topoisomerase I and DNA complex and thereby stabilizing it. This stabilization prevents DNA re-ligation and therefore causes DNA damage which results in apoptosis [155]. Camptothecin has also been shown to inhibit the topoisomerase I of *Leishmania spp.* and thus acting as an apoptosis inducer in the parasites, which results in the manifestation of apoptosis marker such as increased ROS formation, DNA fragmentation and cell shrinkage [176, 47].

Miltefosine:
Miltefosine (hexadecylphosphocholine) is a drug initially developed as an anti-cancer compound in the 80's, which was the first effective oral drug against *Leishmania*. The exact mode of action of the antiprotozoal miltefosine is still not well understood. However, it was demonstrated to target cellular membrane composition by the induction of changes in the biosynthesis of phospholipids and the metabolism of alkyl-lipids [104]. Numerous *in vitro* and *in vivo* studies have shown the cytotoxic effect of miltefosine on both life stages of various *Leishmania* species, including *L. major*. The result is cell death of the parasites showing characteristic apoptosis features like PS externalization, DNA fragmentation and cell shrinkage [38, 51, 54, 83]. An overview of the three described drugs with their distinct targets for apoptosis induction in *Leishmania* parasites is displayed in fig. 2.

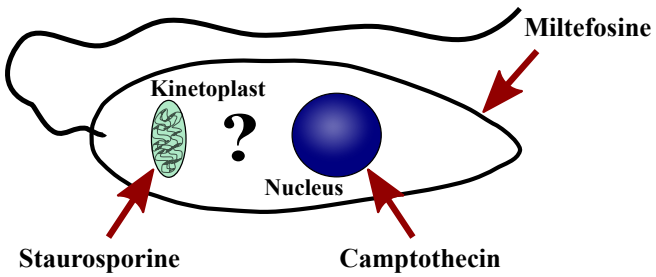

Figure 2: Distinct targets for apoptosis induction in *Leishmania* via different drugs

1.5 *Leishmania* and the adaptive immune system

Leishmania parasites were used as a model organism by immunologists to study the different mechanism of the immune system for the last 40 years. The basic pathogenesis of *Leishmania* infection has been investigated using experimental mouse infection models with mouse strains having different genetic backgrounds. After the successful transfer of the parasites into the final host cells, the MF, the immune response in Leishmaniasis is mediated by T lymphocytes [2]. Resistance of the disease is mediated by a T-helper 1 (Th-1) immune response, whereas disease development is associated with a sustained T-helper 2 (Th-2) response [156, 166]. In mouse infection models with *L. major* this polarized Th response distribution is reflected in resistant C57BL/6 mice which are able to control parasite replication efficiently and the susceptible Balb/c mice, which develop a severe course of disease (reviewed by [22]). For C57BL/6 mice a Th-1 dominated response was demonstrated, characterized by the release of pro-inflammatory cytokines like INF gamma, TNF alpha and IL-12 after infection. These cytokines are responsible for MF activation and the clearance of intracellular parasites. In contrast, susceptible Balb/c mice produce high levels of IL-4 and low amounts of INF gamma and TNF alpha. Additionally, in patients with different forms of Leishmaniasis the most commonly cytokine to find was not IL-4, but IL-10 which leads to down regulation of INF gamma and prevents effective parasite elimination [6, 7]. C57BL/6 mice with a protective Th-1 response are thought to be a model for the self-healing human cutaneous Leishmaniasis [2], whereas Balb/c mice and a strong Th-2 response are associated with non-healing forms of the human disease such as “Kala azar” or diffuse cutaneous Leishmaniasis [25, 24]. However, it has not been possible to associate a Th-2 polarity completely with non-healing or systemic forms of Leishmaniasis in humans [6]. Taken together, these data demonstrate the importance of the Th-1/Th-2 balance for the infection outcome in experimental Leishmaniasis.

1.6 The interaction with human MF

In contrast to PMN where *Leishmania* promastigotes do not differentiate into the amastigote life stage, MF are known to be the final host cells [212]. Inside MF promastigotes

transform into amastigotes and start to multiply. However, MF are a heterogeneous population of cells with various immune and homeostatic functions in the human body. They consist of mature MF and circulating immature monocytes which can migrate into tissue and differentiate after stimulation by different signals into tissue resident MF, such as microglia in the central nervous system or alveolar MF in the alveoli of the lung. For cutaneous Leishmaniasis it is not known which distinct subtype of MF is infected. Blood derived human monocytes were shown to be able to differentiate into two different phenotypes of MF *in vitro* after stimulation with different growth factors. These phenotypes were termed type I and type II MF [184, 202].

Type I MF (MF I):
The incubation with GM-CSF polarizes human blood monocytes into type I MF or classical activated MF. The morphology of this phenotype is fried egg-shaped and the cells are CD14 positive, but CD163 negative. MF I produce pro-inflammatory cytokines when stimulated such as TNF alpha, IL-1, IL-23, and IL-12(p40). In addition they are efficient producers of antimicrobial effector molecules like reactive oxygen and nitrogen intermediates. Type I MF play an important role in the clearance of apoptotic cells and support the Th-1 response by the secretion of IL-12 and IL-6 [109, 202, 203]. Therefore, type I MF are termed pro-inflammatory phagocytes.

Type II MF (MF II):
M-CSF incubation leads to the differentiation of monocytes into type II MF or alternative activated MF. MF II are wide stretched cells and show a spindle-like shape. In contrast to MF I, MF II have a higher phagocytosis capacity [217, 218]. Furthermore, they play an important role in the clearance of necrotic cells [168]. A particular feature of MF II cells is the expression of CD14 and the scavenger receptor CD163, which is supposed to be involved in anti-inflammatory processes [30]. The MF II phenotype is hallmarked by a lack of microbicidal activity as well as IL-12(p40) secretion and release anti-inflammatory IL-10 as the signature cytokine upon activation [202, 203]. Moreover, MF II down-regulate the IL-12 production [88], have poor antigen presentation and were shown to secrete TGF beta upon uptake of apoptotic cells [168, 50]. Therefore, type II MF are termed anti-inflammatory phagocytes. Despite the recognition and characterization of these distinct subtypes of human MF, the consequences of such differently polarized MF interacting with *L. major* like uptake and parasite propagation remain

unclear.

1.7 Defense of Leishmaniasis

The first defense of *Leishmania* inside a mammalian host is mediated by the complement system. Extracellular parasites are targeted by complement compounds such as C3b and C5b leading to complement-mediated lysis. Even though *Leishmania* parasites evolved mechanisms to block an effective lysis via LPG and GP63 as described above, a killing effect of the parasites was described to some extent [164]. Remaining parasites are engulfed by professional phagocytes, which try to eliminate them by diverse antimicrobial effector mechanisms. One of these mechanisms is the induction of several reactive oxygen intermediates (ROI) like O_2^- or H_2O_2 which are generated by the NADPH oxidase and superoxide dismutase [90]. For the experimental mouse model, the production of nitric oxide (NO) which is produced by the inducible isoform of inducible nitric oxide synthase (iNOS) is known to play an important role in the killing of *Leishmania* parasites [100, 66]. However, for the human system NO induction inside infected MF remains controversial [132]. Another eliminating mechanism for intracellular pathogens is the microbicidal effect of several antimicrobial proteins such as defensins (alpha, beta), cathepsins (B, C, D, H, L) or cathelicidins. Defensins are small arginine rich cationic proteins which are present in cells of the immune system to assist in killing of phagocytosed pathogens, for example in granules and phagolysosomes of PMN but also in monocytes and MF [59, 84]. *In vitro*, defensins were shown to have antimicrobial activities against bacteria [59], fungi [1], and distinct viruses [41]. Most defensins function by binding to the microbial cell membrane and forming pores leading to an efflux of essential ions and nutrients resulting in cell lysis [78, 97]. Cathepsins are predominantly endoproteases which are located in lysosomes and phagolysosomes. There are approximately a dozen members of this family, which are distinguished by their structure mainly into cysteine and aspartyl proteases [154]. Most of the members are produced in a pro-form, which becomes activated at a low pH (3 - 5.5 pH) found in mature phagolysosomes [196]. Cathepsins are involved in pathogen degradation which is essential for processing of antigens and further presentation by major histocompatibility class II (MHC II) molecules to establish an immune response [195, 148]. Moreover,

effective clearance of *Leishmania* is correlated with the release of pro-inflammatory cytokines such as INF gamma, TNF alpha and IL-12 acting as potent activators of MF and leading to an activation loop and an improved parasite killing [177].

Cathelicidins (LL-37) comprise another important group of mammalian antimicrobial peptides with a potent antimicrobial activity for bacteria, fungi and viruses [48, 84]. In mammalia, up to seven different protein members were isolated of the cathelicidin family. However, in mouse (CRAMP), rhesus monkey and humans (hCAP18) only one single cathelicidin is present [58, 223, 92]. Cathelicidin is translated as a proform. The hallmark of the cathelicidin family is a highly conserved cathelin-like domain and a variable C-terminal cathelicidin peptide domain representing the proform ot the protein. The C-terminal antimicrobial peptide LL-37 becomes active when released from the pro-region [93, 61]. The microbicidal activity of LL-37 is based on its binding to LPS residues and the subsequent disruption of the foreign cell membrane. Similar to defensins, LL-37 has also a chemotactic activity to neutrophils, monocytes and lymphocytes [29]. An overview of known and potential elimination mechanisms for *Leishmania* parasites is displayed in fig. 3.

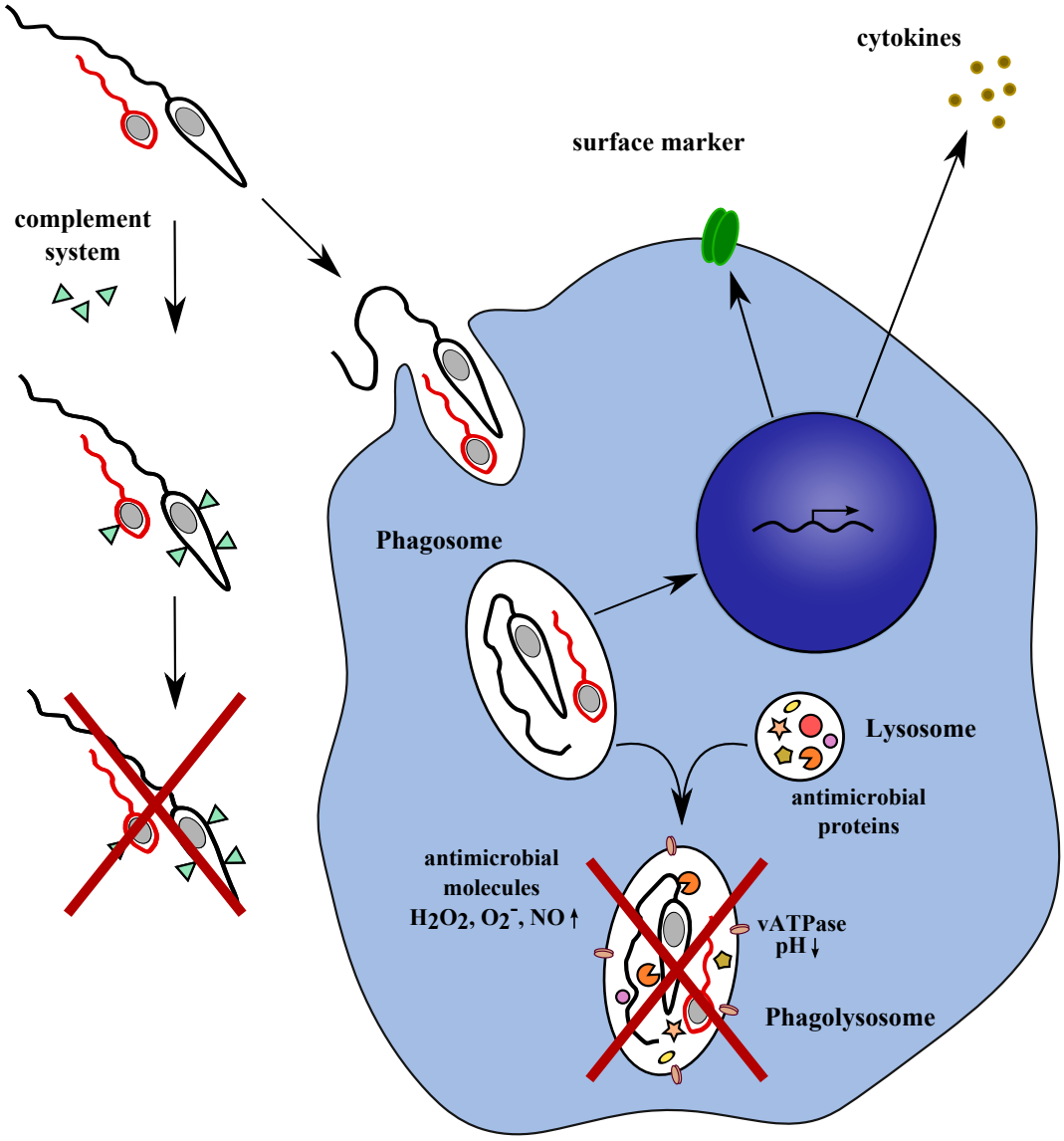

Figure 3: Overview of possible mechanisms for the clearance of *Leishmania*

1.8 Aim of the study

Leishmania major (*L. major*) is the disease causing agent of human cutaneous Leishmaniasis. The dimorphic parasite is characterized by an alteration between two different hosts, a sand fly as the insect vector and the phagocytes of mammalian hosts. The focus of this study was both the stage-specific characterization of the *L. major* parasite itself and the interaction of the parasites with different phenotypes of human macrophages (MF) as their final host cells.

Part 1

The adaption of *L. major* to the two different hosts resulted in two distinct life stages: disease inducing promastigotes and infection propagating amastigotes. For decades it has been tried to generate the amastigote life stage of *L. major* in a pure host free system. As mentioned above our group was the first to successful establish such an *in vitro* method for axenic amastigote generation and culture. We suggest these axenic parasites to represent the multiplying amastigote life stage of *L. major*, which develops inside infected MF and is responsible for disease propagation.

Aim 1: Therefore our first aim was to characterize the generated axenic amastigotes for morphology, state-specific gene expression and surface composition, and compare them with MF-derived amastigotes as well as promastigotes, in order to confirm the generated axenic amastigotes to be the viable amastigote life stage of *L. major*.

Furthermore, the virulent inoculum of *L. major* was demonstrated to consist of viable and apoptotic parasites. However as described above, the machinery for apoptosis in unicellular organisms is up to now poorly understood. Since *Leishmania* parasites lack the metazoan caspases, we speculate that there have to be other proteins responsible for a regulated course of apoptosis.

Aim 2: Consequently we intended to investigate the different steps of the apoptotic cell death in a chronological order for both promastigotes as well as amastigotes and additionally identify new proteins involved in the apoptotic machinery of *L. major*.

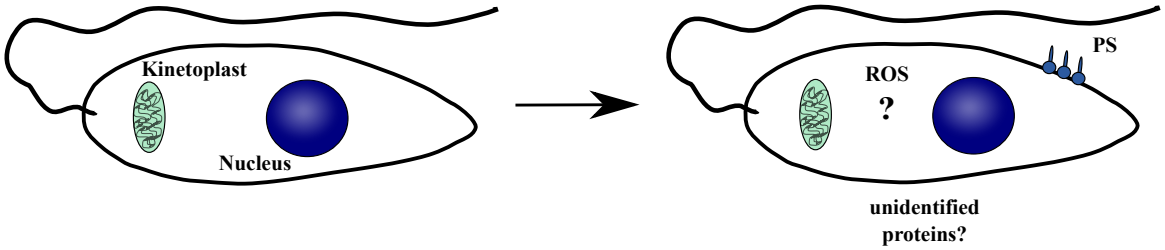

Figure 4: Involved proteins during apoptosis in *L. major* parasites

Part 2

As mentioned above *Leishmania* parasites need to enter MF as their final host cells for replication and establishing a successful infection. However to persist, parasites must prevent efficient MF activation and the development of a protective immune response as well. The mechanisms involved in the propagation of *L. major* parasites inside MF are poorly understood. In addition, it is still not known which phenotype of MF is infected in human cutaneous Leishmaniasis and responsible for parasite propagation and disease development. We hypothesize that pro-inflammatory MF I can eliminate *L. major* parasites leading to a dominantly Th-1 immune response, whereas anti-inflammatory MF II might support disease development resulting in a Th-2 response.

Aim 3: Therefore our aim was to analyze the early and later response of pro- and anti-inflammatory phenotypes of MF in order to investigate their activation state after *L. major* infection. Furthermore, we wanted to study the consequences of possible differential activation, such as the cytokine secretion, which is crucial for the development of an adaptive immune response.

Moreover, we observe a clearance of the intracellular *L. major* parasites after 5 days in both phenotypes of MF, whereas the pro-inflammatory MF I were more efficiently as compared to MF II. Because of this observation we suggest that both types of MF induce their effective pathogen degradation mechanisms to clear the infection, whereas

MF I are expected to kill *L. major* parasites more efficiently as compared to MF II.

Aim 4: Our aim was to identify the degrading mechanisms which are involved in the elimination of *L. major* parasites in infected human MF. In addition, we wanted to know whether there are differences in the responsible mechanisms of parasite clearance in MF I compared to MF II.

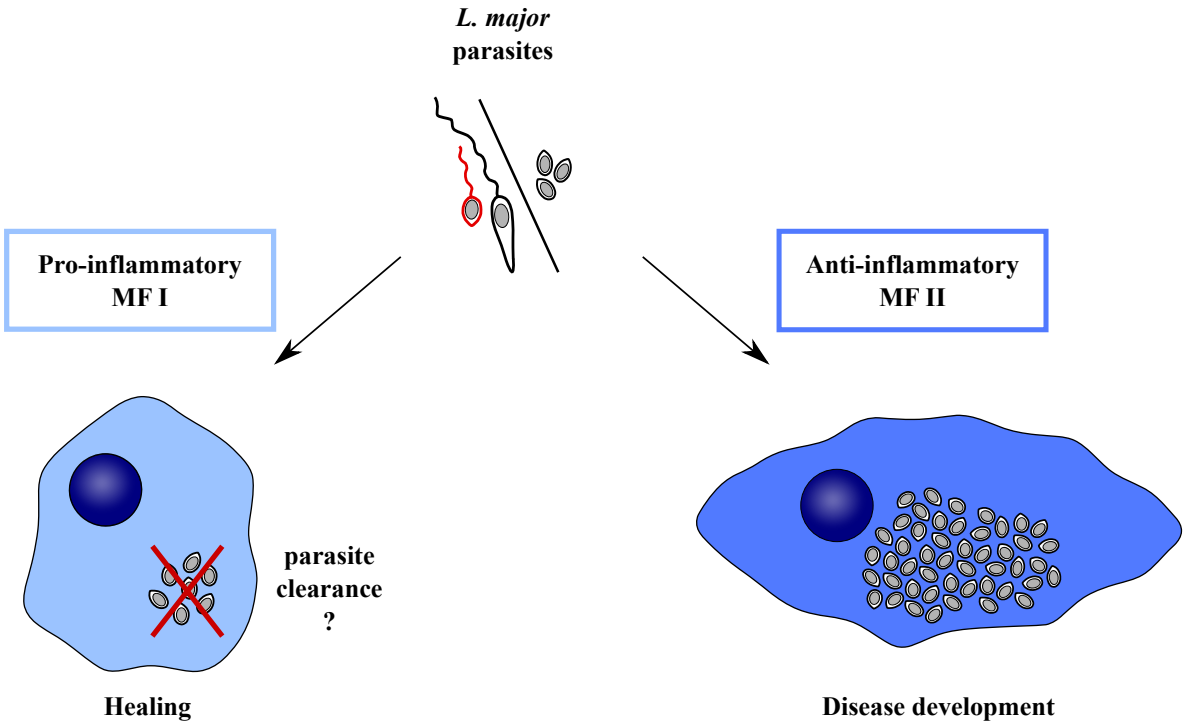

Figure 5: Hypothesis for *L. major* parasite propagation in different phenotypes of human MF

2 Material and Methods

2.1 Material

2.1.1 Chemicals

α-Isonitrosopropiophenone	Sigma, Deisenhof (Ger)
β-Mercaptoethanol	Sigma, Deisenhof (Ger)
Acrylamide-Bis 30 %	Serva, Heidelberg (Ger)
Adenin	Sigma, Deisenhof (Ger)
Agarose	Sigma, Deisenhof (Ger)
Aminocaproic acid	Sigma, Steinheim (Ger)
Ammoniumchloride	Sigma Chemical, St. Louis (USA)
Ammoniumpersulfat (APS)	Serva, Heidelberg (Ger)
Ampuwa H_2O	Fresenius Kabi, Bad Homburg (Ger)
Annexin-V-FITC	Responsif AG, Karlsruhe (Ger)
Annexin-V-Fluos	Roche Applied Science, Mannheim (Ger)
Annexin-V-Alexa 647	Molecular Probes, Eugene (USA)
Biotin	Sigma, Deisenhof (Ger)
Biotinylated Peroxidase	Invitrogen, Camarillo (USA)
Bovine Serum Albumin (BSA)	Sigma, Deisenhof (Ger)
Bromphenol blue dye	Serva, Heidelberg (Ger)
Camptothecin	Bio Vision, San Francisco (USA)

Concanamycin A	Sigma, St. Luois (USA)
D-galactose	Sigma, Steinheim (Ger)
2',7'-Dichlorofuorescein diacetate (H_2DCFDA)	Sigma, Steinheim (Ger)
Difco™ Brain Heart Infusion Agar	BD, Sparks (USA)
Diff-QUIK®	Medion Diagnostics, Düdingen (CH)
Dimethylsulfoxid (DMSO)	Serva, Heidelberg (Ger)
Dithiothreitol (DTT)	Sigma, Steinheim (Ger)
DMEM-Medium (10x)	Biochrom AG, Berlin (Ger)
1 kb DNA Ladder	Promega, Madison (USA)
100 bp DNA Ladder	Promega, Madison (USA)
ECL Blocking Agent	GE Healhcare, Buckinghamshire (UK)
ECL Western Blotting Detection Reagents	GE Healhcare, Buckinghamshire (UK)
EDTA	Sigma, Deisenhof (Ger)
Ethanol, absolut (EtOH)	VWR, Bruchsal (Ger)
Full-Range Rainbow Molecular Weight Marker	GE Healhcare,Buckinghamshire (UK)
Foetal Calf Serum (FCS)	Sigma, Deisenhof (Ger)
Glutamine (L-Glutamine)	Biochrom AG, Berlin (Ger)
Glycerol (99 %)	Sigma, Deisenhof (Ger)
Glycine	Sigma, Steinheim (Ger)
Hemin	Sigma, Deisenhof (Ger)
Hepes-Buffer (1M)	Biochrom AG, Berlin (Ger)
Histopaque®1119	Sigma, Deisenhof (Ger)
Human, recombinant Granolucyte Macrophage Colony Stimulating Factor (GM-CSF)	Genzyme Onkology, NeuIsenburg (Ger)
Human, recombinant Macrophage Colony Stimulating Factor (M-CSF)	R&D Systems, Minneapolis (USA)
Hydrochloric acid, 37 % (HCl)	VWR, Bruchsal (Ger)
Hygromycin B, solution	Invitrogen, San Diego (USA)

Immersion Oil	Carl Zeiss, Jena (Ger)
L-Arginine	Sigma, Steinheim (Ger)
Lectin from *Arachis hypogaea* (peanut)	Sigma, Steinheim (Ger)
Lipopolysaccharides from *E. coli* (LPS)	Sigma, Steinheim (Ger)
Lymphocyte Separation Medium 1077 (LSM 1077)	PAA, Pasching (Aut)
Manganese chloride ($MnCl_2$)	Sigma, Deisenhof (Ger)
Medium 199	Sigma, Deisenhof (Ger)
Methanol	Sigma, Deisenhof (Ger)
Miltefosine	Calbiochem, Darmstadt (Ger)
Human Serum Type AB	Lonza, Walkersville (USA)
Paraformaldehyde (PFA)	Sigma, Deisenhof (Ger)
Peanut Lectin	Sigma, Deisenhof (Ger)
Penicillin/Streptomycin	Biochrom AG, Berlin (Ger)
Phorbol 12-myristate 13-acetate (PMA)	Sigma, Deisenhof (Ger)
Phosphate Buffered Saline (PBS), 1x	PAA, Pasching (Aut)
Phosphoric acid (H_3PO_4)	Merck, Darmstadt (Ger)
Rabbit Blood, defibrinated	Elocin-Lab GmbH, Gladbeck (Ger)
Ringer B. Braun	B. Braun Melsungen, Melsungen (Ger)
RNase AWAY	VWR, Darmstadt (Ger)
Roswell Park Memorial Institute (RPMI) 1640 Medium	Sigma, Deisenhof (Ger)
Roti®-Blue	Carl Roth, Karlsruhe (Ger)
Saponin from *Quillaja* bark	Sigma, Steinheim (Ger)
Sodium Acetat	Sigma, Deisenhof (Ger)
Sodium Azide	Sigma, Deisenhof (Ger)
Sodium Chloride	Sigma, Deisenhof (Ger)
Sodium Dodecyl Sulfate (SDS)	Sigma, Deisenhof (Ger)

Sodium Hydroxide, 1M (NaOH)	Merck, Darmstadt (Ger)
Staurosporine	Sigma, Steinheim (Ger)
Streptavidin	Invitrogen, Camarillo (USA)
Sulfuric acid (H_2SO_4)	Merck, Darmstadt (Ger)
TMB Substrate Solution	Thermo Fisher Scientific, Bonn (Ger)
TEMED	Serva, Heidelberg (Ger)
Trishydroxylmethylaminomethan (Tris)	Sigma, Deisenhof (Ger)
Triton X-100	Sigma, Steinheim (Ger)
Tween 20	Sigma, Steinheim (Ger)
Urea	Roth, Karlsruhe (Ger)

2.1.2 Culture media and buffers

Alex-Amastigote-Medium (AAM)	RPMI 1640 Medium 10 % FCS 3 mM L-Glutamine 100 U/ml Penicillin 100 μg/ml Streptomycin pH 5.5, adjusted with 38 % HCl sterile filtered
FACS-Buffer	1 x PBS 1 % Human Serum 1 % Foetal Calf Serum 1 % Bovine Serum Albumin
FACS-Buffer II	1 x PBS 1 % Human Serum

	1 % Foetal Calf Serum
	1 % Bovine Serum Albumin
	0.5 % Saponin
	sterile filtered
Lm-FACS-Buffer I	1 x Ringer Solution
	1 % Bovine Serum Albumin
Lm-FACS-Buffer II	1 x PBS
	1 % Foetal Calf Serum
	1 % Bovine Serum Albumin
Lm-Medium	RPMI 1640 Medium
	5 % FCS
	2 mM L-Glutamine
	50 μM β-Mercaptoethanol
	100 U/ml Penicillin
	100 μg/ml Streptomycin
	10 mM Hepes Buffer
Lm-Suspension-Medium	Medium 199
	10 % FCS
	100 U/ml Penicillin
	100 μg/ml Streptomycin
	40 mM Hepes Buffer
	5 ml 10 mM Adenine, in 50 mM Hepes
	1 ml 0.25 % Hemin, in 50 % Triethanolamine
	0.5 ml 0.1 % Biotin, in 95 % Ethanol

Novy-Nicolle-McNeal Blood Agar Medium	16.6 % Rabbit blood, defibrinated 16.6 % 1 x PBS 66.2 % Brain Heart Infusion Agar 66.2 U/ml Penicillin 66.2 μg/ml Streptomycin
Complete-Medium	RPMI 1640 Medium 10 % FCS 2 mM L-Glutamine 50 μM β-Mercaptoethanol 100 U/ml Penicillin 100 μg/ml Streptomycin 10 mM Hepes Buffer
Wash-Buffer	1 x PBS 5 % Complete-Medium
MACS-Buffer	1 x PBS 2 mM EDTA 0.5 % Bovine Serum Albumin pH 7.2

2.1.3 Westernblot buffers and solutions

6 x Lämmli-Buffer	A. bidest 4.125 M Glycerol 10 % SDS

	0.6 M DTT
	180 μM Bromphenol blue
Running-Buffer	A. bidest
	25 mM Tris
	0.1 % SDS
	1.44 % Glycine
Separation-Gel-Buffer	A. bidest
	1.5 M Tris
	0.4 % SDS
	pH 6.8 with HCl
Stacking-Gel-Buffer	A. bidest
	500 mM Tris
	0.4 % SDS
	pH 8.8 with HCl
TBST-Solution	A. bidest
	0.5 % Tween
	0.14 M NaCl
	10 mM Tris
	1 mM NaN_3
	pH 8
Anode-Buffer I	A. bidest
	20 % Methanol
	300 mM Tris

Anode-Buffer II	A. bidest 20 % Methanol 25 mM Tris
Cathode-Buffer	A. bidest 20 % Methanol 40 mM Aminocaproic acid 0.01 % SDS
WB-Block-Solution	TBST-Solution 5 % Blocking reagent
Buffer for primary antibody	TBST-Solution 2 % Bovine Serum Albumin 0.02 % NaN_3
Coomassie gel-fixing solution	A. bidest 1 % Phos (85 %) 20 % Methanol
Coomassie staining solution	A. bidest 20 % Roti®-Blue 20 % Methanol
Coomassie gel-washing solution	A. bidest 25 % Methanol

Gels:

Chemicals	Separation gel (30 ml)		Stacking gel (10 ml)
	15 %	12 %	3.3 %
Aqua bidest	7.5 ml	10.5 ml	6.1 ml
Separation-Gel-Buffer	7.5 ml	7.5 ml	-
Stacking-Gel-Buffer	-	-	2.5 ml
Acrylamide stock 30 %	15 ml	12 ml	1.3 ml
TEMED	20 μl	20 μl	10 μl
10 % APS	100 μl	100 μl	50 μl

2.1.4 *Leishmania* strains

Leishmania major isolate MHOM/IL/81/FEBNI: Originally isolated from a skin biopsy of an israeli patient and kindly provided by Dr. Frank Ebert (Bernhard Nocht Institute for Tropical Medicine, Hamburg, Germany).

Leishmania major isolate MHOM/IL/81/FEBNI eGFP: MHOM/IL/81/FEBNI isolate genetically transfected with the green fluorescent eGFP gene.

Leishmania major isolate MHOM/IL/81/FEBNI DsRed: MHOM/IL/81/FEBNI isolate genetically transfected with the red fluorescent DsRed gene.

Leishmania major isolate MHOM/IL/80/Friedlin: Originally isolated from a skin biopsy of an israeli patient with cutaneous leishmaniasis and kindly provided by the Pasteur Institute (Paris, France).

Leishmania donovani isolate MHOM/IN/80/DD8: Originally obtained from an indian Kala-azar patient.

Leishmania tropica isolate MHOM/SU/74/K27: Originally isolated from a skin biopsy of a patient with leishmaniasis in the former Soviet Union.

2.1.5 Human leukocytes

Human peripheral blood mononuclear cells (PBMC) and macrophages (MF) were obtained from buffycoats of healthy donors from the blood bank of the University Hospital of Ulm and the DRK-Blutspendedienst in Frankfurt. Subsequently, cells were isolated as described in Methods 2.2.1.

2.1.6 Ready-to-use kits

CD14 MicroBeads, human	Miltenyi Biotec, Bergisch Gladbach (Ger)
DNeasy Blood and Tissue Kit	Qiagen, Hilden (Ger)
Human TNF-alpha Quantikine Elisa kit	R&D Systems, Minneapolis (USA)
Human IL-12/IL-23 p40 Quantikine Elisa kit	R&D Systems, Minneapolis (USA)
Human IL-10 Duoset Quantikine Elisa kit	R&D Systems, Minneapolis (USA)
ImProm-II Reverse Transkription System	Promega, Mannheim (Ger)
LightCycler® FastStart Master Plus SYBER Green I kit	Roche Applied Science, Mannheim (Ger)
RNeasy Plus Mini kit	Qiagen, Hilden (Ger)
Stemfect™RNA Transfection kit	Stemgent, San Diego (USA)

2.1.7 Anti-Human antibodies

Isotype (FITC), IgG1, MOPC-21 (1:100)	BD Pharmingen, Heidelberg (Ger)
Isotype (FITC), IgG2b, 27-35 (1:25)	BD Pharmingen, Heidelberg (Ger)
Isotype (APC), IgG1, MOPC-21 (1:100)	Caltag Laboratories, Hamburg (Ger)
Isotype (PE), IgG1, MOPC-21 (1:100)	BD Pharmingen, Heidelberg (Ger)

Isotype (PerCP), IgG2a, X39 (1:100)	BD Pharmingen, Heidelberg (Ger)
Chicken anti-mouse (Alexa 488) (1:100)	Molecular Probes, Eugene (USA)
Mouse anti-CD163 (PE), IgG1, GHI/61 (1:10)	BD Pharmingen, Heidelberg (Ger)
Mouse anti-CD206 (PE), IgG1, 19.2 (1:20)	BD Pharmingen, Heidelberg (Ger)
Mouse anti-CD11b (PE), IgG1, ICRF44 (1:100)	BD Pharmingen, Heidelberg (Ger)
Mouse anti-CD14 (FITC), IgG2b, (1:25)	BD Bioscience, Heidelberg (Ger)
Mouse anti-CD35 (FITC), IgG1, E11 (1:25)	BD Pharmingen, Heidelberg (Ger)
Mouse anti-MHC II (PerCP), IgG2a, L243 (1:10)	BD Pharmingen, Heidelberg (Ger)
Mouse anti-CD40 (APC), IgG1, HB14 (1:100)	Caltag Laboratories, Hamburg (Ger)
Mouse anti-CD86 (APC), IgG1, 2331 (1:100)	BD Pharmingen, Heidelberg (Ger)
Mouse anti-phospho-p44/42 MAPK (ERK 1/2) (Alexa Fluor 488), IgG1, 20A (1:10)	BD Pharmingen, Heidelberg (Ger)
Mouse anti-phospho-p38 MAPK (PE), IgG1, 36/p38 (1:10)	BD Pharmingen, Heidelberg (Ger)
Mouse anti-phospho-p38 MAPK , IgG1, 36/p38 (1:2500)	BD Bioscience, Heidelberg (Ger)
Rabbit anti-p38 MAPK , IgG, (1:1000)	Cell Signaling, Danvers (USA)
Rabbit anti-phospho-p44/42 MAPK (ERK 1/2), IgG1, 197G2 (1:1000)	Cell Signaling, Danvers (USA)
Mouse anti-p44/42 MAPK (ERK 1/2), IgG1, 3A7 (1:2000)	Cell Signaling, Danvers (USA)
Goat anti-rabbit-HRP, IgG, (1:4000)	Cell Signaling, Danvers (USA)
Horse anti-mouse-HRP, IgG, (1:4000)	Cell Signaling, Danvers (USA)
Mouse anti-β-Actin, IgG, AC-15 (1:1000)	Sigma, Steinheim (Ger)

2.1.8 Anti-*Leishmania* antibodies

Mouse anti-LPG (WIC79.3) (1:3000)	Kind gift of Dr. G. Späth, Institute Pasteur, Paris (Fra)

2.1.9 Oligonucleotides

Primer	Sequence
45rRNA fwd	5'- CCT ACC ATG CCG TGT CCT TCT A -3'
45rRNA rev	5'- AAC GAC CCC TGC AGC AAT AC -3'
ABC-Transp. homologue fwd	5'- CGG GTT TGT CTT TCA GTC GT -3'
ABC-Transp. homologue rev	5'- CAC CAG AGA GCA TTG ATG GA -3'
Sherp fwd	5'- GAC GCT CTG CCC TTC ACA TAC -3'
Sherp rev	5'- TCT CTC AGC TCT CGG ATC TTG TC -3'
QDPR fwd	5'- ATG AAA AAT GTA CTC CTC ATC G -3'
QDPR rev	5'- TTC ACC CTG CGT ACT GAA CAC AT -3'
alpha-tubulin fwd	5'- ATG CGT GAG GCT ATC TGC ATC CAC AT -3'
alpha-tubulin rev	5'- TAG TGG CCA CGA GCG TAG TTG TTC G -3'
GP63 fwd	5'- ACT GCC CGT TTG TTA TCG AC -3'
GP63 rev	5'- CCG GCG TAC GAC TTG ACT AT -3'
Cpb fwd	5'- TGA TGC GGT GGA CTG GC -3'
Cpb rev	5'- CCA CTC GAA TGC CTG CAG C -3'
GAPDH fwd	5'- GAG TCA ACG GAT TTG GTC GT -3'
GAPDH rev	5'- TTG ATT TTG GAG GGA TCT CG -3'
LL37 fwd	5'- GGA CCC AGA CAC GCC AAA -3'
LL37 rev	5'- GCA CAC TGT CTC CTT CAC TGT GA -3'
ITS1 fwd (LITSR)	5'- CTG GAT CAT TTT CCG ATG -3'
ITS1 rev (L5.8S)	5'- TGA TAC CAC TTA TCG CAC TT -3'

Table 1: Primer for PCR

Primer:
Table 1 contains the used oligonucleotide primer and their sequence. All oligonucleotides were purchased from Thermo Fisher Scientific in Ulm (Ger).

siRNA:

Stealth RNAi siRNA Negative Control Med GC	Invitrogen, Darmstadt (Ger)
ON-TARGET plus SMART pool Human CAMP (LL-37)	Thermo Scientific Dharmacon, Bonn (Ger)

2.1.10 Enzymes

FideliTaq PCR Master Mix (2x)	Affymetrix, Santa Clara (USA)
HaeIII (restriction enzyme)	New England Biolabs, Frankfurt am Main (Ger)
Phusion High Fidelity DNA Polymerase	Finnzymes, Vantaa (Fin)
Phusion High-Fidelity PCR kit	New England Biolabs, Frankfurt am Main (Ger)
Peroxidase	Invitrogen, Camarillo (USA)
Recombinant DNase I	Roche, Mannheim (Ger)
RNaseOUT^{TM} recombinant RNase Inhibitor	Invitrogen, Darmstadt (Ger)

2.1.11 Laboratory supplies

Carbon-coated sapphire discs (3 mm in diameter)	Engineering Office M. Wohlwend GmbH, Sennwald (CH)
Cell culture flasks (25 cm^2; 75 cm^2)	BD labware Europe, Le Pont de Claix (Fra)
Cell culture plates (6-well; 24-well; 96-well)	BD labware Europe, Le Pont de Claix (Fra)
Centrifuge tubes (15 ml; 50 ml)	BD labware Europe, Le Pont de Claix (Fra)
Cryo tubes	Greiner Bio-one, Frickenhausen (Ger)
FACS tubes (2 ml)	Micronic, Lelystad (Ned)
FACS tubes	BD labware Europe, Le Pont de Claix (Fra)

High performance chemiluminescence film (Hyperfilm™ ECL)	GE Healhcare, Buckinghamshire (UK)
Hybond ECL blot membrane	VWR, Darmstadt (Ger)
LightCycler® capillaries 20 µl	Roche Applied Science, Mannheim (Ger)
Microtest plates, 96-well (V-Bottom)	Sarstedt, Nümbrecht (Ger)
Microtest plates, 96-well (Flat-Bottom)	Sarstedt, Nümbrecht (Ger)
Milipore stericup sterile vacuum filter units	Millipore, Schwalbach (Ger)
Multiplier tubes (0.65 ml), biopure	Sarstedt, Nümbrecht (Ger)
Nunc-Immuno™ plate, Maxisorp	NUNC, Langenselbold (Ger)
Pipette filter tips (1-10 µl, 10-100 µl, 50-200 µl, 100-1000 µl)	Sarstedt, Nümbrecht (Ger)
Reaction tubes (0.5 ml; 1.5 ml; 2.0 ml)	Eppendorf, Hamburg (Ger)
Serological pipettes, steril (2.5 ml; 5 ml; 10 ml; 25 ml)	Corning Inc., Corning, New York (USA)
Transfer membrane immobilon-P (PVDF)	Millipore, Billerica (USA)
Transfer pipette (3.5 ml)	Sarstedt, Nümbrecht (Ger)
Whatman paper gel blotting	VWR, Darmstadt (Ger)

2.1.12 Instruments

AutoMACS Pro separator	Miltenyi Biotec, Bergisch Gladbach (Ger)
Analytical balance AG204	Mettler Toledo, Giessen (Ger)
Balance KERN470	Kern & Sohn GmbH, Balingen-Frommern (Ger)
Centrifuge 5471	Eppendorf, Hamburg (Ger)
CO_2-Incubator Forma 3010	Thermo Scientific, Marietta (USA)
CO_2-Incubator Heraeus BBD 6220	Thermo, Dreieich (Ger)
CO_2-Incubator Forma Series II Water Jacket	Thermo Scientific, Marietta (USA)
Cytocentrifuge Cytospin3	Shandon, Frankfurt (Ger)
DNA Engine® Peltier Thermal Cycler	Bio-Rad, München (Ger)

Easy-cast™ Electrophoresis System	Thermo Scientific Owl Separation, Rochester (Ger)
Electrophoresis power supply EPS 600	Amersham Pharmacia, Uppsala (Swe)
EM10 transmission electron microscope	Carl Zeiss, Jena (Ger)
Flow-Cytometer FACS-Calibur II	Becton Dickinson, Heidelberg (Ger)
Flow-Cytometer LSR II	Becton Dickinson, Heidelberg (Ger)
Freezer -20°C	Bosch, Stuttgart (Ger)
Freezer Herafreeze -80°C	Heraeus Sepatech GmbH, Osterode (Ger)
Gel dryer model 543	Bio-Rad, München (Ger)
Gel electrophoresis system SE600	Hoefer, San Francisco (USA)
HPF 01 apparatus	Engineering Office M. Wohlwend GmbH, Sennwald (CH)
Laminar flow workbench MSC-Advantage	Thermo Scientific, Dreieich (Ger)
LightCycler®	Roche Applied Science, Mannheim (Ger)
Magnetic stirrer MR3002	Heidolph, Leverkusen (Ger)
Microscope Axio Imager M2	Carl Zeiss, Jena (Ger)
Microscope Axiovert 40 CFL	Carl Zeiss, Jena (Ger)
Microscope Primo Star	Carl Zeiss, Jena (Ger)
Multichannel Pipette	Eppendorf, Hamburg, (Ger)
Multifuge 3 SR	Heraeus, Thermo, Dreieich (Ger)
Neubauer cell counting chamber depth 0.1mm	VWR, Darmstadt (Ger)
Neubauer cell counting chamber depth 0.02mm	VWR, Darmstadt (Ger)
Power supply Power Pac 300	Angewandte Gentechnologie Systeme GmbH, Heidelberg (Ger)
pH-Meter pH525	WTW, Wellheim (Ger)
Pipettes	Eppendorf, Hamburg, (Ger)
Platform shaker Polymax 1040	Heidolph, Schwabach (Ger)

Shaker	VWR, Darmstadt (Ger)
Shake Table GFL-3016	GFL, Burgwedel (Ger)
Semi-dry transfer unit TE 77 PWR	Amersham Biosciences, Freiburg (Ger)
Table-top processor Curix 60	AGFA, Berlin (Ger)
Tecan infinite M200	Tecan Austria GmbH, Grödig (Aut)
Thermostatic circulator 2219 Multitemp II	LKB Bromma, Stockholm (Swe)
Variofuge 3.OR	Heraeus, Thermo, Dreieich (Ger)
Water bath	GFL, Burgwedel (Ger)

2.1.13 Software

Axiovision 4.7	Carl Zeiss, Jena (Ger)
BD Diva software v6.1.3	Becton Dickinson, Heidelberg (Ger)
CellQuest® Pro	Becton Dickinson, Heidelberg (Ger)
Inkscape v0.48	OpenSource (`http://www.inkscape.org`)
ImageJ	OpenSource (`http://rsbweb.nih.gov/ij/`)
LightCycler® software v3.5	Roche Applied Science, Mannheim (Ger)
Microsoft® Office 2010	Microsoft, Redmont (USA)
Tecan I-Control™ v1.6	Tecan Austria GmbH, Grödig (Aut)

2.2 Methods

2.2.1 Cell culture

The cells were treated and passaged under sterile conditions in endotoxin free environments and all cell cultures were kept in humidified incubators with 5 % CO_2 .

2.2.1.1 Cultivation of *L. major* promastigotes

L. major promastigotes were cultured either in biphasic Novy-Nicolle-McNeal (NNN) blood agar medium or in Lm-Suspension-Medium at 27°C. In the stationary growth phase (stat-phase) after 7 days *L. major* promastigote cultures were passaged up to ten serial passages before the cultures were discarded.
For long-time storage stationary-phase (stat-phase) *L. major* were pelleted at 2400 x g for 8 min and resuspended in ice-cold Lm-Medium supplemented with 20 % FCS and 10 % DMSO. The cell density was adjusted to 2 x 10^8 *L. major*/ml. The cells were transferred into Cryo Tubes and were put in a styropore box at -80°C overnight before they could be stored in liquid nitrogen.
L. major parasites were thawed at 37°C in a water-bath and added drop-wise to Lm-Medium to dilute the DMSO. After pelleting the parasites were washed one more time before the pellet was resuspended in 10 ml Lm-Medium and added on biphasic NNN blood agar medium 100 μl/well. The culture was not used until the second passage.
For eGFP and DsRed promastigotes Lm-Medium was supplemented with 20 μg/ml hygromycin B.

2.2.1.2 Isolation of metacyclic *L. major* promastigotes

4 x 10^8 of stat-phase *L. major* promastigotes were resuspended in 1 ml RPMI supplemented with 100 μg/ml lectin (peanut), incubated at room temperature for 30 min and centrifuged at 545 x g for 10 min. The supernatant was collected and washed with DMEM supplemented with 20 mM D-galactose at 2400 x g for 10 min. The isolated metacyclic parasites were resuspended in Lm-Medium and counted for further analysis.

2.2.1.3 Generation and cultivation of *L. major* amastigotes *in vitro*

Promastigote pre-culture

4 wells of logarithmic growth phsase (log-phase) (day 3 - 4 of NNN blood agar culture) *L. major* promastigotes were cultured in 5 ml Lm-Suspensions-Medium + 0.5 ml FCS for 3 days at 27°C.

For eGFP and DsRed promastigotes Lm-Medium was supplemented with 20 μg/ml hygromycin B.

Amastigote pre-culture

The log-phase promastigote pre-culture was harvested and pelleted at 1450 x g for 8 min. The pellet was resuspended in 10 ml AAM and centrifuged for 8 min at 1450 x g. This step was repeated with 2400 x g. The pellet was resuspended in AAM and adjusted to 2 x 10^7 *L. major*/ml. The cells were incubated in 25 cm^2 culture flasks for 10 - 12 days at 33°C.

Amastigote isolation

To separate the amastigotes from the remaining promastigotes and dead parasites a discontinous Histopaque® 1119 density gradient was used. The amastigote pre-culture was harvested and pelleted at 2400 x g for 8 min. The pellet was resuspended in 50 % (1,0595 g/ml) Histopaque® 1119 and fractionated on a discontinous Histopaque® 1119 density gradient consisting of layers with densities of (from top to bottom) 1,0833 g/ml (70 %), 1,0952 g/ml (80 %), 1,1071 g/ml (90 %) and 1,119 g/ml (100 %). The gradient was centrifuged at 2400 x g for 35 min (with acceleration and deceleration set at the lowest level). The interphases between 80 - 90 % and 90 - 100% were collected, washed twice in AAM and adjusted to 2 x 10^7 *L. major*/ml. The purity of the amastigotes was monitored by analysing Diff QUIK® stained cytospin slides. The purified *L. major* amastigotes were cultured in 25 cm^2 culture flasks at a density of 2 x 10^7 *L. major*/ml at 33°C. The culture is stable for 7 days.

Amastigote retransformation

To assure a constant virulence of the parasites, amastigote-passages were performed using the *in vitro* culture method to generate axenic amastigotes. *L. major* promastigotes were transformed into amastigotes and subsequently, were cultured on biphasic

NNN blood agar medium, where the parasites transformed back to the promastigote stage.

2.2.1.4 Isolation of *L. major* amastigotes from infected MF

Macrophages (MF) were infected as described in 2.2.1.7 with a multiplicity of infection of 1:20 and incubated for 2 - 4 days at 37°C to allow the parasites to differentiate into amastigotes. The infected cells were washed with warm RPMI without supplements and the cell walls were lysed in RPMI supplemented with 0.02 % SDS for 3 min at 37°C to release the intracellular amastigotes. The lysis was stopped with AAM supplemented with 20 % FCS and the MF lysate was washed once at 2400 x g for 8 min. To collect the free parasites the pellet was resuspended in AAM supplemented with 20 % FCS and centrifuged at 75 x g for 8 min. The supernatant was removed and the centrifugation step was repeated twice. The purified amastigotes were pelleted at 2400 x g for 8 min, resuspented in AAM and adjusted to 2 x 10^7 *L. major*/ml. The purity of the amastigotes was monitored by analysing Diff QUIK® stained cytospin slides.

2.2.1.5 Isolation of human peripheral blood mononuclear cells (PBMC)

PBMC were isolated from buffycoats of healthy donors. The buffycoats were diluted 1:5 with sterile PBS, layered on top of 15 ml Lymphocyte Separation Medium 1077 and centrifuged at 545 x g for 30 min (with acceleration and deceleration set at the lowest level). Plasma and the interphase mainly consisting of PBMC were collected and washed with Wash-Buffer at 1024 x g for 8 min. The pellet was resuspendet and washed with Wash-Buffer first at 545 x g and then at 135 x g for 8 min. The pellet was resuspended in 10 ml 0.15 M Ammoniunchloride and the ery-lysis was performed for 10 - 15 min at room temperature. Subsequently, the cells were washed twice with Wash-Buffer at 135 x g for 8 min to remove thrombocytes. After pooling the cells were counted and adjusted to a density of 1 x 10^7 PBMC/ml in Complete-Medium.

2.2.1.6 Generation of blood derived MF

Plastic adherence

Fresh isolated PBMC were incubated in 25 cm^2 culture flasks at a density of 1 x 10^7 PBMC/ml in Complete-Medium supplemented with 1 % human serum for 90 min at 37°C. The supernatant was discarded and the non-adherent cells were removed by washing 2 times with pre-warm Wash-Buffer. The adherent monocytes were cultured in Complete-Medium supplemented with 10 ng/ml GM-CSF (generation of type 1 MF) or 30 ng/ml M-CSF (generation of type 2 MF) for 5 - 7 days at 37°C.

AutoMACS separation

100 x 10^6 PBMC fresh isolated PBMC were washed with 10 ml cold MACS-Buffer at 300 x g for 8 min. The pellet was resuspended in 400 μl MACS-Buffer, 100 μl CD14-Beads were added to the cells and the mixture was incubated at 4° C for 15 min. Subsequently, the cells were washed with 10 ml cold MACS-Buffer at 300 x g for 8 min and the pellet was resuspended in 500 μl MACS-Buffer. The labbeled cells were placed into an AutoMACS device and the separation program posseld was run. After seperation the isolated monocytes were counted and incubated in 6-well plates at a density of 1.6 x 10^6 cells/ml in Complete-Medium supplemented with 10 ng/ml GM-CSF (generation of type 1 MF) or 30 ng/ml M-CSF (generation of type 2 MF) for 5 - 7 days at 37° C with a medium exchange after 3 days.

2.2.1.7 Co-incubation of macrophages with *L. major* parasites

After 5 - 7 days of culture in the presence of either GM-CSF or M-CSF MF were harvested with a cell scraper and counted. Co-incubation of MF with *L. major* parasites was performed by two different methods.

Co-incubation in cell culture plates

1 x 10^6 MF/ml were transfered into 12-well (1 x 10^6 MF) or 96-well (1 x 10^5 MF) cell culture plates. The cells were left to adhere in the cell culture plates for 60 min and the non-adherend cells were removed by discarding the supernatant. Stat-phase *L. major* promastigotes or 1 - 3 days old *L. major* amastigotes were added to the MF

with a multiplicity of infection (MOI) of 1:10. The cell culture plates were centrifuged at 304 x g for 3 min before incubating for 3 h at 37°C. After co-incubation extracellular parasites were removed by washing the cells with Wash-Buffer. Cells and supernatants were collected after 18, 48 or 72 h culture at 37°C for further analyses.

Co-incubation in centrifuge tubes
1 x 10^7 MF/ml were transfered into 15 ml centrifuge tubes or 1.5 ml reaction tubes. Stat-phase *L. major* promastigotes or 1 - 3 days old *L. major* axenic amastigotes were added to the MF with a MOI of 1:10. After 3 h of co-incubation with the parasites either extracellular parasites were removed by washing the cells with Wash-Buffer at 135 x g for 10 min and the cells were cultured for another 18 h at 37°C. Or 1 ml Complete-Medium was added per 1 x 10^6 MF to the cells and after another incubation for 18 h at 37°C the extracellular parasites were removed by centrifuging at 135 x g for 10 min. Cells were collected after 18, 48 or 72 h culture at 37°C for further analyses.

Infection rates were determined by counting at least 200 MF on Diff QUIK® stained cytospin slides. The parasite burdens were evaluated by counting intracellular *L. major* parasites in 20 infected MF.

2.2.1.8 End-point titration

Axenic *L. major* parasites
The amount of viable *L. major* parasites was determined 72 h after the treatment with different drugs by end-point titration. End-point titration experiments were carried out by using 1 x 10^5 parasites in octuplicate wells and a dilution factor of 10. The number of viable *L. major* was assessed after 7 days of incubation on biphasic NNN blood agar medium at 27°C and calculated from the last dilution that showed parasitic growth.

Viable *L. major* parasites inside infected MF
The amount of viable intracellular *L. major* parasites inside human MF was determined 18 and 48 h after 3 h of co-incubation with the parasites by end-point titration.
End-point titration experiments were carried out by using 2000 MF in quadruplicate wells and a dilution factor of 1.5. The number of viable intracellular *L. major* parasites per 1000 MF was assessed after 7 days of incubation on biphasic NNN Blood Agar

Medium at 27°C and calculated from the last dilution that showed parasitic growth and equals 1.5 exp (mean dilution with parasitic growth).

2.2.1.9 Cytocentrifuging cells

2 x 10^6 *L. major* parasites or 1 x 10^5 MF were washed in Medium and resuspended in 100 μl PBS. Cells were centrifuged on slides in a Cytocentrifuge at 500 x g for 10 min for *Leishmania* and at 75 x g for 5 min for MF. Subsequetly, the slides were air-dried for further use.

2.2.1.10 Diff QUIK staining

Air-dried cytospin slides were incubated for 1 min in Fixation Solution of a Qiff QUIK® kit. Subsequently, incubated for 1 min in Staining Solution I followed by 1 min in Staining Solution II. The slides were rinsed in tap water, air-dried and used for further microscopical analyses.

2.2.2 FACS analysis

FACS stainings were performed in 96-well Microtestplates (V-Bottom) in the dark on ice.

2.2.2.1 Extracellular FACS analysis of (infected) MF

2 x 10^5 MF were washed in FACS-Buffer and incubated with α-CD163-PE, α-CD-11b-PE, α-CD14-FITC, α-CD35-FITC, α-CD40-APC, α-CD86-APC, α-CD206-PE and α-MHC II-PerCP in FACS-Buffer for 30 min. For isotype controls, MF were incubated with PE-, FITC-, APC- or PerCP- conjugated matched mouse IgG1 and mouse IgG2 antibodies. The cells were washed in FACS-Buffer, resuspended in 400 μl FACS-Buffer and analysed by a flow cytometer (FACS-Calibur II with CellQuest® Pro software or LSR II with BD Diva software).

2.2.2.2 Intracellular FACS analysis of (infected) MF

5 x 10^5 MF were first washed in FACS-Buffer and then in FACS-Buffer II to permeabilize the cell membrane. Subsequently the cells were incubated with α-phospho Tyr-FITC, α-phospho p38-PE and α-phospho ERK-Alexa 488 in FACS-Buffer II for 30 min. After a washing step with FACS-Buffer II, the MF were washed with FACS-Buffer, resuspended in 400 μl FACS-Buffer and analysed by a flow cytometer (FACS-Calibur II with CellQuest® Pro software).

2.2.2.3 Extracellular FACS analysis of *L. major*

5 x 10^6 *L. major* parasites were washed in Lm-FACS-Buffer I and incubated with α-LPG (WIC79.3) in Lm-FACS-Buffer I for 30 min. After a washing step with Lm-FACS-Buffer I, the cells were incubated with chicken α-mouse-Alexa 488 in Lm-FACS-Buffer I for 30 min. The parasites were washed in Lm-FACS-Buffer I, resuspended in 400 μl FACS-Buffer and analysed by a flow cytometer (FACS-Calibur II with CellQuest® Pro software or LSR II with BD Diva software).

Annexin-binding

5 x 10^6 *L. major* parasites were washed in Lm-FACS-Buffer I and incubated with 0.1 μg/ml Annexin A5 (AnxA5)-FITC or AnxA5-Fluos in Lm-FACS-Buffer I for 20 min. The parasites were washed in Lm-FACS-Buffer I, resuspended in 400 μl Lm-FACS-Buffer I and analysed by a flow cytometer (FACS-Calibur II with CellQuest® Pro software or LSR II with BD Diva software).

2.2.2.4 Intracellular FACS analysis of *L. major*

ROS-detection

5 x 10^6 *L. major* parasites were washed in Lm-FACS-Buffer II and incubated with 50 nM 2',7'-Dichlorofuorescein diacetate (H_2DCFDA) in Lm-FACS-Buffer II for 20 min. The parasites were washed in Lm-FACS-Buffer II, resuspended in 400 μl Lm-FACS-Buffer II and analysed by a flow cytometer (FACS-Calibur II with CellQuest® Pro software).

2.2.3 ELISA analysis

Macrophages were cultured for 18 h in Complete-Medium alone, co-incubated with stat-phase *L. major* promastigotes or with 1-3 days old *L. major* axenic amastigotes at a MOI of 1:10. Supernatants were collected and stored at -80°C until cytokine determination using an enzyme-linked immunosorbent assay (ELISA).

2.2.3.1 TNF alpha

TNF alpha content was measured using sandwich ELISA (Human TNF-alpha Quantikine Elisa kit) according to the manufacturer's instructions. Briefly, a 96-well Immuno™ plate was coated with 2 μg/ml anti-TNF alpha antibody, blocked and washed. The samples were applied to the plate together with a dilution series of a protein standard (for a standard curve) for 1 h at room temperature. TNF alpha was detected using 0.5 μg/ml of a biotinyled anti-human TNF alpha antibody for 1 h. During the incubation the streptavidin-HRP complex was prepared and diluted 1:10000. The plate was washed and incubated with the streptavidin-HRP complex for 30 min. The TMB substrate solution was added after washing to the wells and incubated for 15 - 30 min in the dark. The reaction was stopped using 0.18 M (H_2SO_4) and the optical density was determined with a Tecan infinite M200, wavelength set to 450 nm. The TNF alpha concentration in each well was calculated using the standard curve generated with the optical densities of the standard dilution series.

2.2.3.2 IL-12

Il-12 content was measured using sandwich ELISA (Human IL-12/IL-23 p40 Quantikine Elisa kit) according to the manufacturer's instructions. Briefly, a 96-well Immuno™ plate was coated with 3 μg/ml anti-IL-12/IL-23 p40 antibody, blocked and washed. The samples were applied to the plate together with a dilution series of a protein standard (for a standard curve) for 2 h at room temperature. The plate was washed and IL-12 was detected using 0.2 μg/ml of a biotinyled anti-human IL-12 antibody for 1 h. During the incubation the streptavidin-HRP complex was prepared and diluted 1:10000. The

plate was washed and incubated with the streptavidin-HRP complex for 30 min. The TMB substrate solution was added after washing to the wells and incubated for 15 - 30 min in the dark. The reaction was stopped using 0.18 M (H_2SO_4) and the optical density was determined with a Tecan infinite M200, wavelength set to 450 nm. The IL-12 concentration in each well was calculated using the standard curve generated with the optical densities of the standard dilution series.

2.2.3.3 IL-10

Il-10 content was measured using sandwich ELISA (Human IL-10 Duoset Quantikine Elisa kit) according to the manufacturer's instructions. Briefly, a 96-well Immuno™ plate was coated with 3 μg/ml anti-IL-10 antibody, blocked and washed. The samples were applied to the plate together with a dilution series of a protein standard (for a standard curve) for 2 h at room temperature. The plate was washed and IL-10 was detected using 0.2 μg/ml of a biotinyled anti-human IL-10 antibody for 2 h. During the incubation the streptavidin-HRP complex was prepared and diluted 1:10000. The plate was washed and incubated with the streptavidin-HRP complex for 30 min. The TMB substrate solution was added after washing to the wells and incubated for 15 - 30 min in the dark. The reaction was stopped using 0.18 M (H_2SO_4) and the optical density was determined with a Tecan infinite M200, wavelength set to 450 nm. The IL-10 concentration in each well was calculated using the standard curve generated with the optical densities of the standard dilution series.

2.2.4 Arginase assay

Macrophages were cultured for 18 h in Complete-Medium alone, co-incubated with stat-phase *L. major* promastigotes or with 1 - 3 days old *L. major* axenic amastigotes at a MOI of 1:10. Cells were washed with 10 ml PBS at 1024 x g for 8 min and the pellet was lysed in 100 μl 0.1 % Triton X-100 for 30 min at RT while stirring. 100 μl 25 mM Tris-HCl and 20 μl 10 mM $MnCl_2$ were added to the lysate and the enzyme was activated by incubation for 10 min at 56°C. Subsequently 100 μl 0.5 M L-arginine was added to the whole mixture and incubated for 90 min at 37°C. For a standard curve a dilution series

of a urea protein standard was prepared. 400 μl acid mixture (H_2SO_4/ H_3PO_4/ H_2O (1/3/7)) and 25 μl 9 % α-isonitrosopropiophenone were added to the protein standard and incubated for 30 min at 95°C. The enzyme reaction in the samples was stopped by adding 800 μl acid mixture and 40 μl 9 % α-isonitrosopropiophenone and incubating for 30 min at 95°C. 200 μl of both samples and protein standard were applied to a 96-well plate and the optical density was determined with a Tecan infinite M200, wavelength set to 540 nm after 10 min in the dark. The arginase activity in each well was calculated using the standard curve generated with the optical densities of the standard dilution series.

2.2.5 Molecular biology methods

2.2.5.1 Transfection of primary cells with siRNA

Human MF were generated from buffycoats of healthy donors by AutoMACS separation using a CD14 MicroBeads-isolation kit. For transfection the MF were washed with 1 ml RPMI-Medium without supplements and 1 ml RPMI-Medium without supplements was added per well. For each well: 4 μl of 20 μM siRNA (80 pmole) was mixed with 20 μl of Stemfect Buffer and 4.6 μl of Stemfect Reagent was mixed with 20 μl Stemfect Buffer. Both compounds were mixed together within 5 min and incubated for 20 min at room temperature. Subsequently the whole mixture was added to the MF and incubated for 7 h at 37°C. After incubation the transfection mixture was removed from the cells, 2.5 ml Complete-Medium was added per well and incubated for 2 days at 37°C. After 2 days of siRNA transfection, MF were harvested and proceeded with further experiments.

2.2.5.2 DNA isolation

Genomic DNA was isolated using the DNeasy Blood and Tissue Kit according to the manufacturer's instructions. Briefly, 1 x 10^8 stationary phase *L. major* (MHOM/IL/81/ FEBNI), *L. tropica* (MHOM/SU/74/K27) and *L. donovani* (MHOM/IN/80/DD8) promastigotes were washed in cold PBS and resuspended in 200 μl PBS. 20 μl proteinase K and 200 μl Buffer AL were added and the cells were lysed for 10 min at 56°C. 200

μl ethanol was added to the lysate, vortexed, transfered to a DNeasy Mini spin column and centrifuged at 6000 x g for 1 min. The flow-through was discarded and the column washed with 500 μl Buffer AW1 by centrifugation at 6000 x g for 1 min. Another washing step was performed with 500 μl Buffer AW2 by centrifugation at 18000 x g for 3 min and the column was dried by centrifugation in a fresh collection tube at 18000 x g for 1 min. Subsequently the spin column was placed in a fresh 1.5 ml reaction tube, 200 μl Buffer AE was added to the column, incubated fot 1 min and centrifuged at 6000 x g for 1 min. The isolated DNA was stored at -20°C.

2.2.5.3 Amplification of the ribosomal internal transcribed spacer 1 (ITS1)

The ITS1 of the different *Leishmania spp.* was amplified in a PCR with specific oligonucleotides, which are listed in section 2.1.9 on page 34. For one reaction:

Volume [μl]	Reagent
19	Nuclease-free H_2O
2	Primer fwd (10 μM)
2	Primer rev (10 μM)
25	Phusion High Fidelity DNA Polymerase
48 μl	
+ 150 ng DNA	

Tubes were centrifuged at 800 x g, placed into a PCR cycler and the following program started.

	Temp [°C]	Time
Denaturation	98	30 sec
Amplification (45 cycles)		
Denaturation	98	30 sec
Annealing	53	30 sec
Elongation	72	20 sec
Elongation	72	10 min
Cooling	4	∞

The products were subjected to electrophoresis on a 0.7 % agarose gel and visualized under ultraviolet light.

2.2.5.4 Restriction digest

The PCR products of the different *Leishmania spp.* were incubated with 10 U HaeIII for restriction digest according to the manufacturer's instructions at 37°C for 1 h. The restriction fragments were subjected to electrophoresis on a 0.7 % agarose gel and visualized under ultraviolet light.

2.2.5.5 RNA isolation

RNA was isolated using the RNeasy Plus Mini Kit according to the manufacturer's instructions. Briefly, either 1 x 10^8 *L. major* parasites or 1 x 10^6 MF were washed with cold PBS and the pellet lysed in 350 μl RLT Buffer by pipetting. The lysate was transfered to a gDNA Eliminator spin column and centrifuged at 18000 g for 30 sec. 350 μl 70 % ethanol was added to the flow-through, transfered to a RNeasy spin column and centrifuged at 13000 rpm for 30 sec. The flow-through was discarded and the column was washed with 700 μl RW1 Buffer at 18000 g for 30 sec. The washing

was repeated twice with 500 μl RPE Buffer and the column was dried by centrifugation in a fresh collection tube at 20000 g for 1 min. Subsequently the spin column was placed in a fresh 1.5 ml reaction tube, 40 μl RNase-free water was added to the column and centrifuged at 18000 g for 1 min. The isolated RNA was treated with DNase I to eliminate remaining genomic DNA and stored at -80°C.

DNase digestion
Up to 10 μg RNA was incubated with 1 μl recombinant DNase I (10 U/μl) and 1 μl RNaseOUT™ recombinant RNase Inhibitor (40 U/μl) for 20 min at 37°C. Enzymes were subsequently inactivated for 10 min at 75°C. The DNase digestion was performed twice to ensure the elimination of remaining genomic DNA.

2.2.5.6 Test-PCR

A Test-PCR was performed to check the isolated RNA for genomic DNA contamination. The specific primer for Test-PCR were GAPDH for human MF and 45rRNA for *L. major* parasites, which are listed in section 2.1.9 on page 34. For one reaction:

Volume [μl]	Reagent
19	Nuclease-free H_2O
2	Primer fwd (10 μM)
2	Primer rev (10 μM)
25	FideliTaq PCR Master Mix
48 μl	
+ 150 ng RNA	

Tubes were centrifuged at 800 x g, placed into a PCR cycler and the following program started.

	Temp [°C]	Time
Denaturation	98	30 sec
Amplification (30 cycles)		
Denaturation	98	30 sec
Annealing	60	30 sec
Elongation	72	30 sec
Elongation	72	10 min
Cooling	4	∞

The products were subjected to electrophoresis on a 0.7 % agarose gel and visualized under ultraviolet light. Only the positive control with cDNA as template should show a product. Otherwise the RNA ist contaminated with genomic DNA. Then an additional DNase I digestion step is required.

2.2.5.7 cDNA synthesis

For cDNA synthesis the ImProm-II Reverse Transcription System™ was used according to the manufacturer's instructions. For one reaction:

Volume [μl]	Reagent
1	ImProm-II™ Random Primer Mix
100 - 150 ng	Template RNA
ad 5 μl	Nuclease-free H_2O
5 μl	

The primer/template RNA mix is thermally denatured for 5 min at 70°C and subsequently chilled on ice. A reverse transcription reaction mix was assembled on ice and

added to the mixture. For one reaction:

Volume [μl]	Reagent
6.5	Nuclease-free H_2O
4	ImProm-II™ 5X Reaction Buffer
2	$MgCl_2$
1	dNTP Mix
0.5	Recombinant RNasin® Ribonuclease Inhibitor
1	ImProm-II™ Reverse Transcriptase
15 μl	

Tubes were centrifuged at 800 x g, placed into a PCR cycler and the following program started.

	Temp [°C]	Time
Annealing	25	5 min
cDNA synthesis	42	60 min
Inactivation	70	15 min
Cooling	4	∞

2.2.5.8 Quantitative real-time PCR

For quantitative real-time PCR the LightCycler® FastStart DNA Master^{PLUS} SYBR Green I kit was used according to the manufacturer's instructions. The specific primer for real-time PCR are listed in section 2.1.9 on page 34. For one reaction:

Volume [μl]	Reagent
11	Nuclease-free H_2O
2	Primer Mix (10 μM)
4	LightCycler® FastStart Master Mix
17 μl in capillary	
+ 3 μl	Template cDNA

Capillaries were centrifuged at 3000 rpm for 3 min, placed into a LightCycler and the following program started.

	Temp [°C]	Time	Δ°C/sec
Taq Activation	95	10 min	20
Amplification (45 cycles)			
Denaturation	95	10 sec	20
Annealing	60	10 sec	20
Elongation	72	6 sec	20
Melting of primer dimers	80	5 sec	20
Melting curve	60 - 95	-	0.1
Cooling	20	∞	20

A melting curve analysis was performed to ensure the amplificated product to be specific.

2.2.6 Transmission electron microscopy (EM)

Macrophages were adhered on carbon-coated sapphire discs (3 mm in diameter) in 6-well cell culture plates and infected with stat-phase L. major promastigotes or 1 - 3 days old L. major amastigotes with a MOI of 1:10. After co-incubation for 18 h extracellular parasites were removed by washing the cells with Wash-Buffer and cells were frozen from the living state by high-pressure freezing with an HPF 01 appatus. Samples were freeze substituted in acetone containing 0.1 % (w/v) uranyl acetate, 0.2 % (w/v) osmium tetroxide and 5 % (v/v) water and embedded in epon (as previously described by [205, 32]). Ultrathin sections were prepared on copper grids for transmission electron microscopy. The samples were imaged with the Zeiss EM10 transmission electron microscope at an acceleration voltage of 80 kV.

2.2.7 Westernblot analysis

2.2.7.1 Sample preparation

1 x 10^8 *L. major* parasites or 1 x 10^6 MF were lysed in 100 μl 1 x Lämmli-Buffer by heating at 95°C for 10 min and centrifuged at 12900 x g for 3 min.

2.2.7.2 SDS-PAGE

15 % or 12 % SDS-polyacrylamide gels were prepared according to a standard protocol, see section 2.1.3 on page 28. Either 25 μg/50 μg of total protein or a total number of 0.5 x 10^6 MF were diluted in 1 x Lämmli-Buffer and loaded onto the gel. The electrophoresis was performed with constant 12 Watt for protein passage through the stacking gel and with constant 24 Watt for the separation gel.
The separated proteins were blotted onto a Transfer membrane (PVDF) at 139 mA constant voltage for 2 h. To ensure an equal loading of protein, the gel was stained after blotting with Coommassie staining solution and dried using a gel dryer.

2.2.7.3 Band detection

The membrane was blocked with WB-Block-Solution for 2 h at room temperature or over nigth at 4°C, washed with WB-Wash-Buffer and subsequently exposed to a primary antibody for 2 h at room temperature or over nigth at 4°C by gentle agitation on a shake table. After extensive washing with WB-Wash-Buffer the membrane was incubated with a HRP-conjugated secondary antibody for 1 h at room temperature on a shake table. The menbrane was washed once more and the protein bands were detected using an ECL substrate, high performance ECL films and a processor.

2.2.7.4 Coomassie staining

After electrophoresis gel was incubated in 200 ml Coomassie Gel-fixing solution at room temperature for 1 h, transfered into 200 ml Coomassie staining solution for 2 - 15 h while shaking and destained in 100 ml Coomassie Gel-washing solution for 5 - 15 min while shaking. The stained gel was scanned for further analysis.

2.2.8 Statistical analysis

Data are depicted as mean value ± SEM or standard deviation. To determine whether differences were statistically significant the results were analyzed with student's t test by using a two-tailed distribution and Microsoft Excel 2010 software. * indicates statistically different at $p < 0.05$ and ** at $p < 0.005$.

3 Results

Part 1

3.1 Confirmation of the *L. major* species

This study focused on the *Leishmania* parasite species *L. major*. To ensure the identity of the used *Leishmania* species, a taxonomy analysis was performed. Schönian and colleagues showed the restriction fragment length polymorphism (RFLP) analysis of the internal transcribed spacer 1 (ITS1) marker to be the appropriate method to distinguish between different *Leishmania* species [172]. Therefore the amplicons of ITS1 of the used *Leishmania* strain were digested with the restriction enzyme *HaeIII* and compared with two other *Leishmania* species. In concordance with the literature we found that the different *Leishmania* species showed distinct differential fragment patterns. The obtained fragments varied in size and numbers. We detected two bands of 220 and 140 bp for *Leishmania major* (*Lm*), two fragments of 200 and 45 bp for *Leishmania tropica* (*Lt*) and three bands of 200, 65 and 40 bp for *Leishmania donovani* (fig. 6). In conformity with Schönian et al. these fragment patterns are species specific and can be used to identify the different *Leishmania* species.

3.2 Characterisation of *L. major* FEBNI parasites

The lifecycle of *Leishmania* includes two different life stages of the parasite: the disease inducing promastigote form, which replicates in the insect vector and the disease propagating obligate intracellular amastigote form, which multiplies in a mammalian host.

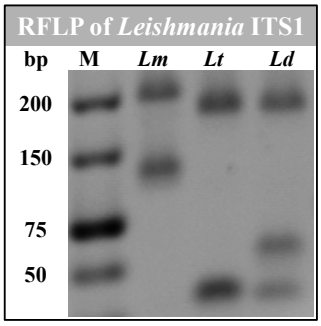

Figure 6: RFLP analysis of the *Leishmania spp.* ITS1 marker: Genomic DNA isolated from log-phase promastigotes of 3 different *Leishmania* species was amplified with ITS1 specific oligonucleotides. Products were digested with the restriction enzyme *HaeIII* and displayed by gel electrophoresis. *L. major* MHOM/IL/81/FEBNI (*Lm*) in lane 2, *L. tropica* MHOM/SU/74/K27 (*Lt*) in lane 3 and *L. donovani* MHOM/IN/80/DD8 (*Ld*) in lane 4 were analyzed and a representative restriction pattern is depicted. A 100 bp DNA ladder was used as molecular size marker (M) in lane 1.

Molecular biology methods, flow cytometry and different microscopic techniques were used to characterize both parasite forms, studying the morphology, the expression of distinct surface markers and mRNA expression levels.

3.2.1 Morphological characteristics of *L. major* promastigotes

In vitro cultured logarithmic-phase (log-phase) promastigotes were analyzed microscopically (fig. 7). Light microscopy of Diff QUIK stained log-phase promastigotes (fig. 7 A) and phase contrast microscopy (fig. 7 B) showed an elongated body with a length of 10 - 15 μm, a diameter of 1 - 2 μm and one apical flagellum (F). Transmission electron microscopy (EM) revealed that the flagellum is anchored within the flagellum pocket (FP) (fig. 7 C). In addition, the nucleus (N) and the characteristic kinetoplast (KP) are visible in EM and Diff QUIK stained micrographs (fig. 7 A + C).

The virulent inoculum of *L. major* consists of viable and apoptotic promastigotes [198] as represented by in vitro cultured stationary-phase (stat-phase) parasites (fig. 8). About 50 % of the cells are apoptotic and show different morphological features like cell shrinkage and rounding of the cell body (fig. 8 A, black arrow 2). Another characteristic

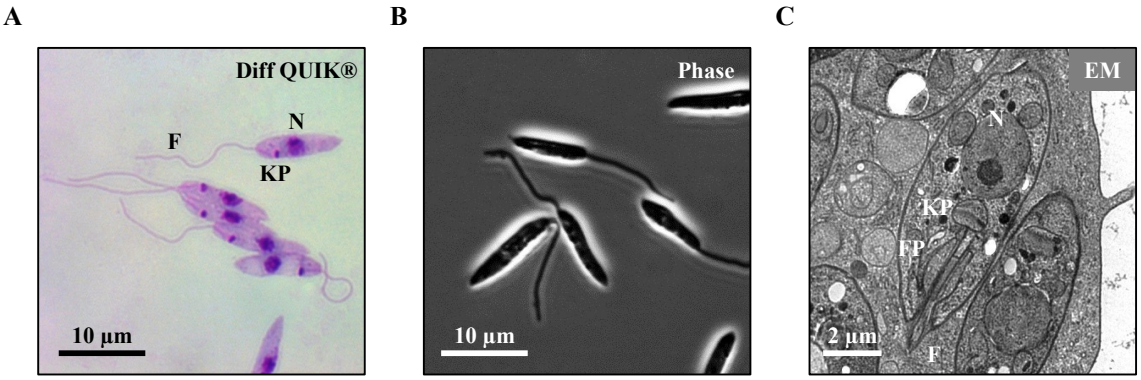

Figure 7: Morphology of log-phase *L. major* FEBNI promastigotes: Representative micrographs of 3 independent experiments. A) Micrograph of fixed and Diff QUIK®stained log-phase *L. major* promastigotes. B) Phase contrast micrograph of unstained log-phase *L. major* promastigotes. C) Transmission Electron micrograph (EM) of a longitudinal parasite section of *L. major* promastigotes inside a MF after 3 h of co-incubation. The Nucleus (N), kinetoplast (KP), flagellum (F) and the flagellum pocket (FP) are indicated. Bars indicating 2 or 10 μm.

of apoptotic stat-phase promastigotes is the externalization of phosphatidylserine (PS). PS was detected using the PS binding protein Annexin-A5 (AnxA5) Fluos as indicated by the green staining of the round shaped parasite (fig. 8 B, white arrow 2).

3.2.2 Morphological characteristics of *L. major* amastigotes

In vitro cultured axenic amastigotes were generated as described by Wenzel et al. [212] and analyzed microscopically (fig. 9). In contrast to promastigotes, amastigotes have a smaller elliptic shaped body with a length of 2 - 3 μm, a diameter of 2 μm and they have no extracellular flagellum (fig. 9 A + B). Using electron microscopy we were able to visualize the nucleus, the kinetoplast and the flagellum pocket with the remains of a flagellum inside (fig. 9 C). Furthermore, micrographs of Diff QUIK stained amastigotes showed dividing amastigotes in the axenic *in vitro* culture (fig. 9 A).

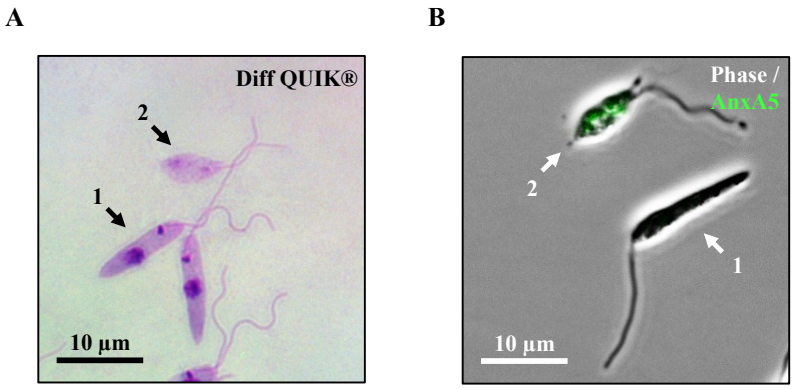

Figure 8: Morphology of stat-phase *L. major* FEBNI promastigotes: Representative micrographs of 3 independent experiments. A) Micrograph of fixed and Diff QUIK®stained stat-phase *L. major* promastigotes, displaying two viable parasites (black arrow 1) and an apoptotic one (black arrow 2). B) Fluorescent micrograph of Annexin A5-Fluos (green) stained stat-phase *L. major* promastigotes analyzed by fluorescent microscopy, displaying a viable parasite (white arrow 1) and an apoptotic one (white arrow 2). Bars indicating 10 μm.

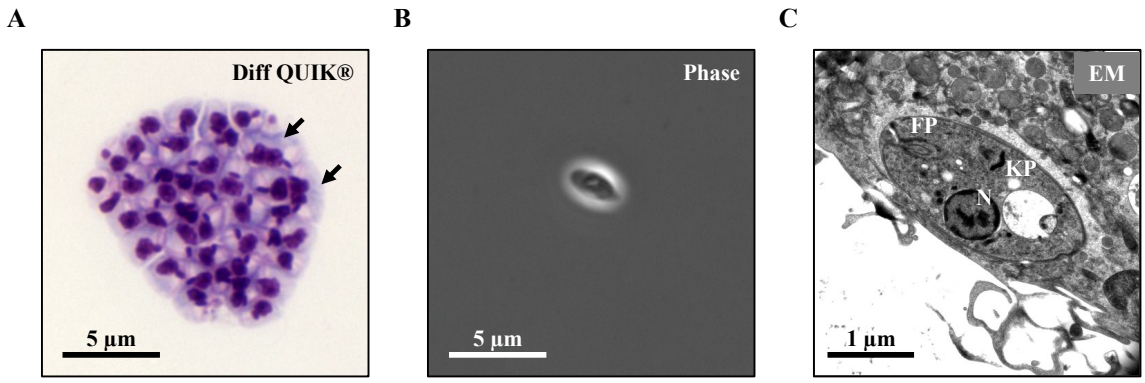

Figure 9: Morphology of *L. major* FEBNI amastigotes: Representative micrographs of 3 independent experiments. A) Micrograph of Diff QUIK®stained *L. major* axenic amastigotes, displaying viable dividing parasites (black arrows). B) Phase contrast micrograph of an unstained *L. major* amastigote. C) Transmission Electron micrograph of a longitudinal parasite section of a *L. major* amastigote inside a MF after 3 h of co-incubation. The Nucleus (N), kinetoplast (KP) and the flagellum pocket (FP) are indicated. Bars indicating 1 or 5 μm.

3.2.3 Annexin binding

As mentioned above the virulent inoculum of *L. major* consists of viable and apoptotic promastigotes [198]. Therefore log-phase and stat-phase promastigotes as well as axenic amastigotes were additionally analyzed for their PS expression by flow cytometry (FACS) (fig. 10 A + B). Stat-phase promastigotes were found to consist of 59.8 % ± 1.4 PS positive parasites, whereas for log-phase promastigotes 13 % ± 4.4 were found to be PS positive (fig. 10 B). Furthermore, axenic amastigote showed only 11.2 % ± 1.2 PS positive parasites (fig. 10 B).

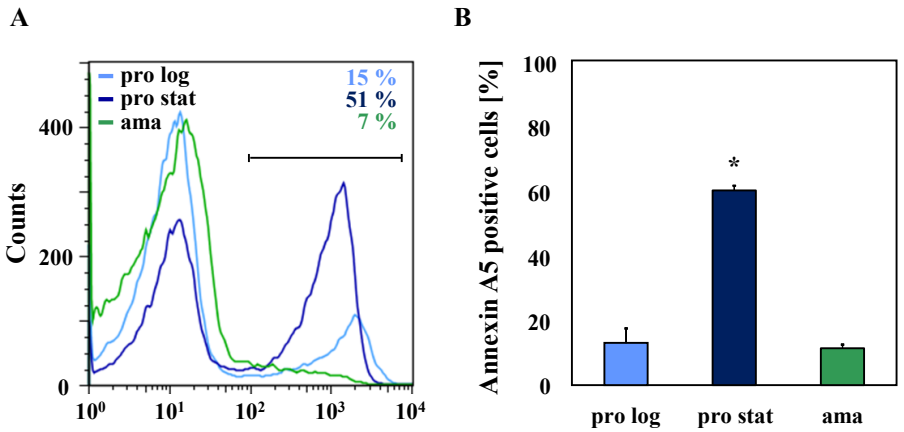

Figure 10: Annexin A5 staining of the different stages of *L. major* parasites: Log-phase promastigotes, stat-phase promastigotes and axenic amastigotes were stained for phosphatidylserine exposure with Annexin A5 (AnxA5)-Flous and analyzed by flow cytometry (FACS). A) Representative FACS histogram of one experiment out of 6 independent experiments. Log-phase promastigotes (light blue), stat-phase promastigotes (blue) and axenic amastigotes (green) with the percentages of AnxA5 positive parasites inside the indicated gate. B) Phosphatidylserine exposure on the cell surface of the different parasite stages. Depicted are percentages of AnxA5 positive cells. Data are shown as means ± SEM, n = 6. ∗ P-value < 0.05.

3.2.4 Stage-specific gene expression levels

Several studies revealed that only 0.2 % to 5 % of the total genes are differentially regulated between the different *L. major* life stages [36, 106]. To characterize the different *Leishmania* life stages in more detail, the expression of these stage-specific genes was an-

alyzed (fig. 11 + 12). The small hydrophilic endoplasmic reticulum-associated protein (SHERP, LmjF23.1050) has been described previously to be specifically up-regulated in the infective non-replicative metacyclic parasite stage [86]. On the other hand the putative ABC transporter homologue (ABC, LmjF11.0040) was shown to be a marker for the amastigote form [36, 98]. The gene expression was assessed by RT-PCR analysis and normalized to the endogenous reference gene rRNA45 (LmjF32.3420) [139]. Comparing metacyclic promastigotes with axenic and macrophage-derived amastigotes, we found that the promastigote-specific gene SHERP showed a 5-fold lower expression in axenic and macrophage-derived amastigotes as compared to metacyclic promastigotes (fig. 11 A). Furthermore, the ABC transporter was expressed 2-fold higher in both axenic and macrophage-derived amastigotes as compared to the metacyclic promastigotes (fig. 11 B). In addition, we found similar expression patterns for both the axenic cultured amastigotes as well as the macrophage-derived amastigotes for these markers (fig. 11 A + B).

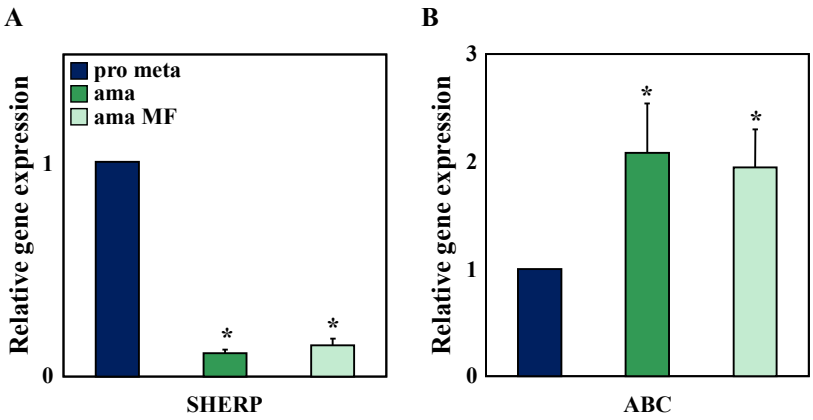

Figure 11: Stage-specific mRNA expression of SHERP and ABC-transporter homologue in *L. major*: Total RNA was isolated, cDNA generated and relative gene expression of *L. major* metacyclic promastigotes (pro meta; blue bars), axenic amastigotes (ama; green bars), and amastigotes isolated from infected MF (ama MF; light green bars) was determined by LightCycler analysis. Depicted are fold mRNA change compared to *L. major* metacyclic promastigotes. A) Promastigote-specific SHERP mRNA expression. B) Amastigote-specific ABC-transporter homologue mRNA expression. Data are shown as means ± SEM, n = 5. ∗ P-value < 0.05 vs. metacyclic promastigotes.

Moreover, we analyzed four additional genes by RT-PCR: The quinonoid-dihydropteridine reductase (QDPR, LmjF34.4390), alpha-tubulin (LmjF13.0390), the cysteine protease b

(Cpb, LmjF08.1040) and the major surface glycoprotein (GP63; LmjF10.0470) as shown in fig. 12 [105, 98, 129, 116]. For QDPR we found a significantly higher expression in axenic amastigotes compared to stat-phase promastigotes, whereas alpha-tubulin was significantly down-regulated in amastigotes (fig. 12 A). Furthermore, Cpb and GP63 were both significantly higher expressed in the amastigote stage compared to stat-phase and log-phase promastigotes (fig. 12 B). These data demonstrate that the different life stages of *L. major* show a stage-specific gene expression.

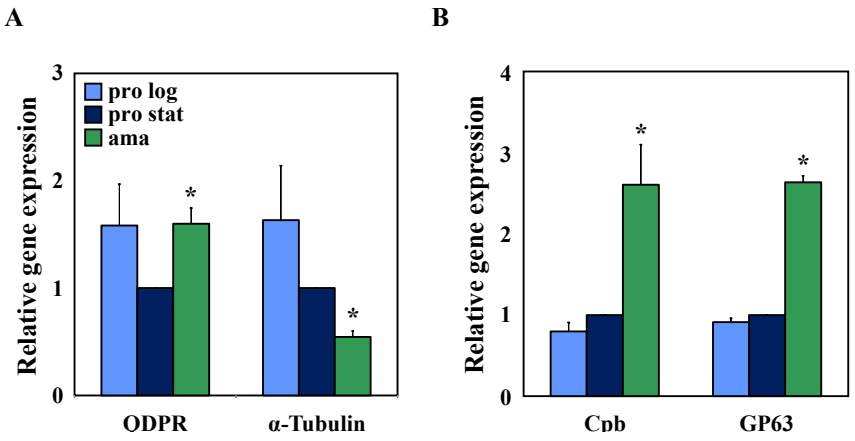

Figure 12: Stage-specific mRNA expression of QDPR, alpha-tubulin, Cpb and GP63 in *L. major*: Total RNA was isolated, cDNA generated and relative gene expression of log-phase *L. major* promastigotes (pro log; light blue bars), stat-phase promastigotes (pro stat; blue bars) and axenic amastigotes (ama; green bars) was determined by LightCycler analysis. Depicted are fold mRNA change compared to stat-phase *L. major* promastigotes. A) Gene expression of QDPR and alpha-tubulin. B) Gene expression of Cpb and GP63. Data are shown as means ± SEM, n = 3. ∗ P-value < 0.05 vs. stat-phase promastigotes.

3.2.5 The surface marker lipophosphoglycan (LPG)

The most abundant surface macromolecule on the promastigote stage of *Leishmania* parasites is the polymorphic lipophosphoglycan (LPG). Glaser et al. demonstrated that this promastigote-specific LPG is nearly absent on the amastigote life stage [63]. The expression of promastigote-specific LPG was analyzed on the parasite surface of the different life stages by FACS analysis (fig. 13) and by western blot (fig. 14). LPG was detected with the murine WIC79.3 antibody (Ab) and visualized with Alexa

488-labeled anti-mouse Ab using FACS analysis. In concordance with the literature, log-phase promastigotes and axenic amastigotes were found to express a significant lower level of LPG as compared to stat-phase promastigotes (fig. 13 B). These results were confirmed by western blot analysis (fig. 14 A). Parasite lysates were separated by SDS-PAGE and LPG was detected by the murine WIC79.3 Ab. The band intensity was normalized with the whole protein amount gained by coomassie staining (fig. 14 B).

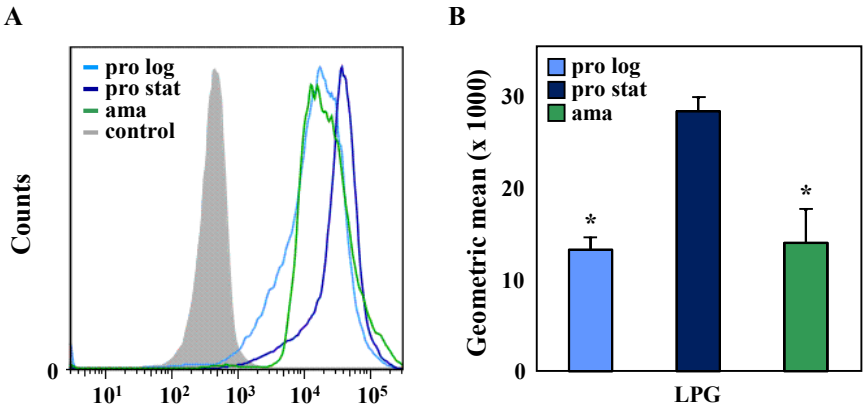

Figure 13: Stage-specific protein expression of LPG on the cell surface of *L. major*: Log-phase promastigotes, stat-phase promastigotes and axenic amastigotes were stained for lipophosphoglycan (LPG) expression with mouse anti-LPG WIC79.3 (1:3000), detected with Alexa 488-labeled chicken anti-mouse Ab (2 μg) and analyzed by flow cytometry (FACS) A) Representative FACS histogram of one experiment out of 3 independent experiments. Log-phase promastigotes (light blue), stat-phase promastigotes (blue) and axenic amastigotes (green) with the corresponding control (grey). B) LPG expression on the cell surface of the different parasite stages. Depicted are geometric means x 1000. Data are shown as means $\pm$ SEM, n = 3. $*$ P-value < 0.05 vs. stat-phase promastigotes.

3.2.6 Generation of axenic amastigotes in other *L. major* strains

To validate the method for amastigote generation described by Wenzel et al. [212], several other *L. major* strains were transformed into the amastigote stage. Using our standardized protocol we found that for the transfected *L. major* FEBNI eGFP strain the incubation time of the amastigote pre-culture in AAM was too long, resulting in many dead parasites in the culture. In contrast, for the *L. major* FEBNI DsRed strain the transformation into amastigotes was not fully completed after the pre-culture, which

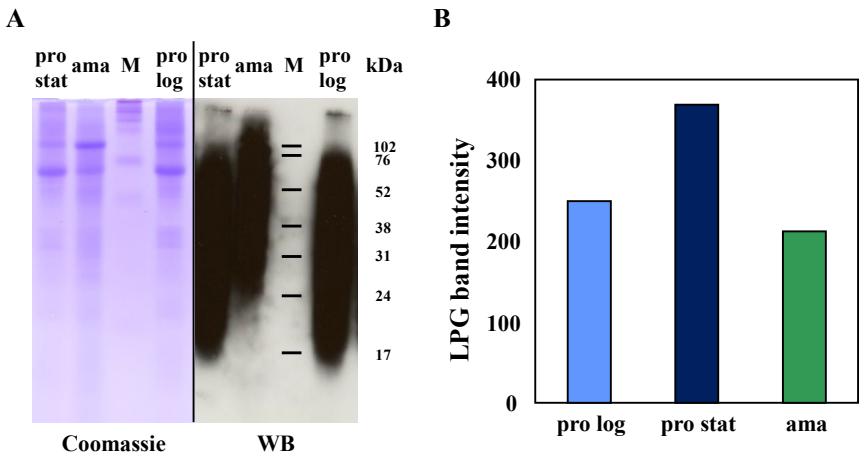

Figure 14: Stage-specific protein expression of LPG in *L. major*: Log-phase promastigotes (pro log), stat-phase promastigotes (pro stat) and axenic amastigotes (ama) were lysed in 1x-Lämmli Buffer and subjected to SDS-PAGE. LPG was detected with mouse anti-LPG WIC79.3 (1:1000) and Anti-mouse HRP (1:1000). Gel was stained with Coomassie blue. A) Coomassie staining and LPG western blot of the different parasite stages. A full range rainbow marker was used as molecular size marker (M). B) LPG band intensity of the different parasite stages after normalization with the whole protein amount. Log-phase promastigotes (light blue), stat-phase promastigotes (blue) and axenic amastigotes (green), n = 1.

led to a high contamination with promastigotes. Therefore small modifications in the transformation procedure had to be assessed. We defined a pre-culture of amastigotes to be completely transformed and viable, when the developed amastigotes started dividing. Focusing on this characteristic feature, different time points were tested for the amastigote pre-culture to achieve a complete transformation resulting in diving amastigotes. We could successfully convert the genetically modified fluorescent strains *L. major* FEBNI eGFP and DsRed into amastigotes by adjusting the incubation time (data not shown). For the transgenic *L. major* FEBNI eGFP strain the incubation time was shorted to 7 - 10 days of amastigote pre-culture at 33°C. Whereas in case of the transgenic *L. major* FEBNI DsRed strain 12 - 14 days of amastigote pre-culture at 33°C were required to get dividing amastigotes.

In addition to *L. major* FEBNI, we wanted also to transform the well characterized *L. major* strain MHOM/IL/80/Friedlin. This was the first *Leishmania* strain whose genome was completely sequenced [125, 76]. To find the adequate conditions for the amastigote transformation of the Friedlin strain, different parameters like the incubation

time, temperature, the pH value of the AAM and the density of the cultured parasites were tested (tab. 2). As already mentioned, the cell division of the cultured amastigotes was a characteristic feature of a complete transformation as well as the viability of the amastigote culture. For the transformation of *L. major* Friedlin, an elevated temperature to 35°C combined with a shorter incubation time for the amastigote pre-culture to 5 - 8 days turned out to be the most effective conditions.

Incubation temp	**33°C**	**35°C**	**37°C**
20 Mio/ml parasite density	+-	++	-
50 Mio/ml parasite density	+-	++	ND
5.3 pH value	-	+	ND
5.5 pH value	+-	+++	-
5.7 pH value	-	+	ND
5 days incubation time	+-	+++	-
9 days incubation time	-	+++	-
10 days incubation time	-	+	-
12 days incubation time	-	-	-

Table 2: Different conditions for the generation of axenic *L. major* Friedlin amastigotes: Different tested conditions for amastigote generation of *L. major* Friedlin and the appropriate results. - parasite death, +- no trasformation, + transformation, ++ transformation and few dividing cells, +++ transformation and many dividing cells, ND = no data

Several different developmental steps of the amastigote transformation were compared between the *L. major* FEBNI (fig. 15 A - C) and Friedlin (fig. 15 D - F) strains, to ensure an equivalent and complete amastigote transformation. Therefore parasites were fixed and Diff QUIK stained during promastigote pre-culture, the amastigote pre-culture and after the isolation of pure amastigotes by a density gradient. Fig. 15 D - F illustrates the corresponding transformation steps in both strains from procyclic promastigotes (fig. 15 A + D) over the amastigote pre-culture, containing promastigotes (fig. 15 B + E, arrow 1 + 4) as well as amastigotes (fig. 15 B + E, arrow 2 + 5), to the pure amastigote culture with dividing amastigotes after isolation via histopaque density gradient (fig. 15 C + F, arrow 3 + 6).

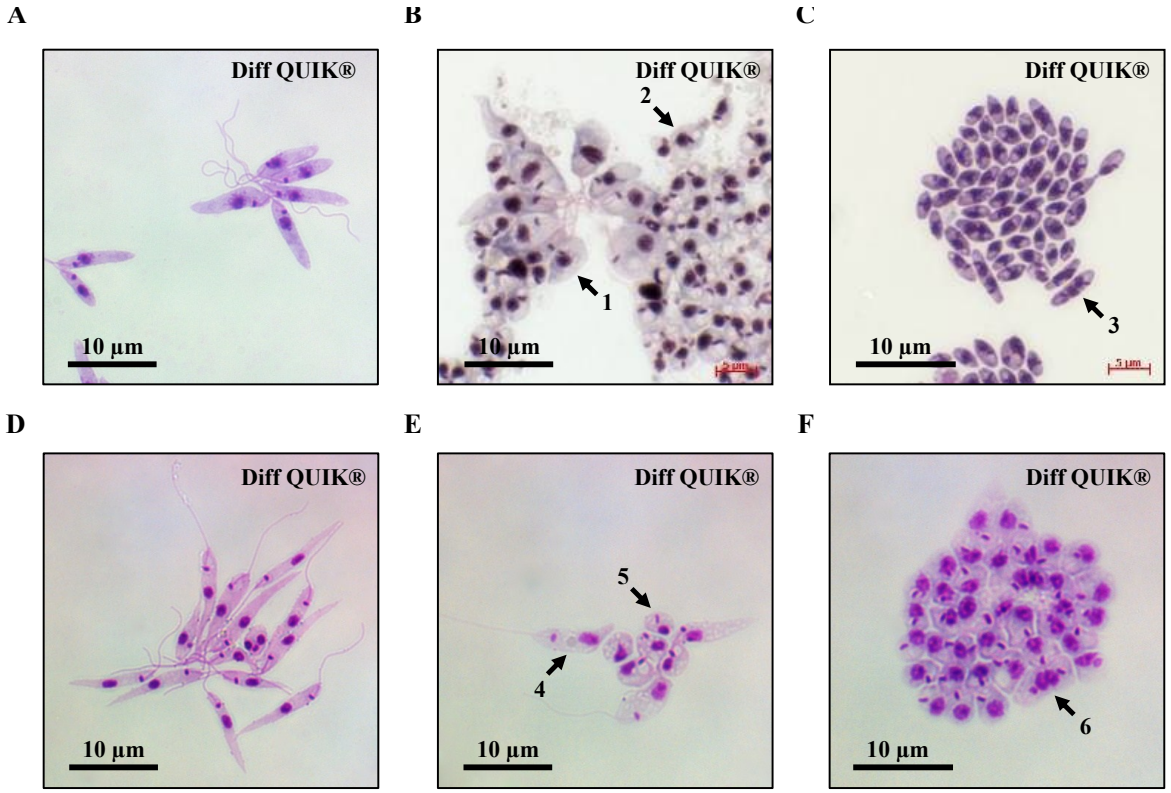

Figure 15: Generation of *L. major* Friedlin axenic amastigotes: *L. major* FEBNI (A-C) and Friedlin (D-F) promastigotes were cultured in Liquid Medium (27°C) for promastigote pre-culture, transferred into AAM (33°C / 35°C) for transformation into the amastigote stage and purified by histopaque density gradient as described. Representative micrographs of fixed and Diff QUIK®stained *L. major* parasites of 3 independent experiments. A) Micrograph of log-phase *L. major* FEBNI parasites during the promastigote pre-culture. B) Micrograph of *L. major* parasites after amastigote pre-culture, displaying a mixture of promastigotes (arrow 1) and amastigotes (arrow 2). C) Micrograph of Diff QUIK®stained *L. major* parasites after amastigote purification from the 80 % layer, displaying viable dividing amastigotes (arrow 3). D) Micrograph of log-phase *L. major* Friedlin parasites during the promastigote pre-culture. E) Micrograph of *L. major* parasites after amastigote pre-culture, displaying a mixture of promastigotes (arrow 4) and amastigotes (arrow 5). F) Micrograph of Diff QUIK®stained *L. major* parasites after amastigote purification from the 80 % layer, displaying viable dividing amastigotes (arrow 6). Bars indicating 10 μm.

3.3 Detection of Apoptotic characteristics in *L. major* parasites

In multicellular organisms, apoptosis is a tightly regulated pathway of the cell to die. An early sign is the externalization of PS from the inner to the outer leaflet of the cell membrane [110]. Another early marker which is connected to apoptosis is the intracellular formation of reactive oxygen species (ROS) [160, 176]. To investigate the presence of extracellular expression of PS and intracellular expression of ROS in *L. major* parasites after apoptosis induction we used flow cytometry.

3.3.1 Apoptosis mechanisms in promastigotes

L. major promastigotes were treated with three different drugs to induce apoptosis: Staurosporine which triggers the mitochondrial pathway, the anti-leishmanial drug miltefosine which affects the parasite membrane and camptothecin, a nucleus dependent apoptosis inducer. After the treatment the parasites were analyzed for PS exposure with the PS recognizing protein AnxA5, labeled with Alexa 647 and ROS was detected with 5-(and-6)-chloromethyl-2',7'-dichlorodihydrofluorescein diacetate (H_2DCFDA). We found a significant higher PS expression of 72.7 % $\pm$ 6.9 for the miltefosine treated promastigotes as compared to 28.3 % $\pm$ 2.6 positive parasites for the untreated promastigotes after 18 hours (fig. 18 A). However, 42 hours of treatment resulted in a significant higher level of PS positive promastigotes in both miltefosine (81.3 % $\pm$ 2) and staurosporine (61 % $\pm$ 8.9) treated parasites. Camptothecin had no effect on the PS externalization. Detecting the formation of ROS, we found significant higher percentages of ROS positive parasites only for staurosporine treated promastigotes compared to the low ROS level in the untreated parasites (fig. 18 B). 18 hours after treatment there was a maximum of 60 % $\pm$ 4.1 ROS positive parasites and then decreased to 39.7 % $\pm$ 10 ROS positivity after 42 hours. Moreover, these ROS positive parasites were detected to have a significant higher mean fluorescence intensity (MFI) for ROS after 18 hours (fig. 18 C). In contrast, miltefosine induced a non-significant increase in ROS over time (p-value = 0.078), whereas camptothecin showed no ROS induction.

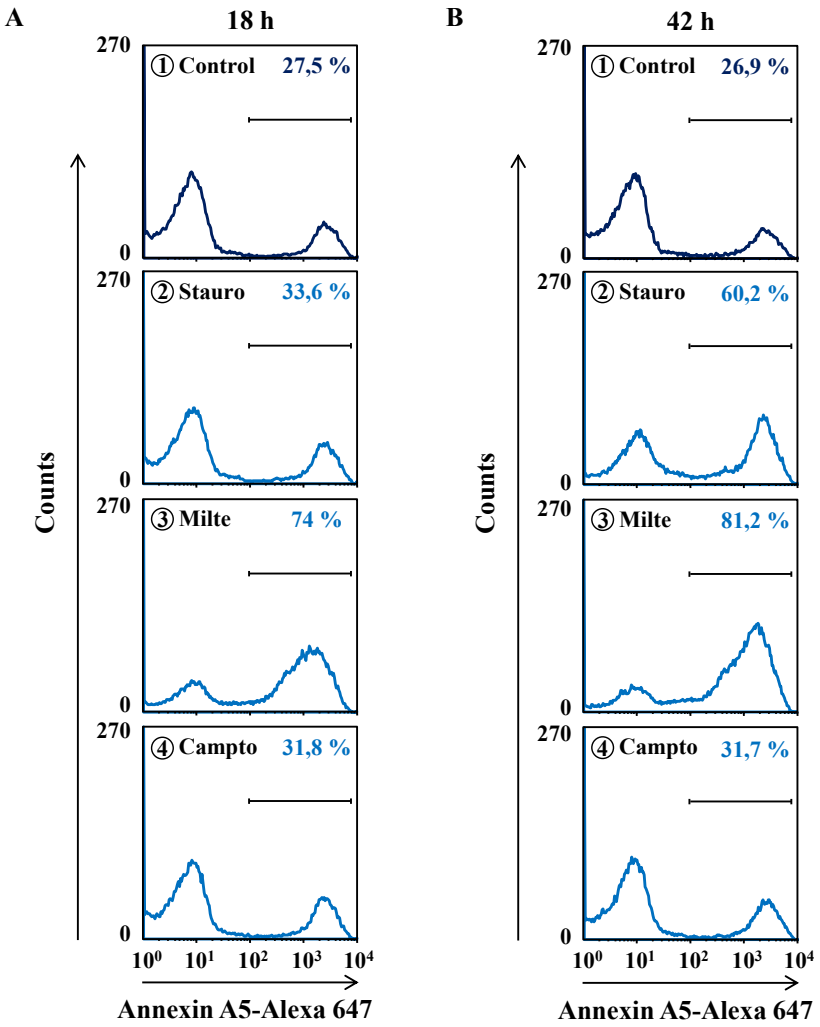

Figure 16: Phosphatidylserine externalisation after apoptosis induction in *L. major* FEBNI promastigotes: Log-phase promastigotes were incubated with 15 μM staurosporine (2), 25 μM miltefosine (3), 10 μM camptothecin (4) and medium (1) for 18 and 42 hours to induce apoptosis. Parasites were stained for phosphatidylserine (PS) exposure with Annexin A5-Alexa 647 and analyzed by flow cytometry (FACS). Representative histograms of 3 independent experiments. A) FACS histogram of PS exposure after apoptosis induction for 18 hours with the percentages of AnxA5 positive parasites inside the indicated gate. B) FACS histogram of PS exposure after apoptosis induction for 42 hours with the percentages of AnxA5 positive parasites inside the indicated gate.

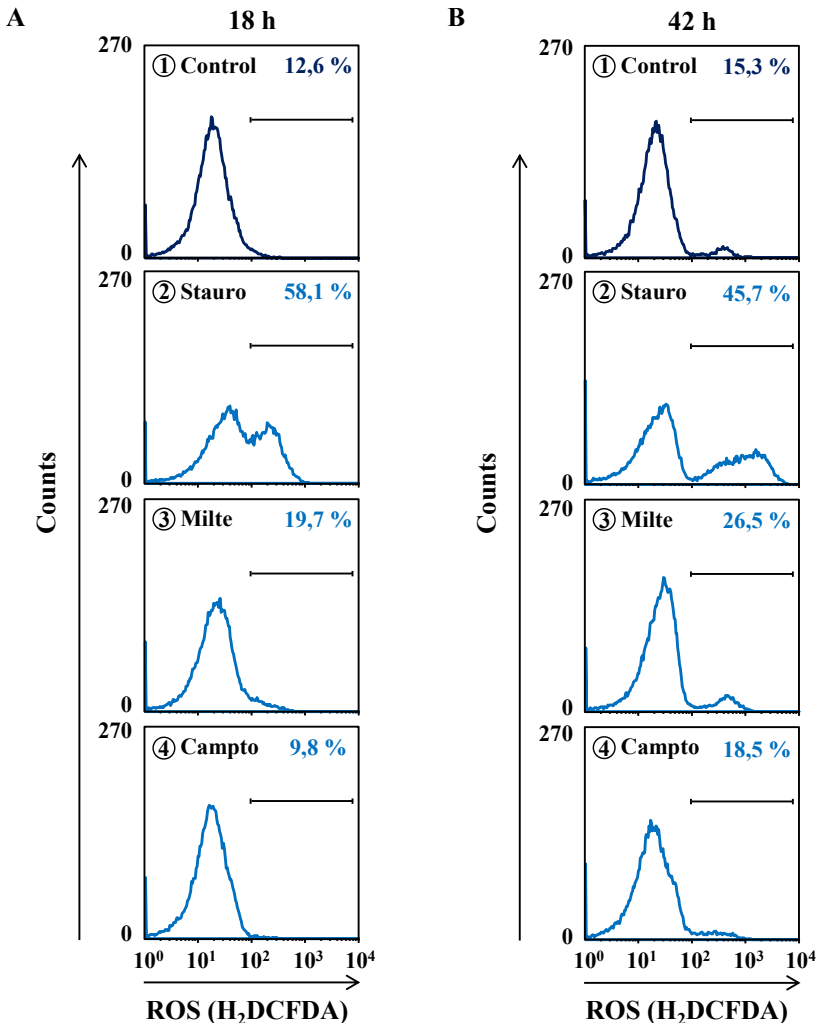

Figure 17: Formation of reactive oxygen species after apoptosis induction in *L. major* FEBNI promastigotes: Log-phase promastigotes were incubated with 15 μM staurosporine (2), 25 μM miltefosine (3), 10 μM camptothecin (4) and medium control (1) for 18 and 42 hours to induce apoptosis. Parasites were stained for reactive oxygen species (ROS) with 5-(and-6)-chloromethyl-2',7'-dichlorodihydrofluorescein diacetate (H_2DCFDA) and analyzed by flow cytometry (FACS). Representative histograms of 3 independent experiments. A) FACS histograms of ROS presence after apoptosis induction for 18 hours with the percentages of ROS positive parasites inside the indicated gate. B) FACS histograms of ROS presence after apoptosis induction for 42 hours with the percentages of ROS positive parasites inside the indicated gate.

3.3.2 Apoptosis mechanisms in amastigotes

Corresponding to the apoptosis induction in promastigotes, the amastigote life stage parasites were treated with the same drugs and concentrations: staurosporine, milte-

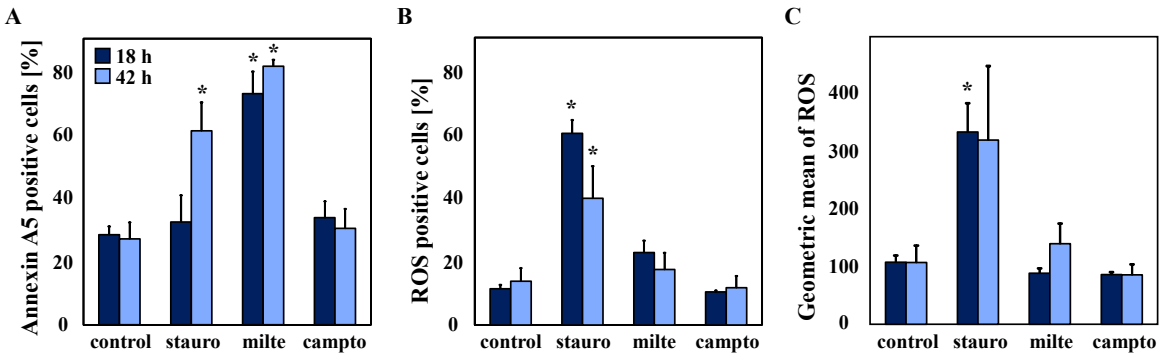

Figure 18: Modulation of markers after apoptosis induction in *L. major* FEBNI promastigotes: Log-phase promastigotes were incubated with 15 μM staurosporine (stauro), 25 μM miltefosine (milte), 10 μM camptothecin (campto) and medium control for 18 (dark blue bars) and 42 hours (sky blue bars) to induce apoptosis. Parasites were stained for phosphatidylserine (PS) exposure with Annexin A5-Alexa 647 and present reactive oxygen species (ROS) with 5-(and-6)-chloromethyl-2',7'-dichlorodihydrofluorescein diacetate (H_2DCFDA) and analyzed by flow cytometry (FACS). A) Depicted are the percentages of PS positive promastigotes after apoptosis induction for 18 and 42 hours. B) Depicted are the percentages of ROS positive promastigotes after apoptosis induction for 18 and 42 hours. C) Geometric mean of ROS positive promastigotes after apoptosis induction for 18 and 42 hours. Data are shown as means $\pm$ SEM, n = 3. $*$ P-value < 0.05.

fosine and camptothecin. PS exposure was analyzed with AnxA5 labeled with Alexa 647 and ROS formation was detected with H2DCFDA (fig. 19). Combined data from three independent experiments showed a significant higher PS expression only for staurosporine treated parasites. After 18 hours we found 44 % $\pm$ 12.6 PS positive amastigotes and the even higher percentage of 62.3 % $\pm$ 6.3 after 42 hours of incubation as compared to untreated amastigotes with 13.7 % $\pm$ 2.4 positive parasites (fig. 19 A). The treatment with miltefosine resulted in a non-significant increase of PS positive parasites after 42 hours, whereas camptothecin had no effect on the PS externalization (fig. 19 A).

Detecting ROS formation in amastigotes, we found a high percentage of ROS positive parasites (82.3 % $\pm$ 2.4) in untreated amastigotes (fig. 19 B). After staurosporine incubation we obtained a decrease of ROS positive amastigotes. First we found a non-significant trend with 45.5 % $\pm$ 18.6 ROS positive amastigotes after 18 hours. However, after 42 hours of treatment became a significant down-regulation with 23.6 % $\pm$ 10.8 ROS positive amastigotes. In addition, these ROS positive parasites were detected to

have a significant lower MFI for ROS after 18 hours compared to untreated amastigotes (fig. 19 C). Interestingly, even though miltefosine treatment had no effect on the percentage of ROS positive amastigotes, these parasites had a significant higher MFI for ROS after 18 hours. The treatment with camptothecin showed no significant difference in ROS formation.

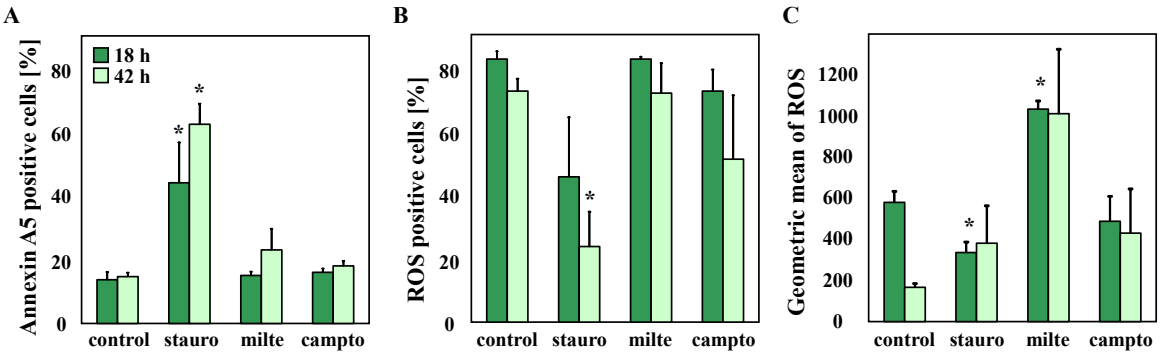

Figure 19: Modulation of markers after apoptosis induction in *L. major* FEBNI amastigotes: Axenic amastigotes were incubated with 15 μM staurosporine (stauro), 25 μM miltefosine (milte), 10 μM camptothecin (campto) and medium control for 18 (green bars) and 42 hours (light green bars) to induce apoptosis. Parasites were stained for phosphatidylserine (PS) exposure with Annexin A5-Alexa 647 and present reactive oxygen species (ROS) with 5-(and-6)-chloromethyl-2',7'-dichlorodihydrofluorescein diacetate (H_2DCFDA) and analyzed by flow cytometry (FACS). A) Depicted are the percentages of PS positive amastigotes after apoptosis induction for 18 and 42 hours. B) Depicted are the percentages of ROS positive amastigotes after apoptosis induction for 18 and 42 hours. C) Geometric mean of ROS positive amastigotes after apoptosis induction for 18 and 42 hours. Data are shown as means $\pm$ SEM, n = 3. $*$ P-value < 0.05.

3.3.3 FACS analysis of apoptotic parasites

Previous experiments using microscopy analyses showed that promastigotes round up and decrease in size when becoming apoptotic [211]. This is also detectable by flow cytometry. The forward light scatter (FSC) indicates the size of analyzed cells, whereas the side scatter (SSC) detects their granularity. A virulent promastigote culture, consisting of viable and apoptotic parasites, shows two distinct populations displayed in a density plot of FSC and SSC in FACS analysis. The right population with the higher

density and size represents the viable promastigotes and the apoptotic parasites are found in the other population (left) with the lower density and size. We found such two distinct populations of parasites in FACS after the treatment of promastigotes with miltefosine (fig. 20 A + B). Further analysis revealed the right population with the higher density to consist of PS negative and thus viable promastigotes (fig. 20 B). In contrast, we found the PS positive promastigotes in the population with the lower density and size.

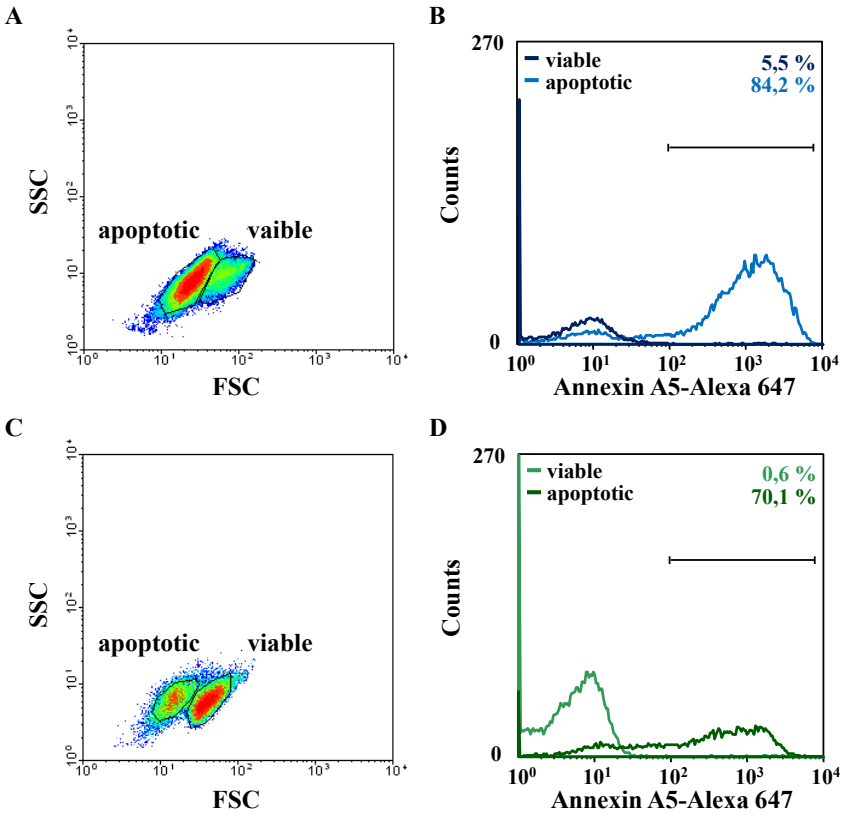

Figure 20: Viable and apoptotic *L. major* FEBNI parasites in flow cytometry: Log-phase promastigotes were incubated with 25 μM miltefosine and axenic amastigotes with 15 μM staurosporine for 18 hours to induce apoptosis. Parasites were stained for phosphatidylserine exposure with Annexin A5-Alexa 647 and analyzed by flow cytometry (FACS). Representative plots of 3 independent experiments. A) FACS density plot of viable and apoptotic promastigotes after apoptosis induction display two different populations. B) FACS histograms of promastigotes gated on the viable (dark blue) and apoptotic (blue) parasite population. C) FACS density plot of viable and apoptotic amastigotes after apoptosis induction display two different populations. D) FACS histograms of amastigotes gated on the viable (dark blue) and apoptotic (blue) parasite population.

Furthermore, a similar distribution of the parasites was found in a density plot of FSC and SSC for amastigotes after the induction of apoptosis (fig. 20 C + D). Two distinct populations were detected after incubation of amastigotes with staurosporine. Analyzing these populations for PS revealed the right more dense population to consist of PS negative viable amastigotes, while the left less dense population resulted to be mainly PS positive parasites (fig. 20 D).

Part 2

3.4 Interaction of *L. major* with human MF

In Leishmaniasis MF are known to be the final host cells. But it is still not clear which type of MF is involved in disease development or parasite clearance. There are different phenotypes of human MF present in the human body, such as pro-inflammatory type I (MF I) and anti-inflammatory type II (MF II) MF [203]. Both phenotypes, MF I as well as MF II can be possible host cells for *L. major* parasites (fig. 21). Therefore, the interaction of *L. major* promastigotes and amastigotes with pro-inflammatory as well as anti-inflammatory human MF was investigated.

3.4.1 Infection of different phenotypes of MF with *L. major*

Initially, we characterized the infectivity of both *L. major* parasite life stages for the different phenotypes of MF. In pro-inflammatory MF I we found a significant lower infection rate of 38.7 % ± 3.5 as compared to 51.5 % ± 4.5 for anti-inflammatory MF II after co-incubation with promastigotes (fig. 22 A). In addition, in pro-inflammatory MF I we found a significant lower infection rate, after co-incubation with amastigotes of 66.3 % ± 3.5 as compared to 80.6 % ± 1.5 for anti-inflammatory MF II. Moreover we found that amastigotes are more infective than promastigotes for both phenotypes of MF. Next to infection we assessed the parasite burden by quantifying the number of intracellular parasites per MF. In concordance with the MF phenotype specific as well as parasite stage specific infection rates, we found a significant lower parasite burden of 2.8 ± 0.2 parasites/MF in pro-inflammatory MF I as compared to 4.0 ± 0.5 in anti-inflammatory MF II after promastigote co-incubation (fig. 22 C). Furthermore, the co-incubation with amastigotes resulted also in lower parasite uptake in MF I of 18.3 ± 2.7 compared to 25.6 ± 2.2 in MF II (fig. 22 D), however in higher parasite burdens than after promastigote co-incubation.

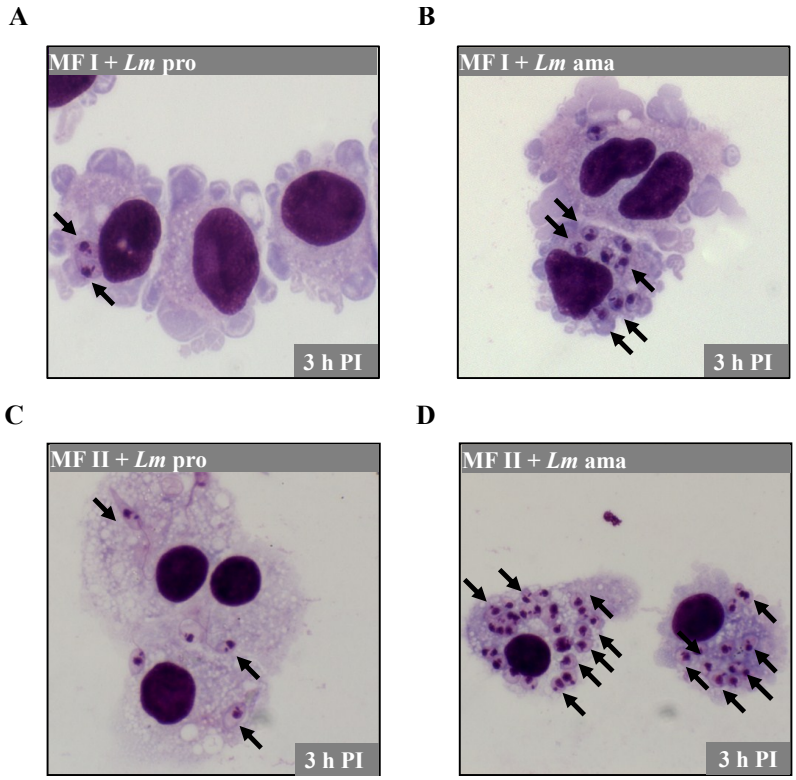

Figure 21: Infected human MF with *L. major* parasites: Pro-inflammatory type I MF (MF I) and anti-inflammatory type II MF (MF II) were co-incubated with stat-phase promastigotes (A and C) or axenic amastigotes (B and D). Extracellular parasites were removed 3 hours post infection (PI) and the cells stained with Diff QUIK®. Representative micrographs of 3 independent experiments. A) Micrograph of MF I infected with *L. major* promastigotes. B) Micrograph of MF I infected with *L. major* amastigotes. C) Micrograph of MF II infected with *L. major* promastigotes. D) Micrograph of MF II infected with *L. major* amastigotes. Magnification: 63x objective with 10x ocular.

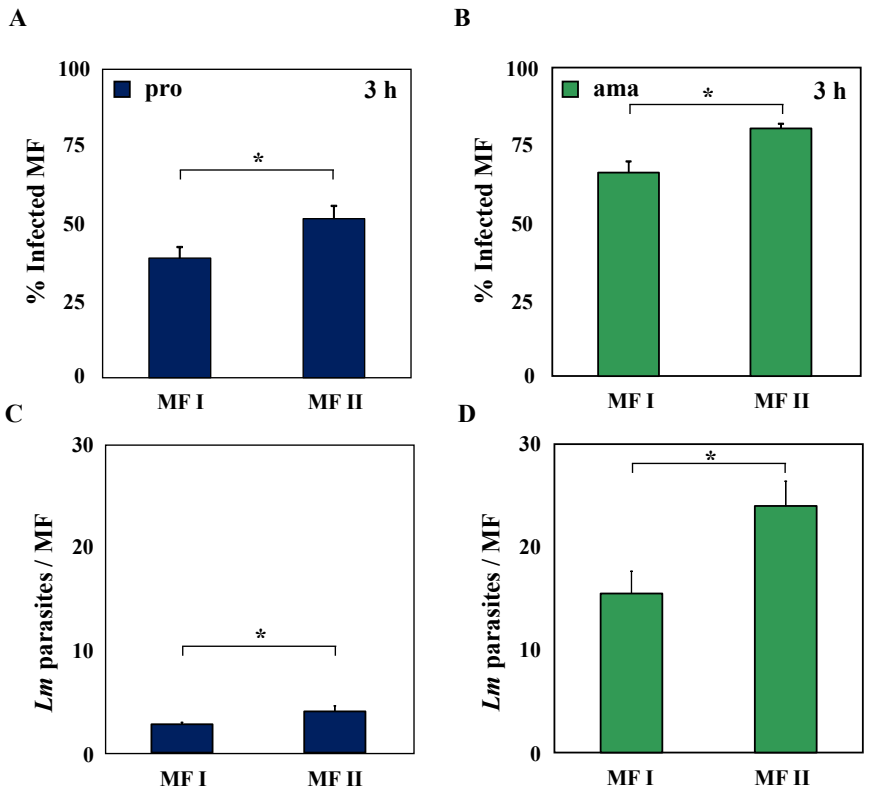

Figure 22: Stage-specific interaction of *L. major* parasites with human MF: Pro-inflammatory type I MF (MF I) and anti-inflammatory type II MF (MF II) were co-incubated with stat-phase promastigotes (A and C) or axenic amastigotes (B and D). Extracellular parasites were removed 3 hours post infection, cells were Diff QUIK® stained and infection rates were determined by counting > 200 phagocytes. Parasite burdens were assessed by counting intracellular parasites in 20 infected MF. A) Infection rates as percentage of infected MF after 3 h of co-incubation with promastigotes (blue bars), n = 13. B) Infection rates as percentage of infected MF after 3 h of co-incubation with amastigotes (green bars), n = 13. C) Number of parasites per MF after 3 h of co-incubation with promastigotes (blue bars), n = 5. D) Number of parasites per MF after 3 h of co-incubation with amastigotes (green bars), n = 5. Data are shown as means ± SEM. $*$ P-value < 0.05.

3.4.2 Infection with eGFP expressing *L. major*

Subsequently we used a transgenic eGFP expressing *L. major* strain to asses infection in the different phenotypes of human MF [118, 186].

3.4.2.1 *L. major* eGFP parasites

L. major FEBNI eGFP was generated by transfection of the *L. major* FEBNI wildtype strain with the eGFP expressing gene into the kinetoplast genome of the parasite. The eGFP gene is integrated into a locus which is known to be up-regulated in the amastigote life stage [118]. To characterize the different life stages of the parasites for their fluorescence *L. major* parasites were analyzed by flow cytometry. Log-phase promastigotes were found to be green fluorescent with a mean fluorescence intensity (MFI) of 71. In addition we used Annexin A5 (AnxA5) staining for detection of PS externalization and apoptosis. We found only 5 % of the log-phase cultures to express PS (fig. 23 A). In contrast, the stat-phase promastigotes split in two distinct populations: an eGFP fluorescent + PS negative population (54 %) with a similar MFI compared to log-phase promastigotes and a non-fluorescent + PS positive population (46 %) (fig. 23 B). This data suggest that leishmanial apoptosis mechanisms lead to the loss of the fluorescence in the parasites.
When we generated axenic amastigotes form eGFP expressing promastigotes, we found a 3-fold increase in eGFP expression (fig. 23 C). These axenic eGFP amastigotes were found to express only 4 % PS.

3.4.2.2 Parasite development in infected MF

We wanted to analyze, whether the transgenic *L. major* FEBNI eGFP parasites are still green fluorescent inside infected MF and are detectable by FACS. Therefore human MF were co-incubated either with *L. major* FEBNI eGFP promastigotes or amastigotes and analyzed by flow cytometry. We were able to detect the intracellular green fluorescent parasites inside the infected MF. In addition, the infected green fluorescent MF were found to have a comparable MFI to the MFI of the parasites alone. Amastigote infected

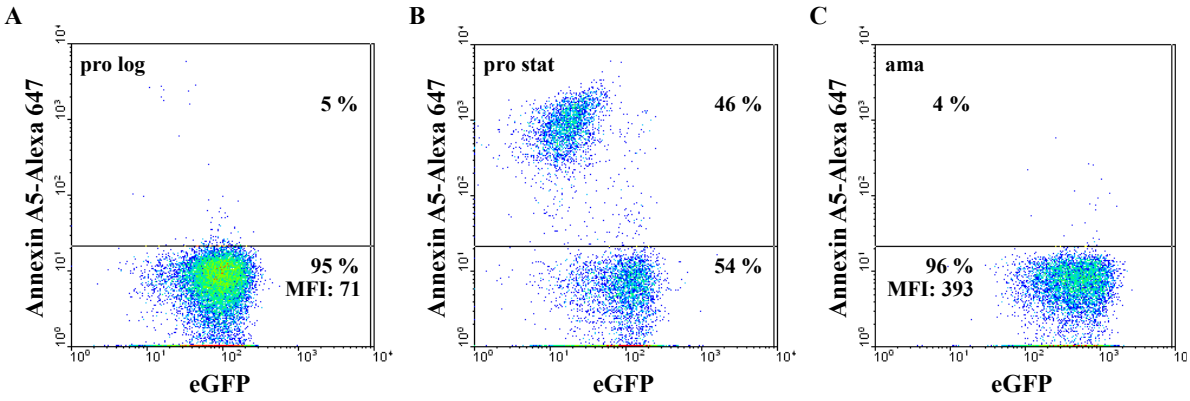

Figure 23: Characteristics of *L. major* FEBNI eGFP parasites: *L. major* eGFP parasites were stained for phosphatidylserine (PS) exposure with Annexin A5-Alexa 647 and analyzed by flow cytometry (FACS). Indicated are the percentages of PS positive and negative parasites with the corresponding eGFP mean fluorescence intensity (MFI). Representative density plots of 3 independent experiments. A) Log-phase *L. major* eGFP promastigotes. B) Stat-phase *L. major* eGFP promastigotes. C) Axenic *L. major* eGFP amastigotes.

MF showed a higher green fluorescent level as compared to promastigote infected cells (data not shown). Furthermore, the parasite stage differentiation from promastigotes into the amastigote life stage was followed over time after infection. Pro-inflammatory MF I and anti-inflammatory MF II were infected with *L. major* eGFP promastigotes and cells were analyzed by FACS at given time points (fig. 24). We found an infection rate of 35 % and a MFI of 77 in pro-inflammatory MF I 18 hours post infection (fig. 24 A), whereas anti-inflammatory MF II showed a higher infection rate of 65 % and a MFI of 118 (fig. 24 C). After the incubation for 72 hours the infection rates remained with 32 % in MF I and 60 % in MF II nearly the same, however the fluorescence intensity of the infected MF shifted to a higher eGFP fluorescence level. We obtained a 2.7-fold increase of the MFI to 210 in pro-inflammatory MF I and for anti-inflammatory MF II a 2.2-fold increase to 255 (fig. 24 B + D).

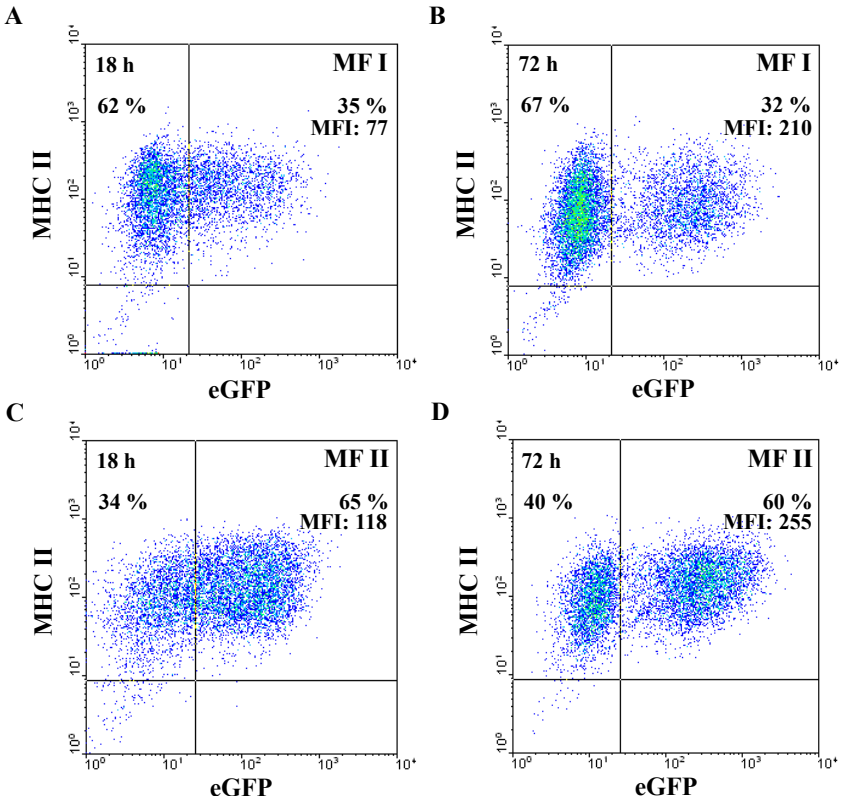

Figure 24: *L. major* eGFP parasite development in different types of human MF: Pro-inflammatory MF I and anti-inflammatory MF II were infected with stat-phase *L. major* eGFP promastigotes. Extracellular parasites were removed 18 hours post infection and infection rates as well as eGFP mean fluorescence intensity (MFI) were determined 18 and 72 hours post infection by flow cytometry (FACS). Indicated are the percentages of non-infected and infected MF with the corresponding eGFP MFI. Representative density plots of 3 independent experiments. A) Infected pro-inflammatory MF I 18 hours post infection. B) Infected pro-inflammatory MF I 72 hours post infection. C) Infected anti-inflammatory MF II 18 hours post infection. D) Infected anti-inflammatory MF II 72 hours post infection.

3.5 Phenotype and parasites stage-specific MF surface marker expression

We found a MF phenotype and parasite stage-specific infection after co-incubation with *L. major*. Now we wanted to know whether these differences have an effect on distinct surface markers on the infected MF. Therefore, we infected pro-inflammatory MF I and anti-inflammatory MF II with either *L. major* promastigotes or amastigotes and analyzed the phenotypically expression of the following cell surface molecules by flow cytometry.

3.5.1 CD163

The scavenger receptor CD163 is a specific marker for anti-inflammatory MF II and plays a role in the resolution of inflammation [119, 135]. We found CD163 expression to be low on MF I (5.3 % ± 1.8) independent of an infection (fig. 26 A), whereas 52.4 % ± 5.5 of the uninfected MF II expressed CD163 on their cell surface. However, the percentage of CD163 positive MF II decreased significantly upon infection with both *L. major* promastigotes and amastigotes, 36.1 % ± 5.8 and 36.8 % ± 5.7 respectively (fig. 25 B). Furthermore, there was not only a reduction of CD163 positive MF II, but also the MFI of infected and CD163 positive cells shifted to a significant lower level upon the infection with promastigotes (fig. 25 C + D) and amastigotes (data not shown). In addition to the expression of CD163 on the cell surface, we monitored the relative gene expression by RT-PCR analysis. We found no significant difference in the CD163 mRNA expression of untreated MF I and II, 1.6 ± 0.2 and 1.3 ± 0.2 respectively (fig. 26 C + D). However, there was a significant reduction of the CD163 mRNA expression to 0.7 ± 0.5 for MF I and 0.9 ± 0.2 for MF II after the infection of both phenotypes of MF with the promastigote life stage. The infection with amastigotes resulted in a non-significant decrease of CD163 expression.

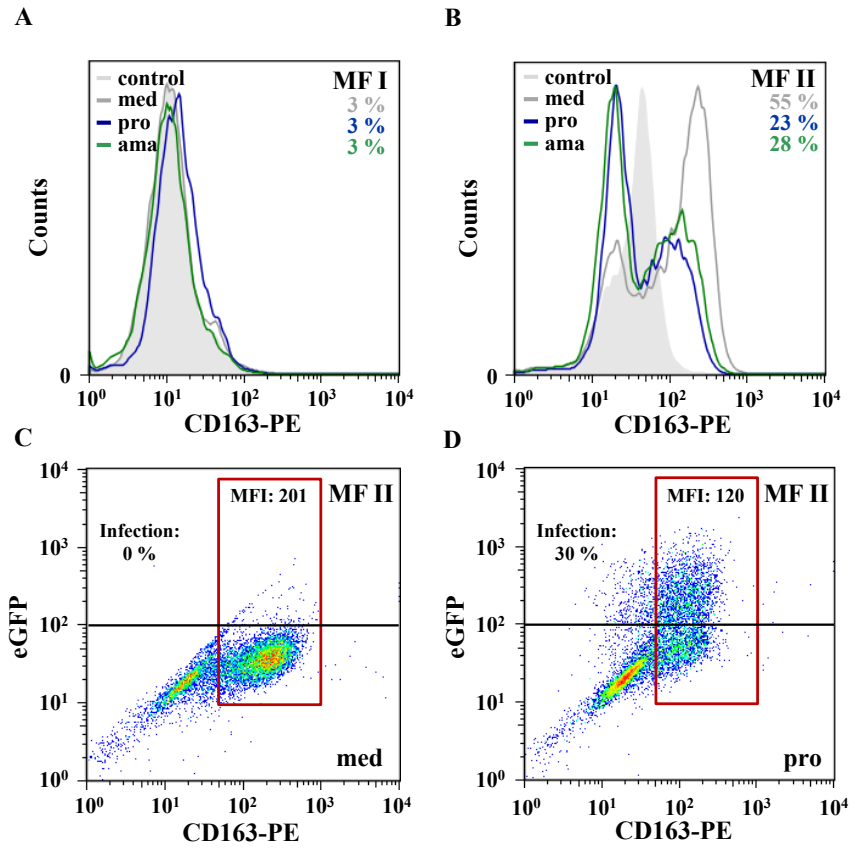

Figure 25: Downregulation of CD163 on the cell surface in human MF II after infection with *L. major* parasites: Pro-inflammatory MF I and anti-inflammatory MF II were infected with stat-phase promastigotes or axenic amastigotes. Extracellular parasites were removed 3 hours post infection and cells were stained 18 hours post infection for CD163 surface expression with mouse anti-CD163 labeled with PE (1:10) with the corresponding isotype (PE) control and analyzed by flow cytometry (FACS). A)+B) Representative FACS histograms of one experiment out of 6 independent experiments. Control MF (grey line), promastigote infected (blue line) and axenic amastigote infected MF (green line) with the percentages of CD163 positive cells compared to the isotype control (filled light grey). C)+D) Representative FACS density plots of control MF II and infected with *L. major* eGFP promastigotes. Displayed is the mean fluorescent intensity (MFI) for the CD163 positive MF and the infection rate.

3.5.2 CD206

The mannose receptor CD206 is involved in recognizing pathogens that have mannose on their cell surface, like mannosylated glycoproteins present on a variety of pathogens [31].

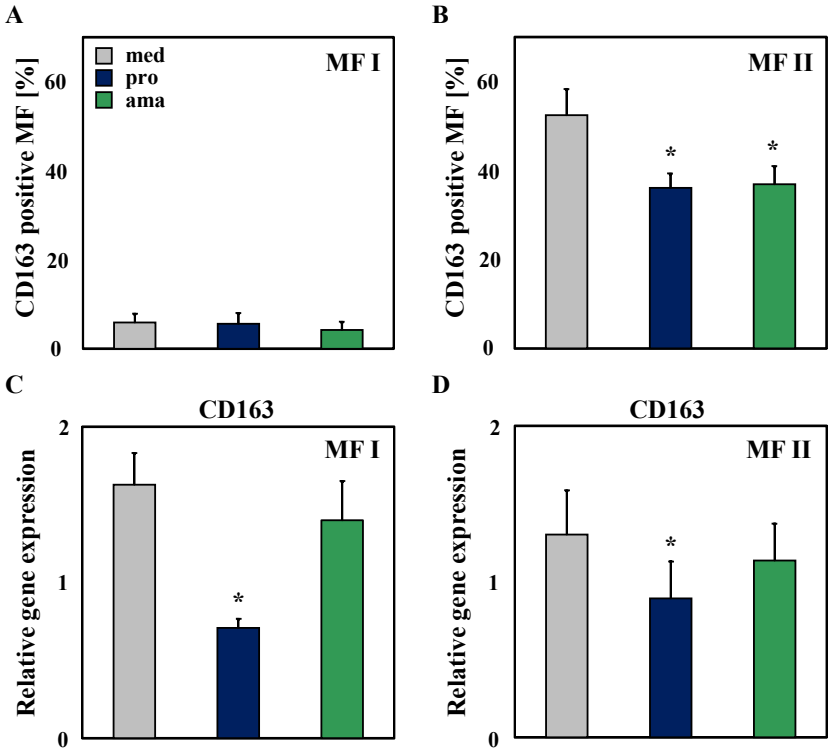

Figure 26: Downregulation of CD163 on the cell surface and mRNA expression in human MF II after infection with *L. major* parasites: Pro-inflammatory MF I and anti-inflammatory MF II were infected with stat-phase promastigotes or axenic amastigotes. Extracellular parasites were removed 3 hours post infection and cells were harvested 18 hours post infection from medium controls (grey bars), promastigote infected MF (blue bars) and amastigote infected MF (green bars). A)+B) MF I and II were stained for CD163 surface expression with mouse anti-CD163 labeled with PE (1:10) with the corresponding isotype (PE) control and analyzed by flow cytometry (FACS). Depicted are percentages of CD163 positive cells, n = 6. C)+D) Total RNA was isolated, cDNA generated and the relative gene expression was determined by LightCycler analysis. Depicted is the relative gene expression of MF I and II, n = 5. Data are shown as means ± SEM. ∗ P-value < 0.05.

Therefor CD206 plays a role in receptor-mediated endocytosis and receptor-mediated facilitated antigen presentation [167, 192, 31]. We found that there is no significant difference in CD206 expression on uninfected MF I and II, 49.7 % ± 12.3 and 55.1 % ± 9.3 respectively (fig. 27 C + D).

However, we did find significant higher percentages of CD206 positive MF upon the infection with both life stages of *L. major* parasites. For MF I we observed an up-regulation of CD206 positive cells to 82.1 % ± 2.2 after the infection with promastigote

and to 79.1 % ± 4.2 after amastigote infection. In addition, the infection with promastigotes resulted in an up-regulation of CD206 positive cells to 74.5 % ± 8.4 and to 74.8 % ± 8.3 upon amastigote infection in MF II.

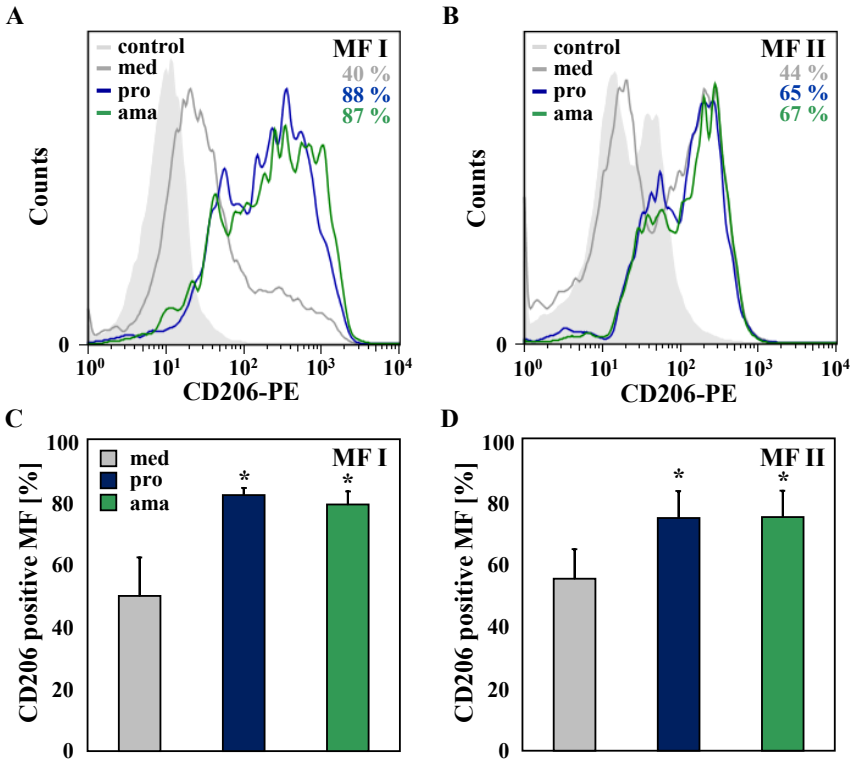

Figure 27: Up-regulation of CD206 on the cell surface in human MF after infection with *L. major* parasites: Pro-inflammatory MF I and anti-inflammatory MF II were infected with stat-phase promastigotes or axenic amastigotes. Extracellular parasites were removed 3 hours post infection and cells were stained 18 hours post infection for CD206 surface expression with mouse anti-CD206 labeled with PE (1:20) with the corresponding isotype (PE) control and analyzed by flow cytometry (FACS). A)+B) Representative FACS histograms of one experiment out of 4 independent experiments. Control MF (grey line), promastigote infected (blue line) and axenic amastigote infected MF (green line) with the percentages of CD206 positive cells compared to the isotype control (filled light grey). C)+D) Depicted are the percentages of CD206 positive control MF (grey bars), promastigote infected MF (blue bars) and amastigote infected MF (green bars). Data are shown as means ± SEM, n = 4. $*$ P-value < 0.05.

3.5.3 MHC class II (MHC II)

Major histocompatibility complex (MHC) class II molecules are essential for antigen presentation of ingested pathogens in MF [152, 28].

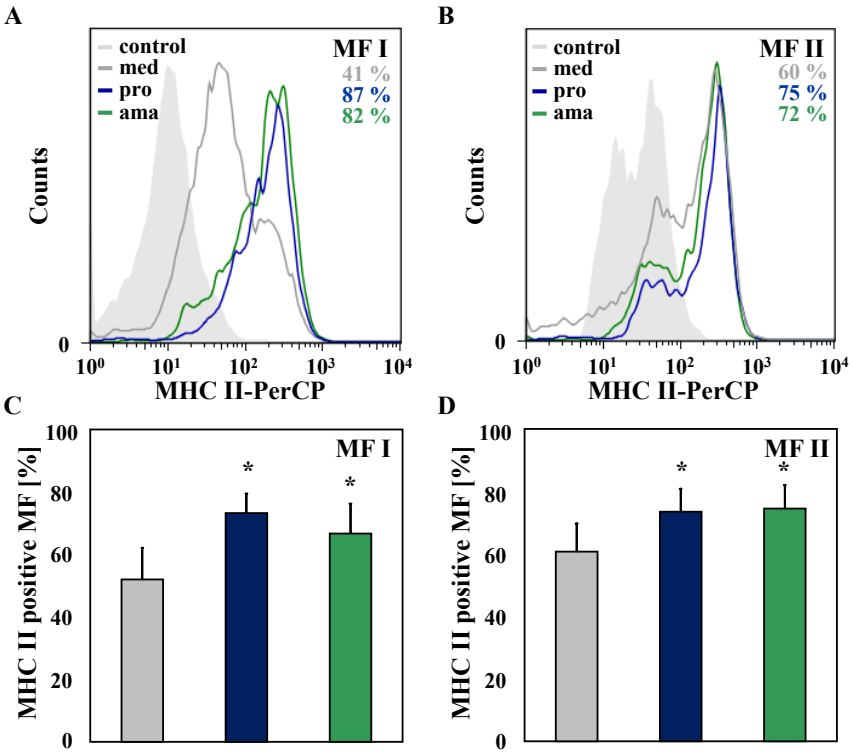

Figure 28: Up-regulation of MHC II on the cell surface in human MF after infection with *L. major* parasites: Pro-inflammatory MF I and anti-inflammatory MF II were infected with stat-phase promastigotes or axenic amastigotes. Extracellular parasites were removed 3 hours post infection and cells were stained 18 hours post infection for MHC II surface expression with mouse anti-MHC II labeled with PerCP (1:10) with the corresponding isotype (PerCP) control and analyzed by flow cytometry (FACS). A)+B) Representative FACS histograms of one experiment out of 4 independent experiments. Control MF (grey line), promastigote infected (blue line) and axenic amastigote infected MF (green line) with the percentages of MHC II positive cells compared to the isotype control (filled light grey). C)+D) Depicted are the percentages of MHC II positive control MF (grey bars), promastigote infected MF (blue bars) and amastigote infected MF (green bars). Data are shown as means $\pm$ SEM, n = 4. $*$ P-value < 0.05.

We found no significant differences in MHC II expression of uninfected MF I and II, 51.9 % ± 10.1 and 60.6 % ± 8.9 respectively (fig. 28 C + D). However, after the infection with both life stages of *L. major* parasites, we found significant higher expression of MHC II on the surface of both phenotypes of MF. For MF I we observed an up-regulation of MHC II positive cells to 73.2 % ± 6.2 after the infection with promastigote and to 66.8 % ± 9.4 after amastigote infection. In addition, the infection with promastigotes resulted in an up-regulation of MHC II positive cells to 73.5 % ± 7.3 and to 74.4 % ± 7.5 upon amastigote infection in MF II.

3.5.4 CD86

CD86 is expressed on MF and other antigen-presenting cells and is involved in providing co-stimulatory signals necessary for T cell activation and survival [108, 179, 174]. Uninfected MF were found to show a significant higher expression of CD86 of 37.4 % ± 6 on the cell surface of MF II as compared to 15 % ± 1.4 on MF I (fig. 29 A + B). Furthermore, we found significant higher expression of CD86 on the surface of both phenotypes of MF after the infection with both life stages of *L. major* parasites. For MF I we observed an up-regulation of CD86 positive cells to 28.8 % ± 5.2 after the infection with promastigote and to 24.3 % ± 3.2 after amastigote infection. In addition, we found for MF II an up-regulation of CD86 positive cells to 59.3 % ± 3.9 after promastigote infection and to 51.3 % ± 5.3 upon amastigote infection.
In addition, the analysis of complement receptor 3 (CD11b), a protein which plays a role in phagocytosis, adhesion and migration revealed no significant differences in CD11b expression on uninfected MF I and II. Moreover, we found no influence of an infection with *L. major* parasites on CD11b surface expression in MF I. However, MF II resulted in a significant higher CD11b expression upon the infection with both parasite life stages of *L. major* (data not shown). Furthermore, we investigated the surface expression of the co-stimulatory protein CD40, which is responsible for MF activation. We found a high CD40 expression on the cell surface of both phenotypes of MF (94.8 % ± 0.8). The infection with *L. major* parasites had no influence on the surface expression, neither for MF I nor for MF II (data not shown).

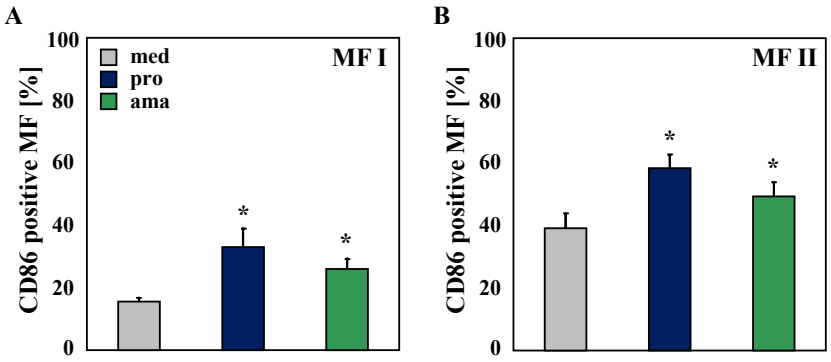

Figure 29: Up-regulation of CD86 on the cell surface in human MF after infection with *L. major* parasites: Pro-inflammatory MF I and anti-inflammatory MF II were infected with stat-phase promastigotes or axenic amastigotes. Extracellular parasites were removed 3 hours post infection and cells were stained 18 hours post infection for CD86 surface expression with mouse anti-CD86 labeled with APC (1:100) with the corresponding isotype (APC) control and analyzed by flow cytometry (FACS). A)+B) Depicted are the percentages of CD86 positive control MF (grey bars), promastigote infected MF (blue bars) and amastigote infected MF (green bars). Data are shown as means ± SEM, n = 4. $*$ P-value < 0.05.

3.6 Phenotype and parasites stage-specific cytokine production

In addition to different parasite uptake, which resulted in altered surface expression of distinct markers on the infected MF, we wanted to investigate whether these differences have consequences for further cell functions. Therefore we analyzed the cytokine production of MF after the infection with different stages of *L. major* parasites using RT-PCR or ELISA.

3.6.1 TNF alpha

Tumor necrosis factor (TNF) alpha is a pro-inflammatory cytokine which induces systemic inflammation and has also been reported to be involved in host defense against a broad range of pathogens, including *Leishmania* [56, 182, 220]. We found a low TNF alpha secretion of 38.1 pg/ml ± 27.9 in uninfected pro-inflammatory MF I and 12.9

pg/ml ± 4.9 in anti-inflammatory MF II. After the infection with *L. major* promastigotes, we could detect a significant increase in TNF alpha production in both phenotypes of MF, with a significantly higher increase in MF II (1079 pg/ml ± 237) as compared to MF I (113.3 pg/ml ± 53, fig. 30 A + B). In contrast, amastigote infection do not induce TNF alpha, neither in MF I (20.2 pg/ml ± 10.4) nor in MF II (16.7 pg/ml ± 5.8, fig. 30 A + B).

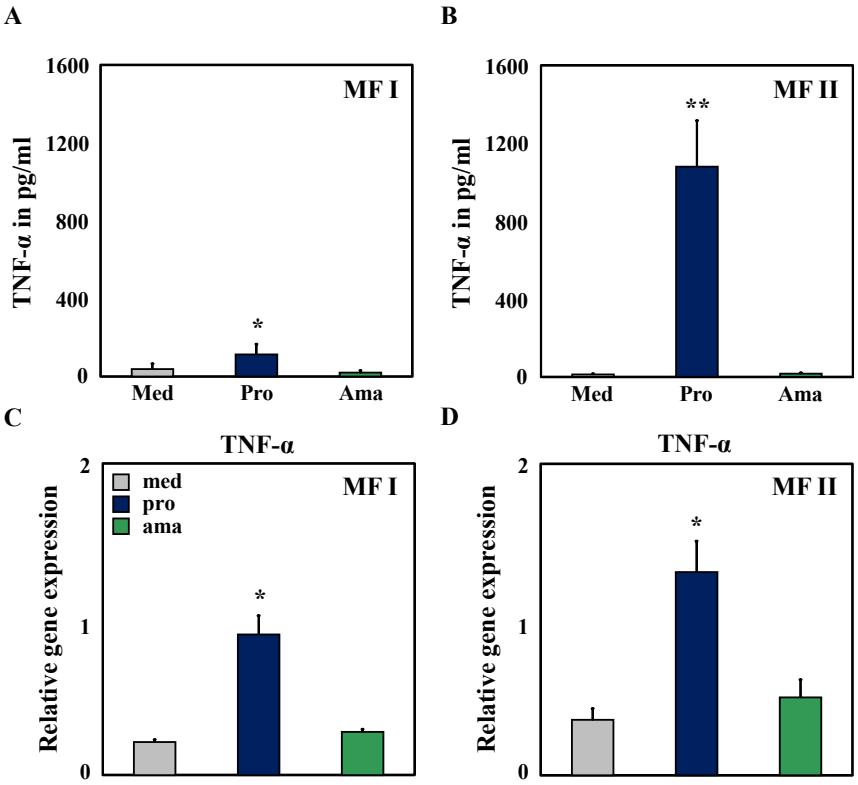

Figure 30: Different cytokine production of TNF alpha in human MF after infection with *L. major* parasites: Pro-inflammatory MF I and anti-inflammatory MF II were infected with stat-phase promastigotes or axenic amastigotes. Extracellular parasites were removed 3 hours post infection and supernatants and cells were harvested 18 hours post infection from medium controls (grey bars), promastigote infected MF (blue bars) and amastigote infected MF (green bars) for TNF alpha sandwich ELISA and mRNA expression analysis. Total RNA was isolated, cDNA generated and the relative gene expression was determined by LightCycler analysis. A) TNF alpha production of pro-inflammatory MF I (n = 3). B) TNF alpha production of anti-inflammatory MF II (n = 3). C) TNF alpha mRNA expression of pro-inflammatory MF I (n = 4). D) TNF alpha mRNA expression of anti-inflammatory MF II (n = 4). Data are shown as means ± SEM. ∗ P-value < 0.05, ∗∗ P-value < 0.005.

In addition to TNF alpha production, we monitored the relative gene expression of TNF alpha by RT-PCR analysis. We found no significant differences in uninfected MF I and II, 0.22 ± 0.02 and 0.35 ± 0.07 respectively (fig. 30 C + D). However, in concordance with the cytokine expression on protein level, we found a significant up-regulation of the TNF alpha expression on the mRNA level after promastigote infection in MF I to 0.9 ± 0.1 and to 1.3 ± 0.2 in MF II (fig. 30 C + D). Upon the infection with the amastigote life stage we found, similar to the results of ELISA analysis, no significant differences in the TNF alpha expression in MF I and II.

3.6.2 IL-12

Interleukin 12 (IL-12) is a heterodimer consisting of the IL-12p40 and the IL-12p35 subunit [87]. IL-12 is a pro-inflammatory regulatory cytokine and is shown to promote the differentiation of naive T lymphocytes into Th-1 cells, which is crucial in determining resistance and clearance of a particular pathogen [73, 107]. The IL-12p40 subunit was detected by ELISA analysis for the IL-12 measurement (fig. 31).

Uninfected MF I and II showed a low level of IL-12 secretion of 3.8 pg/ml ± 1.2 in pro-inflammatory MF I and 1.3 pg/ml ± 0.1 in anti-inflammatory MF II. We found a significant increase of IL-12 secretion to 778.6 pg/ml ± 307 only in pro-inflammatory MF I after the infection with promastigotes (fig. 31 A). The infection with amastigotes in MF I as well as both parasite life stages in MF II had no effect on IL-12 production (fig. 31 A + B).

3.6.3 CCL3 and CCL4

Macrophage inflammatory protein-1 (MIP-1) alpha and MIP-1 beta belong both to the family of chemotactic cytokines, which are known as chemokines and are now officially named CCL3 and CCL4, respectively. Both CCL3 and CCL4 are demonstrated to have a chemotactic activity towards monocytes and T lymphocytes, as well as pro-inflammatory effects [111]. The relative gene expression of CCL3 and CCL4 was analyzed by RT-PCR (fig. 32). For CCL3 we found no significant differences in the

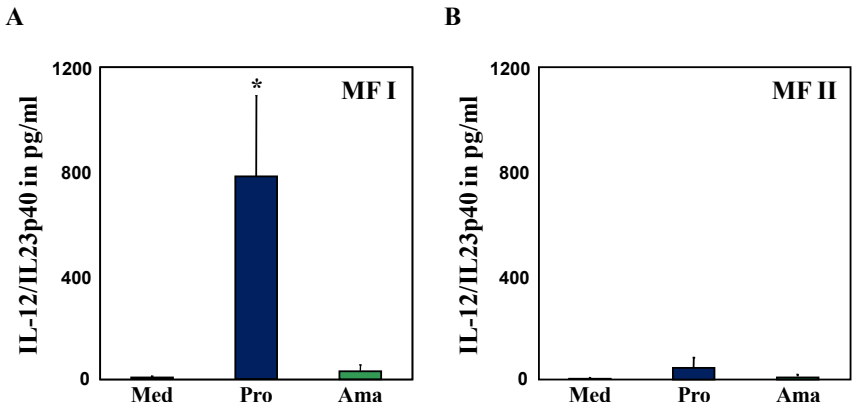

Figure 31: Different cytokine production of IL-12 in human MF after infection with *L. major* parasites: Pro-inflammatory MF I and anti-inflammatory MF II were infected with stat-phase promastigotes or axenic amastigotes. Extracellular parasites were removed 3 hours post infection and supernatants were collected 18 hours post infection from medium controls (grey bars), promastigote infected MF (blue bars) and amastigote infected MF (green bars) for IL-12/IL23p40 sandwich ELISA analysis. A) IL-12 production of pro-inflammatory MF I. B) IL-12 production of anti-inflammatory MF II. Data are shown as means ± SEM, n = 5. $*$ P-value < 0.05.

expression of uninfected MF I and II, 0.39 ± 0.19 and 0.43 ± 0.07 respectively. However, there was a significant up-regulation of the CCL3 expression to 1.0 ± 0.3 for MF I and to 1.2 ± 0.2 for MF II after the infection with the promastigote life stage of both phenotypes of MF (fig. 32 A + B). Upon the infection with amastigotes we found no significant differences. Comparable to the CCL3 expression, we found no significant differences for CCL4 between uninfected MF I and II, 0.14 ± 0.06 and 0.35 ± 0.08 respectively (fig. 32 C + D). However, a significant up-regulation of the CCL4 expression to 0.55 ± 0.14 for MF I and to 1.3 ± 0.3 for MF II was found upon the infection with promastigotes. Amastigote infection showed no effect on the CCL4 expression.
Moreover, we found CCL2, which has the same immunomodulating repertoire as CCL3 and CCL4 and was formally known as monocyte chemotactic protein-1 (MCP-1), to show the same gene expression pattern like CCL3 + 4 upon the infection with *L. major* parasites (data not shown).

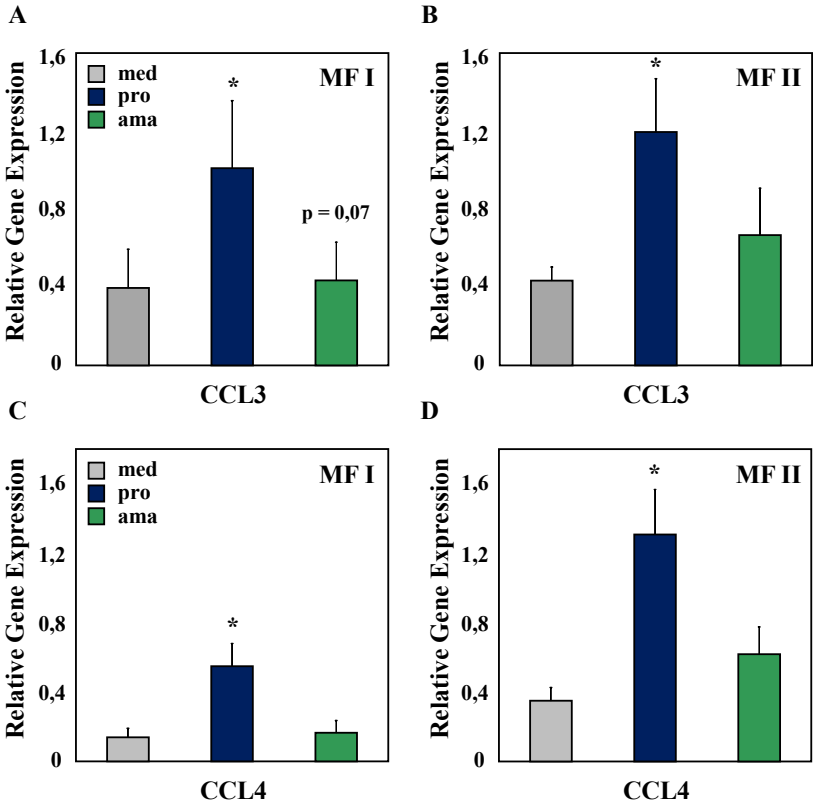

Figure 32: Different cytokine mRNA expression of CCL3 and CCL4 in human MF after infection with *L. major* parasites: Pro-inflammatory MF I and anti-inflammatory MF II were infected with stat-phase promastigotes or axenic amastigotes. Extracellular parasites were removed 3 hours post infection and cells were harvested 18 hours post infection from medium controls (grey bars), promastigote infected MF (blue bars) and amastigote infected MF (green bars). Total RNA was isolated, cDNA generated and the relative gene expression was determined by LightCycler analysis. A) CCL3 mRNA expression of pro-inflammatory MF I. B) CCL3 mRNA expression of anti-inflammatory MF II. C) CCL4 mRNA expression of pro-inflammatory MF I. D) CCL4 mRNA expression of anti-inflammatory MF II. Data are shown as means ± SEM, n = 4. $*$ P-value < 0.05.

3.6.4 IL-10

Interleukin 10 (IL-10) is able to profoundly inhibit a broad spectrum of activated MF functions such as cytokine secretion, NO production and the expression of MHC II molecules [23, 55, 60, 45, 138, 151, 124] and thus serves as an anti-inflammatory cytokine.

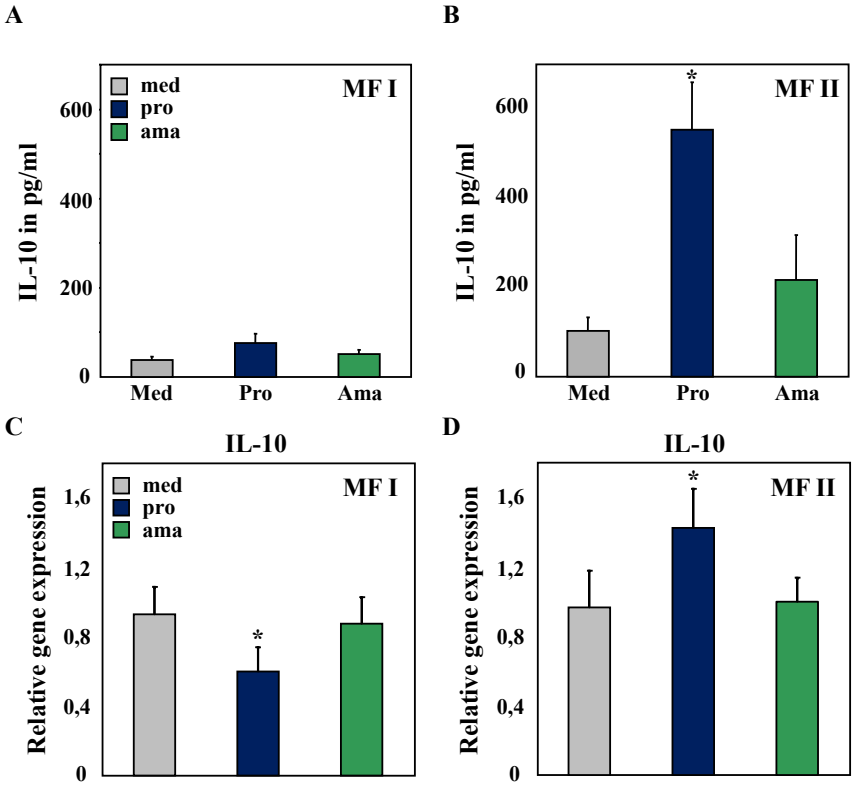

Figure 33: Different cytokine production of IL-10 in human MF after infection with *L. major* parasites: Pro-inflammatory MF I and anti-inflammatory MF II were infected with stat-phase promastigotes or axenic amastigotes. Extracellular parasites were removed 3 hours post infection and supernatants and cells were harvested 18 hours post infection from medium controls (grey bars), promastigote infected MF (blue bars) and amastigote infected MF (green bars) for IL-10 sandwich ELISA and mRNA expression analysis. Total RNA was isolated, cDNA generated and the relative gene expression was determined by LightCycler analysis. A) IL-10 production of pro-inflammatory MF I. B) IL-10 production of anti-inflammatory MF II. C) IL-10 mRNA expression of pro-inflammatory MF I. D) IL-10 mRNA expression of anti-inflammatory MF II. Data are shown as means ± SEM, n = 5. ∗ P-value < 0.05 vs medium control.

In contrast to TNF alpha and IL-12, we found a significant higher secretion of IL-10 in uninfected anti-inflammatory MF II of 89 pg/ml ± 31 as compared to 34.4 pg/ml ± 7.6 in pro-inflammatory MF I (fig. 33 A + B). Furthermore, MF II resulted in a significant increase in IL-10 production to 579.2 pg/ml ± 118 after the infection with the promastigote life stage. Amastigote infection showed no influence on the secretion of IL-10 in MF II, as well as both parasite life stages in MF I (fig. 33 A + B). Subsequently to IL-10 production, the relative gene expression was monitored by RT-PCR analysis. Interestingly, we found a significant down-regulation of IL-10 expression from 0.9 ± 0.15 in uninfected MF I to 0.6 ± 0.14 in promastigote infected pro-inflammatory MF I, whereas amastigotes had no influence on IL-10 expression in MF I (fig. 33 C). In contrast, anti-inflammatory MF II showed a significant up-regulation upon promastigote infection to 1.43 ± 0.2 as compared to 0.97 ± 0.2 in uninfected MF II. Amastigotes showed no effect on the IL-10 expression in MF II (fig. 33 D).

3.7 Phosphorylation of MAP kinases (MAPK) after *L. major* infection

In order to understand the differential cytokine production in the different phenotypes of MF as well as after infection with both life stages of the *L. major* parasite, we investigated intracellular signal transduction pathways. Therefore we selected the following two pathways based on their involvement in the intracellular signaling network [141, 35]: P38 mitogen-activated protein kinase (p38) and extracellular signal-regulated kinases (ERK1/2). Both are mitogen-activated protein (MAP) kinases of the family of protein kinase cascades. They belong to the serine/threonine-specific protein kinases that respond to extracellular stimuli such as pro-inflammatory cytokines, ultra violate radiation, heat shock, growth factors and mitogens. MAPK activation is regulated by phosphorylation cascades of a serial of molecules resulting in modulation of distinct transcription factors with effects on various cellular activities like cell proliferation, differentiation and cell survival/apoptosis [142]. For both there have been hints that they might be affected in parasite infection [77, 16, 15].
Preliminary data (n = 2) from an intracellular FACS staining showed a slight in-

crease in the phosphorylation of p38 and ERK1/2 after infection with *L. major* in pro-inflammatory MF I (fig. 34 C + D). Furthermore, we used western blot analysis, which is a standard method to investigate the phosphorylation level of p38 and ERK1/2.

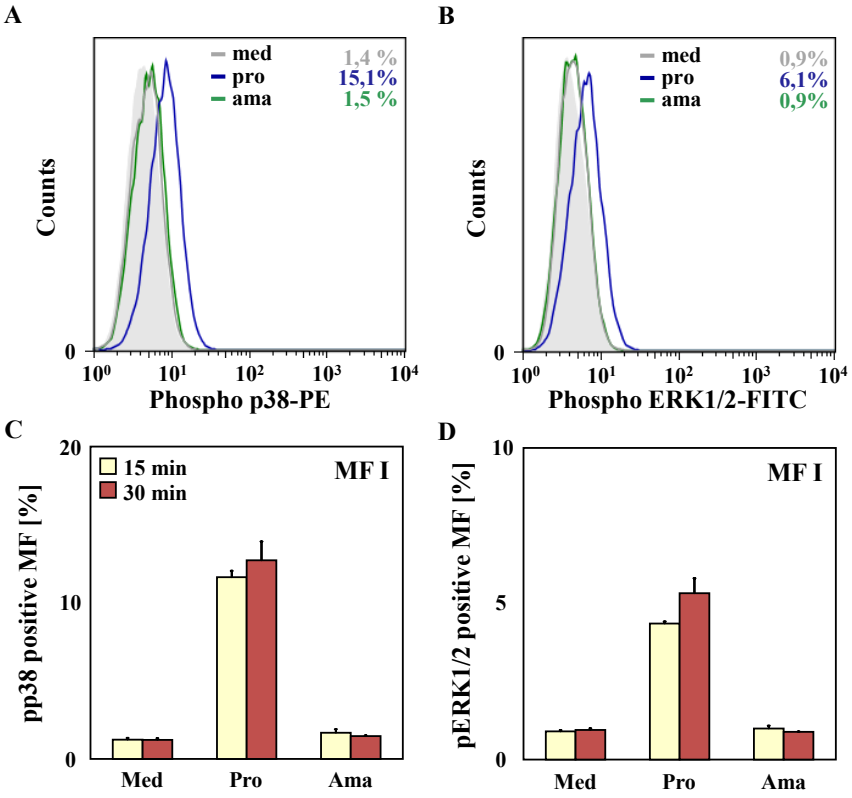

Figure 34: Different phosphorylation state of p38 and p44/42 (ERK1/2) MAP kinases (MAPK) in human type I MF after infection with *L. major* parasites: Pro-inflammatory MF I were infected with stat-phase promastigotes or axenic amastigotes. Extracellular parasites were removed 15 and 30 minutes post infection and cells were harvested from medium controls (med), promastigote infected MF (pro) and amastigote infected MF (ama). Intracellular staining was performed for phospho p38 and phospho ERK1/2 MAPK with mouse anti-phospho p38 MAPK labeled with PE (1:10) and anti-phospho ERK1/2 MAPK labeled with Alexa Fluor 488 (1:10) and analyzed by FACS. A)+B) Representative FACS histograms of one experiment out of 2 independent experiments. Control MF I (grey line), promastigote infected (blue line) and axenic amastigote infected (green line) with the percentages of phospho p38 and phospho ERK1/2 positive cells compared to the isotype control (filled light grey) after 30 minutes infection. C)+D) Positive MF I for phospho p38 and phospho ERK1/2 after 15 (yellow bars) and 30 (brown bars) minutes of *L. major* infection. Depicted are percentages of phospho p38 and phospho ERK1/2 positive cells. Data are shown as means ± SEM, n = 2.

3.7.1 p38 MAP kinases

P38 MAPK is activated mainly by inflammatory cytokines, like TNF alpha, TGF beta and IL-1, as well as by lipopolysaccharides (LPS) [150]. It was demonstrated that the activation of p38 leads to different effects such as cytokine production, cell motility, apoptosis or elimination of pathogens [137, 136]. We found first a significant up-regulation of phospho p38 in promastigote infected MF I after 15 min (1.18 ± 0.04), however after 30 min there was a subsequent significant decrease of phospho p38 (0.75 ± 0.05, fig 35 A). Amastigote infection showed no significant effect on p38 phosphorylation. In contrast, we obtained a significant up-regulation of phospho p38 only after 15 min of infection with both parasite life stages in MF II, 1.59 ± 0.06 after promastigote and 2.17 ± 0.27 upon amastigote infection (fig. 35 B).

3.7.2 ERK1/2 MAP kinases

In contrast to p38, ERK1/2 MAPK are induced by hormones, growth factors and a vast number of extracellular stimuli [35]. Activation of ERK1/2 leads to altered transcription of genes that are important amongst others for the cell cycle. Feng et al. showed *Leishmania* to activate ERK1/2 and subsequently decrease IL-12 production in MF [52]. However, for MF I and II there are no data published. Preliminary data ($n = 2$) showed for MF I a down-regulation of phospho ERK1/2 in promastigote infected cells after 15 min (0.74 ± 0.02) as well as after 30 min (0.51 ± 0.02, fig. 36 A). An even stronger decrease was found upon amastigote infection 15 min (0.38 ± 0.04) and 30 min (0.23 ± 0.04) after co-incubation. However, MF II showed an up-regulation after 15 min in both promastigote (1.36 ± 0.01) and amastigote (1.82 ± 0.04) infected MF II for phospho ERK1/2 (fig. 36 B). After 30 min of co-incubation no differences in ERK 1/2 phosphorylation could be detected any more.

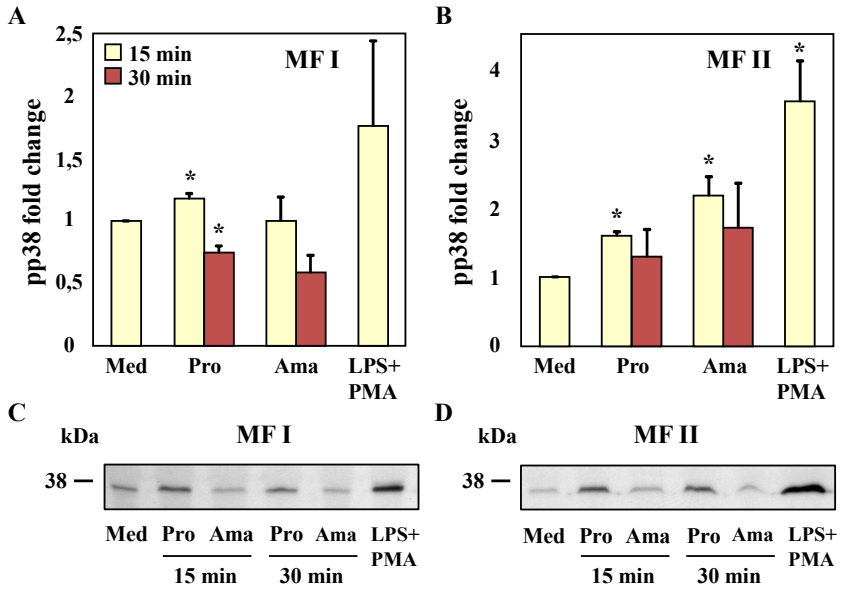

Figure 35: Different phosphorylation state of p38 MAP kinases (MAPK) in human MF after infection with *L. major* parasites: Pro-inflammatory MF I and anti-inflammatory MF II were infected with stat-phase promastigotes or axenic amastigotes. Extracellular parasites were removed 15 (yellow bars) and 30 (brown bars) minutes post infection and cells were harvested from medium controls (med), promastigote infected MF (pro), amastigote infected MF (ama) and MF treated with 2 μg/ml LPS and 160 nM PMA. Cells were lysed, separated by SDS-Page and western blot analysis was performed for phosphorylated p38 MAPK (pp38) with rabbit anti-phospho p38 MAPK (1:1000) detected with anti-rabbit Ab labeled with HRP (1:1000). Band intensity was normalized to protein amount detected by coomassie staining. A)+B) Fold change of band intensity of phospho p38 MAPK in MF I (A) and MF II (B) after infection and LPS + PMA treatment. Data are shown as means $\pm$ SEM, n = 3. $*$ P-value < 0.05 vs. medium control. C)+D) Representative western blot of phospho p38 MAPK in infected and LPS + PMA treated MF I (C) and MF II (D). A full range rainbow marker was used as molecular size marker and the 38 kDa band is indicated.

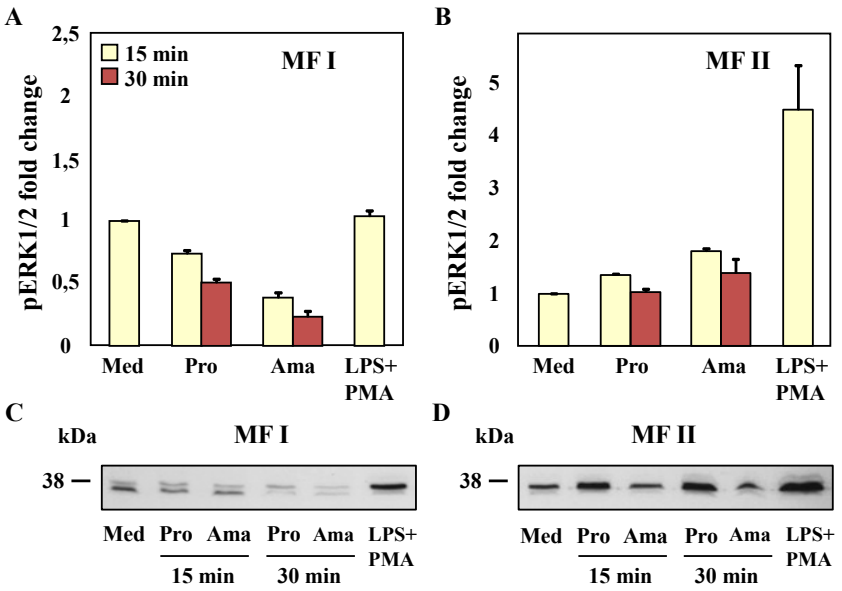

Figure 36: Different phosphorylation state of ERK1/2 MAP kinases (MAPK) in human MF after infection with *L. major* parasites: Pro-inflammatory MF I and anti-inflammatory MF II were infected with stat-phase promastigotes or axenic amastigotes. Extracellular parasites were removed 15 (yellow bars) and 30 (brown bars) minutes post infection and cells were harvested from medium controls (med), promastigote infected MF (pro), amastigote infected MF (ama) and MF treated with 2 μg/ml LPS and 160 nM PMA. Cells were lysed, separated by SDS-Page and western blot analysis was performed for phosphorylated ERK1/2 MAPK (pERK 1/2) with rabbit anti-phospho ERK1/2 MAPK (1:1000) detected with anti-rabbit Ab labeled with HRP (1:1000). Band intensity was normalized to protein amount detected by coomassie staining. A)+B) Fold change of band intensity of phospho ERK1/2 MAPK in MF I (A) and MF II (B) after infection and LPS + PMA treatment. Data are shown as means ± SEM, n = 2. C)+D) Representative western blot of phospho ERK1/2 MAPK in infected and LPS + PMA treated MF I (C) and MF II (D). A full range rainbow marker was used as molecular size marker and the 38 kDa band is indicated.

3.8 *L. major* parasite escape from phagolysosomes

After the analysis of the cytokine production and intracellular cell signaling of MF upon the infection with *L. major* parasites, we wanted to look at the compartment where the parasites reside inside MF. *L. major* promastigotes are known to end up in phagolysosomes, where they need the special environmental conditions like a low pH-value to start stage differentiation into the amastigote form and multiplication [22]. Concanamycin A is an inhibitor of the vacuolar ATPase, a proton pump that carries H^+ in the lumen of a compartment and acidifies the pH inside this compartment [26, 57, 74]. Therefore, treatment of MF with concanamycin A leads to the inhibition of the vacuolar ATPase in the phagolysosomal membrane by binding to the proteolipid subunit, which results in an increase of the pH-value inside the phagolysosome after treatment. Investigating the effect of such a pH increase on the fate of infection of human MF, we analyzed infected MF I and II with *L. major* parasites after subsequently treated with concanamycin A.

We found no significant differences in the resulting infection rates for both phenotypes of MF upon promastigote infection, neither after 18 hours (data not shown) nor after 42 hours any (fig. 37 A). In addition, the infection with amastigotes showed no differences after 18 hours. However, after 42 hours we found a significant higher percentage of infected MF in concanamycin A treated cells as compared to the untreated control cells in both MF I and MF II. For MF I the infection rate increased from 55.1 % ± 9.2 in untreated control MF to 78 % ± 6.2 in concanamycin A treated cells and for MF II from 80.4 % ± 4.5 to 90.6 % ± 2.1 respectively (fig. 37 B).

Subsequently, we analyzed the location of *L. major* parasites inside MF using electron microscopy (EM) in infected MF I (data not shown) and MF II (fig. 37 C + D). We found promastigote infected MF II to show two double membrane structures, one from the host compartment (phagolysosome) and one parasite double membrane (fig. 37 C). We found the promastigote double membrane to be associated with the characteristic subpellicular microtubular structure of the *L. major* parasites surface. In contrast, for amastigote infected MF II, we found some phagolysosomes with one intact parasite membrane and a second disrupted host membrane around the parasite, in addition to phagolysosomes with two double membranes (data not shown). Furthermore, some infected MF II showed only one double membrane of the parasite without any host

membranes of the MF (fig. 37 D, white arrows). In addition, *L. major* amastigotes show the same characteristic subpellicular microtubular structure associated with the parasite membrane as compared to the promastigote form.

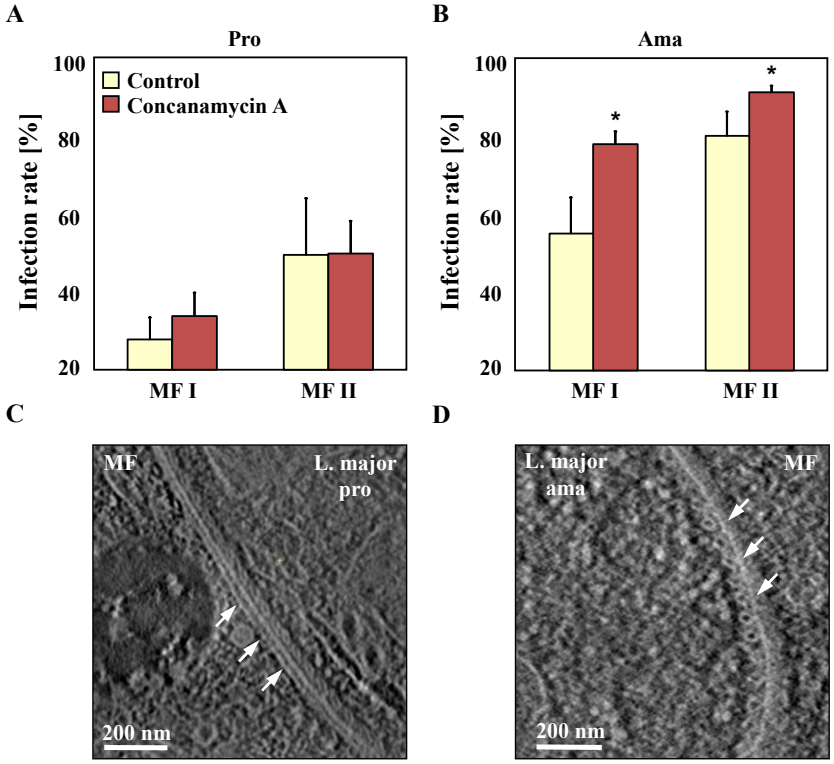

Figure 37: Infection rates after concanamycin A treatment and parasite location in human MF after *L. major* infection: A)+B) Pro-inflammatory MF I and anti-inflammatory MF II were infected with stat-phase promastigotes (A) or axenic amastigotes (B) in the presence of 22 nM Concanamycin A (brown bars) or medium (yellow bars). Extracellular parasites were removed 3 hours post infection and cells were Diff QUIK® stained 42 hours post infection. Infection rates were determined by counting $>$ 200 phagocytes. Depicted are infection rates as percentages of infected MF. Data are shown as means $\pm$ SEM, n = 4. $*$ P-value < 0.05. C)+D) Represatative EM micrpgraghs of 3 independent experiments of MF II infected with stat-phase promastigotes (C) or axenic amastigotes (D) 18 hours post infection.

3.9 Arginase in infected MF

In addition to *L. major* parasite stage differentiation inside phagolysosomes, parasites are either degraded by the infected MF or manage to survive inside the host MF. After the analysis of different parasite uptake and cell surface markers as well as the cytokine production of infected MF, we wanted to know what happens to the engulfed parasites in the different phenotypes of MF. Fully activated MF are known to eliminate intracellular *L. major* parasites, whereas "alternatively" activated MF were demonstrated to have an induced arginase pathway, which is regulated opposite to nitric oxide synthase II expression. Activation of arginase is shown to enhance *L. major* parasite replication and persistence in MF [75, 65, 206]. In order to investigate which mechanisms could be responsible for the different infection rates in pro-inflammatory MF I and anti-inflammatory MF II, we analyzed the gene expression and enzyme activity of arginase in both MF I and II after infection.
We found no significant differences in the arginase activity upon *L. major* promastigote or amastigote infection, neither in MF I nor in MF II (fig. 38 A + B). Moreover, the arginase gene expression showed no significant differences in MF I and MF II and an infection with *L. major* resulted in no effects on the expression of arginase (fig. 38 C + D).

3.10 Cathelicidin (LL-37) in infected MF

The different phenotypes of MF we found to show different infection rates, accompanied by differential cell signaling and resulted in phenotype specific cytokine production of infected MF. Furthermore, we could observe a clearance of the *L. major* parasites after 5 days in both MF I and II (data not shown). Therefore we wanted to investigate which processes are involved in intracellular *L. major* parasite degradation. In the murine model inducible nitric oxide synthases (iNOS) are well characterized to be important for the killing of *Leishmania* [100, 66]. However, for the human system the involvement of iNOS has been discussed controversy (reviewed by [132]. Since we were not able to detect iNOS activation in both phenotypes of human MF, we searched for other antimicrobial molecules in pro-inflammatory MF I and anti-inflammatory MF II.

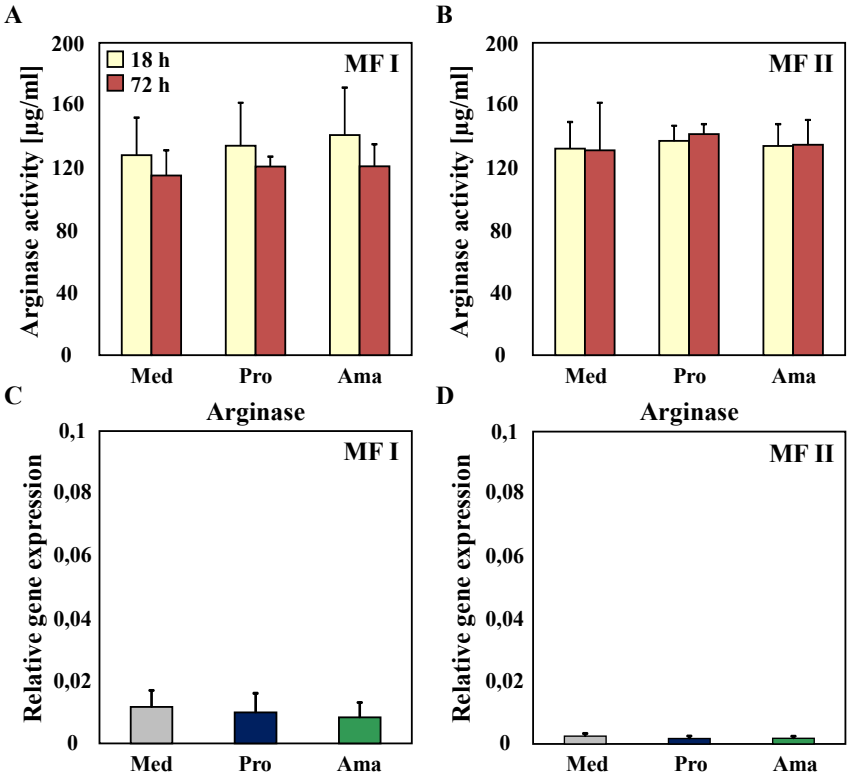

Figure 38: Arginase activity and mRNA expression in human MF after infection with *L. major* parasites: Pro-inflammatory MF I and anti-inflammatory MF II were infected with stat-phase promastigotes or axenic amastigotes. Extracellular parasites were removed 3 hours post infection and cells were harvested 18 and 72 hours post infection for arginase activity determination and mRNA expression analysis. A)+B) Arginase activity in MF I and MF II after 18 (yellow bars) and 72 (brown bars) hours, n = 3. C)+D) Total RNA was isolated, cDNA generated and the relative gene expression was determined by LightCycler analysis in medium controls (grey bars), promastigote infected (blue bars) and amastigote infected (green bars) MF I and MF II, n = 5. Data are shown as means ± SEM. $*$ P-value $<$ 0.05.

3.10.1 Different LL-37 expression in MF I and MF II

Using RT-PCR we found a significant higher gene expression of LL-37 in pro-inflammatory MF I as compared to anti-inflammatory MF II (0.14 ± 0.07, fig. 39 A). Furthermore, we also monitored the LL-37 expression upon *L. major* infection and found no significant differences after the infection with both parasite life stages, neither in MF I nor in MF II (fig. 39 B + C). However, human cathelicidin, also named LL-37, revealed to be a promising candidate for *L. major* parasite degradation, because of its effective antimicrobial activity against a variety of pathogens [187, 64, 12, 71].

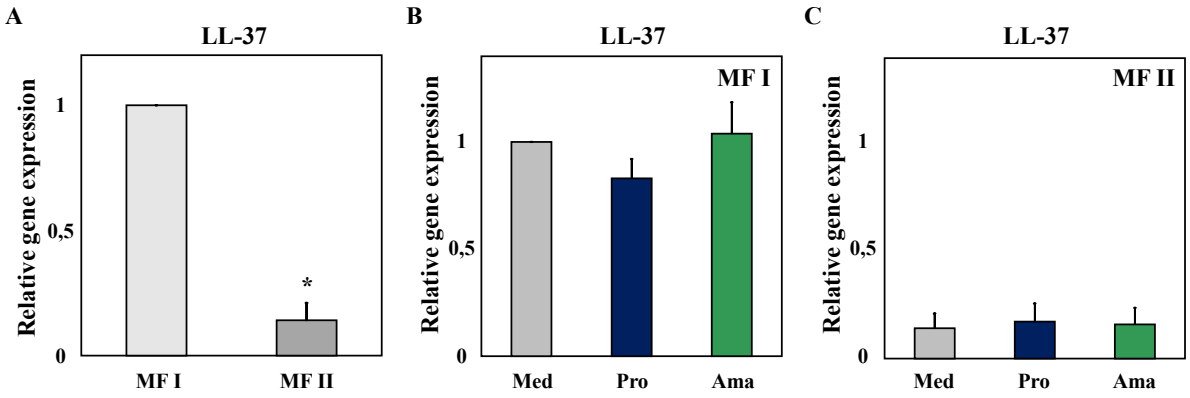

Figure 39: Different cathelicidin (LL-37) mRNA expression in human MF: Pro-inflammatory MF I and anti-inflammatory MF II were infected with stat-phase promastigotes or axenic amastigotes. Extracellular parasites were removed 3 hours post infection and cells were harvested 18 hours post infection from medium controls (grey bars), promastigote infected MF (blue bars) and amastigote infected MF (green bars). Total RNA was isolated, cDNA generated and the relative gene expression was determined by LightCycler analysis. Depicted are fold mRNA change compared to medium control of MF I. A) LL-37 mRNA expression of control pro-inflammatory MF I (light grey) and anti-inflammatory MF II (dark grey). B) LL-37 mRNA expression of pro-inflammatory MF I. C) LL-37 mRNA expression of anti-inflammatory MF II. Data are shown as means ± SEM, n = 5. $*$ P-value < 0.05.

3.10.2 Killing effect of rhLL-37 on *L. major* promastigotes

In order to investigate whether human LL-37 is able to be involved in the degradation of *L. major*, the parasites were treated with different concentrations of the recombinant human LL-37 (rhLL-37).

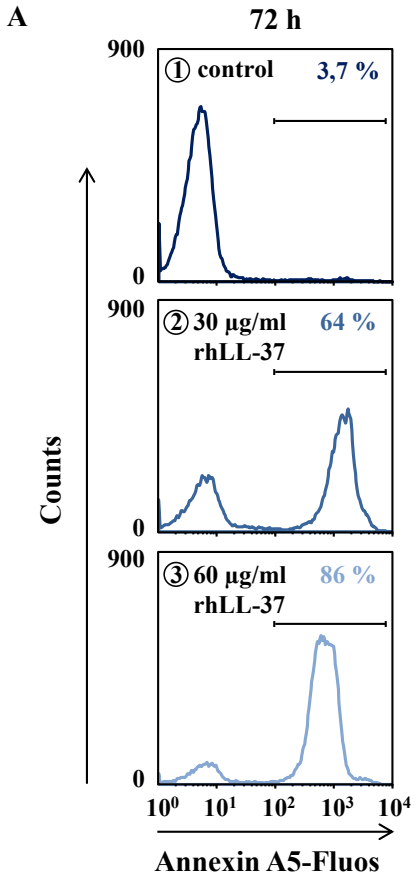

Figure 40: Crucifying effect of rhLL-37 on *L. major* promastigotes: Log-phase promastigotes were incubated with 30 μg/ml and 60 μg/ml recombinant human LL-37 (rhLL-37) for 72 hours. After treatment the parasites were stained for phosphatidylserine exposure with Annexin A5-Flous (AnxA5). A) Representative FACS histograms of one experiment out of 4 independent experiments. Log-phase control promastigotes (1), 30 μg/ml rhLL-37 treated promastigotes (2) and 60 μg/ml rhLL-37 treated promastigotes (3) with the percentages of AnxA5 positive parasites inside the indicated gate.

Using FACS analysis we found a significant increase in the percentage of PS positive apoptotic promastigotes after the treatment with 30 μg/ml rhLL-37 from 6.1 % $\pm$ 1.6 in untreated parasites to 63.3 % $\pm$ 8 in LL-37 treated promastigotes (fig. 41 A). And after the incubation with 60 μg/ml rhLL-37, there was an even higher increase of PS positive promastigotes to 91.3 % $\pm$ 2.1. Moreover, the end-point titration assay which is a more quantitative method to monitor parasite survival revealed that only 13.4 % $\pm$ 3.4 of the treated promastigotes remained viable after 30 μg/ml rhLL-37 treatment

(fig. 41 B). An even higher decrease of viable promastigotes to 0.07 % ± 0.03 was found after the treatment with 60 μg/ml rhLL-37, compared to 100 % viable parasites in the untreated control.

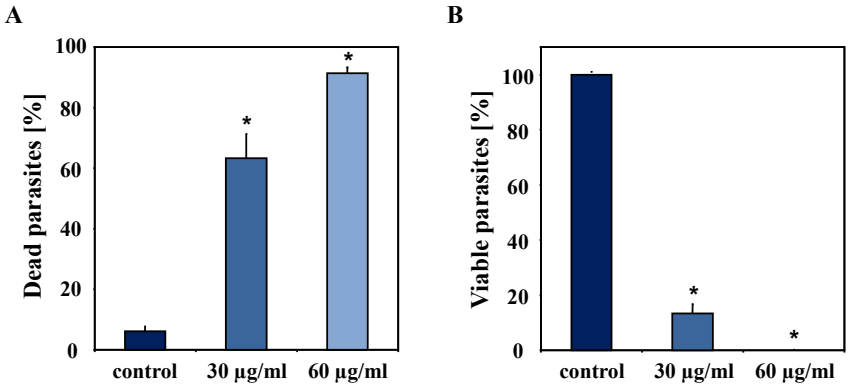

Figure 41: Killing effect of rhLL-37 on *L. major* promastigotes: Log-phase promastigotes were incubated with 30 μg/ml and 60 μg/ml recombinant human LL-37 (rhLL-37) for 72 hours. After treatment parasites were stained for phosphatidylserine exposure with Annexin A5-Flous (AnxA5) and end-point titration assay was performed. A) Phosphatidylserine exposure on the cell surface of log-phase control promastigotes (dark blue), 30 μg/ml rhLL-37 treated promastigotes (blue) and 60 μg/ml rhLL-37 treated promastigotes (light blue). Depicted are percentages of AnxA5 positive parasites. B) Viability of the promastigotes after the different treatments with rhLL-37. Depicted are percentages of viable parasites. Data are shown as means ± SEM, n = 4. $*$ P-value < 0.05.

In addition to the analysis of the PS staining by FACS, we analyzed the parasites via fluorescence microscopy (fig. 42). Untreated control promastigotes were found to have elongated bodies and show no green fluorescence of the AnxA5-Fluos, which indicates them to be viable (fig. 42 A). In contrast, after the incubation with 30 μg/ml rhLL-37 the promastigotes revealed to be rounded up and PS positive, as shown by the green AnxA5-Fluos staining which indicates this promastigotes to be apoptotic (fig. 42 B).

3.10.3 No effect of rhLL-37 on *L. major* amastigotes

For the amastigote life stage of *L. major*, we found no significant differences in the percentage of PS positive parasites compared to untreated amastigotes, neither after the treatment with 30 nor 60 μg/ml rhLL-37 (fig. 43 A). In concordance to the FACS

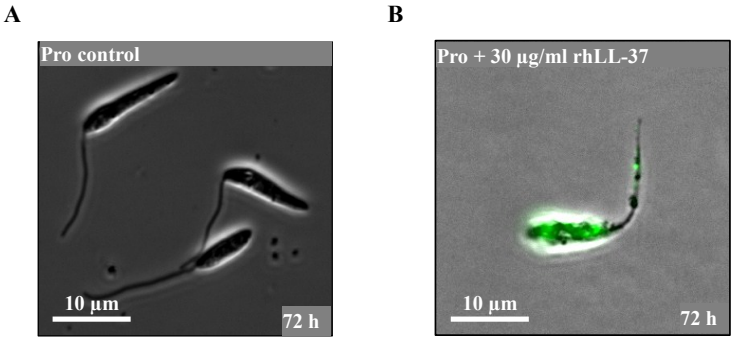

Figure 42: Morphology of rhLL-37 treated *L. major* promastigotes: Representative phase contrast micrographs of Annexin A5-Fluos (green) stained *L. major* promastigotes analyzed by fluorescent microscopy. A) Micrograph of control promastigotes after 72 hours. B) Micrograph of promastigotes treated with 60 μg/ml recombinant human LL-37 for 72 hours, displaying an apoptotic parasite. Bars indicating 10 μm.

analysis, the end-point titration assay revealed also no effect of rhLL-37 on the survival of the treated amastigotes compared to 100 % viable parasites in the untreated control (fig 43 B).

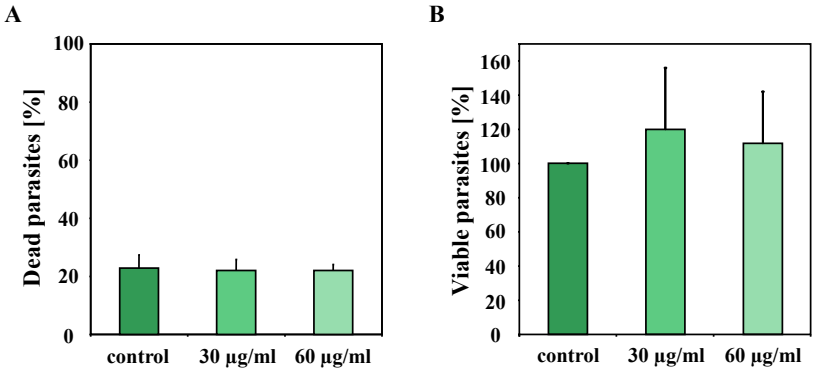

Figure 43: No effect of rhLL-37 on *L. major* amastigotes: Axenic amastigotes were incubated with 30 μg/ml and 60 μg/ml recombinant human LL-37 for 72 hours. After treatment parasites were stained for phosphatidylserine exposure with Annexin A5-Flous (AnxA5) and end-point titration assay was performed. A) Phosphatidylserine exposure on the cell surface of control amastigotes (dark green), 30 μg/ml rhLL-37 treated amastigotes (green) and 60 μg/ml rhLL-37 treated amastigotes (light green). Depicted are the percentages of AnxA5 positive parasites. B) Viability of the amastigotes after the different treatments with rhLL-37. Depicted are percentages of viable parasites. Data are shown as means $\pm$ SEM, n = 4. $*$ P-value < 0.05.

3.10.4 Knockdown of LL-37 in human MF

We found the gene expression of LL-37 to be up-regulated in the pro-inflammatory MF I as compared to anti-inflammatory MF II. Since LL-37 was reported to have effective microbicidal activity against a wide range of pathogens [187, 64, 12, 71], we treated both parasite life stages with human recombinant LL-37. The resulting dose dependent killing effect was only detected for the promastigote life stage. Amastigotes were not affected by LL-37. Finally we wanted to investigate whether LL-37 is also able to degrade intracellular *L. major* parasites inside infected MF. Therefore a knockdown for LL-37 was established in primary human MF. Different Transfection kits and protocols were tested to achieve a reliable knockdown for LL-37. The "Transfection kit" from Qiagen reached knockdown efficiencies only up to 9 % for MF I and 50 % for MF II, in addition it provided unreliable results. Another kit, the "Stemfect RNA Transfection kit" from Stemgent achieved knockdown efficiencies up to 87 % for MF I and 92 % for MF II. With this kit we were able to accomplish stable results for the LL-37 knockdown efficiency. Furthermore, different incubation times were tested for the transfection to gain the optimum between the viability of the cells and an adequate knockdown. The incubation of the MF for 7 hours with the siRNA revealed to meet this goal most adequate (data not shown).

3.10.4.1 Infection and parasite burden

To investigate whether LL-37 is involved in intracellular parasite elimination, we analyzed the infection rates and parasite uptake in LL-37 knockdown and control MF after the infection with *L. major* parasites in both phenotypes of MF. We found no significant differences in the infection rates between the knockdown MF and the controls for both MF I and II (data not shown). Furthermore, the parasite burdens showed no different parasite uptake after 18 hours (fig. 44 A - D). However, after 48 hours we found significant higher parasite burdens in LL-37 knockdown pro-inflammatory MF I only upon promastigote infection with 5.9 $\pm$ 0.2 as compared to nonsense control MF I with 3.2 $\pm$ 0.6 (fig. 44 A). In contrast, for anti-inflammatory MF II we could not detect any differences in parasite burdens after 48 hours.

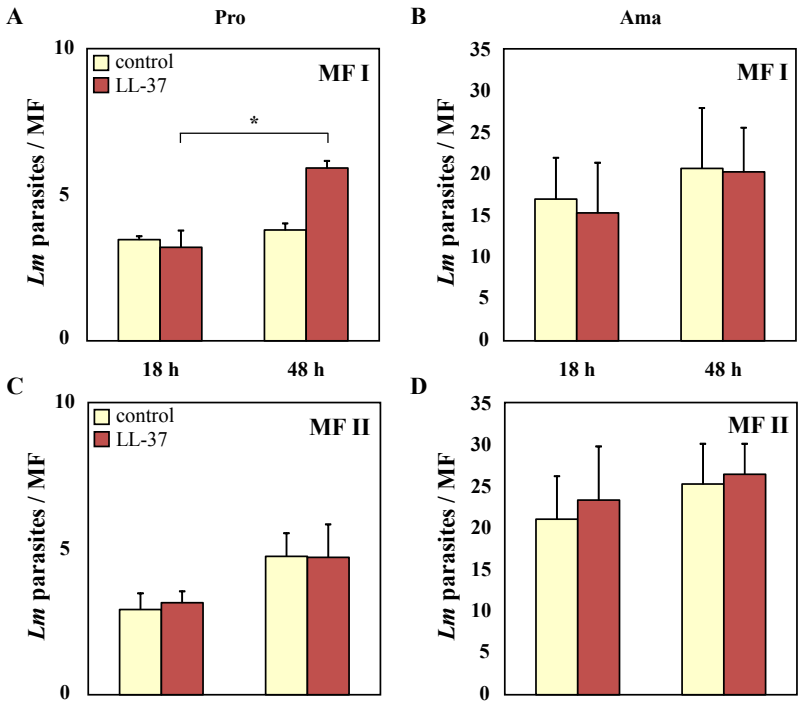

Figure 44: Parasite burden in LL-37 knockdown pro-inflammatory and anti-inflammatory human MF: MF I and MF II were treated with control nonsense siRNA (yellow bars) and LL-37 siRNA (brown bars) to maintain a knockdown. MF were co-incubated with stat-phase promastigotes or axenic amastigotes, extracellular parasites were removed 3 hours post infection, 18 and 48 hours post infection cells were Diff QUIK® stained and parasite burdens were assessed by counting intracellular parasites in 20 infected MF. Depicted are the number of parasites per MF. A)+B) Parasite burdens in pro-inflammatory MF I. C)+D) Parasite burdens in anti-inflammatory MF II. Data are shown as means ± SEM, n = 3. $*$ P-value < 0.05.

3.10.4.2 Survival of *L. major* parasites in knockdown MF

A more sensitive and quantitative method to analyze intracellular parasite survival of *L. major* is the end-point titration assay. Therefore this method was also performed to determine intracellular parasitic survival in LL-37 knockdown and control MF of both phenotypes. In concordance with the results of the parasite burdens, we found again a significant higher number of viable parasites per 1000 MF (681.9 $\pm$ 139.8) only in the LL-37 knockdown of pro-inflammatory MF I and only after promastigote infection as compared to nonsense control MF I (227.2 $\pm$ 58.9, fig. 45 A - D). Furthermore, amastigote infected LL-37 knockdown MF I were found to showed a trend to higher numbers of viable parasites in knockdown cells with a p-value of 0.1 (fig. 45 C).

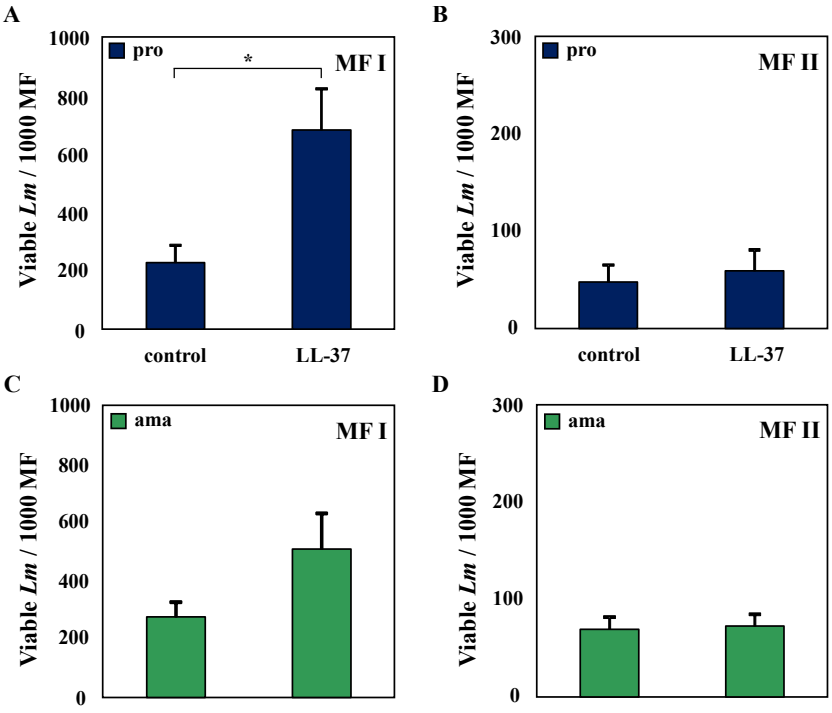

Figure 45: Survival of *L. major* parasites in LL-37 knockdown pro- and anti-inflammatory human MF: MF I and MF II were treated with control siRNA and LL-37 siRNA to maintain a knockdown. MF were co-incubated with stat-phase promastigotes (blue bars) or axenic amastigotes (green bars), extracellular parasites were removed 3 hours post infection, MF were harvested 18 hours post infection and an end-point titration assay was performed. Depicted are the number of viable parasites per 1000 MF. A) Viable parasites in pro-inflammatory MF I after promastigote infection. B) Viable parasites in anti-inflammatory MF II after promastigote infection. C) Viable parasites in pro-inflammatory MF I after amastigote infection. D) Viable parasites in anti-inflammatory MF II after amastigote infection. Data are shown as means ± SEM, n = 4. $*$ P-value < 0.05.

4 Discussion

First we characterized both life stages of *L. major* FEBNI parasites, promastigotes as well as amastigotes. We found that in contrast to previous findings the virulence marker GP63 was also expressed by axenic amastigotes. In addition to the *L. major* FEBNI strain, we applied and successfully modified our novel *in vitro* method to generate axenic amastigotes of the *L. major* Friedlin and 5ASKH strains. Interestingly, these *L. major* strains needed another temperature to be transferred into amastigotes in the axenic culture system. Investigating apoptotic mechanisms in both parasite life stages of *L. major* FEBNI we found both ROS dependent and ROS independent cell death mechanisms. Focusing on promastigote and amastigote interaction with pro-inflammatory (MF I) and anti-inflammatory (MF II) macrophages we found amastigotes to be more infective as compared to promastigotes. Moreover, we could demonstrate that pro-inflammatory MF I were less susceptible to infection as compared to anti-inflammatory MF II. Finally we investigated parasite stage specific macrophages (MF) responses and defense mechanisms against *L. major*. We identified a new mechanism in MF enabling killing of promastigotes. This mechanism depends on the antimicrobial molecule cathelicidin, LL-37.

Part 1

4.1 Different life stages of the parasite *L. major*

Characterizing the generated axenic amastigotes on a genetic level, we could demonstrate that they showed the same stage-specific gene expression as compared to MF-derived amastigotes focusing on markers such as ABC and Sherp. Analyses of the virulence factor GP63 revealed an up-regulation in the amastigote life stage. In con-

trast, using mouse derived *L. major* amastigotes Schneider et al. reported GP63 to be only expressed in promastigotes, but not in the amastigote life stage [170]. However, for *L. major*, seven distinct genes are described on chromosome 10, which can encode for the protein GP63 [204]. We analyzed the gene expression of the GP63 gene 3. Furthermore, for all *Leishmania* species studied to date GP63 is reported to be encoded by a multigene family [33, 208, 115, 204]. Here the GP63 genes are arranged in one gene locus containing several tandemly repeated genes and additional dispersed genes from this tandem array. We suggest that these distinct genes for GP63 could be expressed differently during the different life stages of the *L. major* parasites. In addition, such a stage-specific expression of the structurally distinct GP63 genes was already shown for *L. mexicana* [116, 115]. Here three different gene classes were found for the GP63 gene family: C1 - 3. Only the C1 gene class is up-regulated and transcribed in amastigotes, while the C2/3 gene classes are expressed in promastigotes [161]. A comparable C1 gene class for GP63 was also found in *L. donovani* [153]. Although there are no reports for such gene classes in *L. major* to date, these findings support our suggestion of a stage-dependent expression of the different GP63 genes in *L. major*.

Investigating GP63 on the protein level, we found GP63 to be almost absent on the cell surface of amastigotes. In contrast, log-phase promastigotes showed a high surface expression of GP63, which was decreased but still present on stat-phase promastigotes (data not shown). GP63 is encoded by several distinct genes, which may be expressed stage-specifically in *L. major* parasites. We hypothesize that the distinct GP63 genes code for GP63 proteins, which are structurally different in the amastigote and promastigote life stage. This may result in a different surface distribution of the distinct GP63 proteins. In agreement, Medina-Acosta et al. found in *L. mexicana* such a differential posttranslational processing and localization of GP63 proteins in amastigotes as compared to promastigotes [116, 115]. These alterations of GP63 in the different life stages could lead to an altered 3-dimensional conformation and surface distribution of GP63, which may be stage-specific. Moreover, Medina-Acosta et al. reported a lack of the promastigote characteristic "membrane-form" of GP63 on the amastigote cell surface of *L. mexicana*, whereas it was present within the flagellar pocket of the parasite [116]. In addition, they demonstrated that altered GP63 proteins were the most abundant proteins on the surface of the amastigote life stage and that different antibodies raised against GP63 showed different reactivity to both life stages, being promastigote

or amastigote specific [116]. The monoclonal antibody for GP63 used for FACS analysis in this study was generated for *L. major* promastigote specific recombinant GP63 [34], resulting in binding only to a specific GP63 protein structure. GP63 proteins which are structurally different cannot be detected by this antibody. This would explain the absence of GP63 detection on axenic amastigotes by FACS analysis in our results.

As it was described for *L. mexicana*, there is a different gene expression of the three GP63 gene clusters C1 - 3 in promastigotes and amastigotes [161]. Our data suggest such a stage-specific gene expression of GP63 genes also in *L. major* parasites. Furthermore, we would suggest an organization of the seven GP63 genes in gene clusters as compared to *L. mexicana* [161]. We suggest that the analyzed GP63 gene 3 belongs to a gene cluster which is up-regulated during the amastigote life stage. Since there is no data concerning such gene clusters for *L. major* parasites. This should be investigated using our new *in vitro* culture method to generate axenic *L. major* amastigotes.

4.2 *In vitro* culture method for axenic *L. major* amastigotes

Different factors are of importance to transform *L. major* promastigotes into amastigotes. In our axenic culture for *L. major*, we found the temperature to be critical. Using either 35°C or 31°C instead of 33°C we were able to generate *L. major* Friedlin and 5ASKH amastigote cultures in addition to *L. major* FEBNI. The different *L. major* isolates used in this study originate from different geographic regions, namely Israel (Friedlin) and the former Soviet Union (5ASKH). It has been described previously that *Leishmania* species differ in their sensitivity to temperature stress [224]. For *L. tropica* it was shown that amastigotes replicate more rapidly at 35°C than at 37°C, and are completely eliminated at 39°C [18]. Furthermore, the growth of *L. mexicana* is also reported to be temperature sensitive [21]. While parasites of this species grow and proliferate well within cultured MF at 34°C, infection does not proceed at 37.5°C. Similar findings were reported for *L. panamensis* [222, 162], where parasite survival is restricted to 33°C.

These reports all indicate that the temperature is of immense importance during the stage differentiation of the different *L. major* isolates, which are adapted to the local temperatures of their origin. Therefore we suggest that that the complex process of *L. major* stage differentiation and generation of axenic *in vitro* cultures is restricted to a narrow temperature range and depends on exact temperature settings fitting to the specific natural environmental conditions of the corresponding isolate and its origin.

4.3 Apoptosis in *L. major* parasites

To investigate the underlying processes of the apoptosis machinery in unicellular organisms, we aimed to analyze the different steps of the apoptotic cell death in *L. major* parasites and identify new proteins involved in the leishmanial apoptotic machinery. Inducing apoptosis with staurosporine we found a strong up-regulation of ROS accompanied by a time-delayed PS externalization and cell rounding in the promastigote life stage. In *Leishmania*, staurosporine is reported to strongly induce apoptosis resulting in PS externalization, cytochrome c release, DNA fragmentation and cell shrinkage [13, 9]. However, the exact mechanism of apoptosis induction is not known. Our data showed that there was first a high ROS formation after staurosporine treatment followed by PS externalization. This could indicate that *Leishmania* have a mitochondrial triggered apoptotic pathway similar as in mammalian cells [190, 191]. For *L. donovani* such a mitochondria-dependent ROS-mediated programmed cell death was reported by Roy et al. [160]. They found first a stimulation of mitochondrial generated ROS, followed by a depolarization of the mitochondrial membrane potential. Subsequently, the mitochondrial membrane disrupts, leading to the release of ROS together with cytochrome c into the cytosol of the parasite and finally resulting in DNA fragmentation [160]. These findings fit with our results after staurosporine treatment. Therefore a similar mechanism is conceivable also in *L. major* parasites for the induction of apoptosis by staurosporine. Another mechanism for staurosporine-induced apoptosis in *L. major* could be the induction of the endoplasmic reticulum (ER) stress-induced apoptotic pathway [46]. Here the exposure of the ER to stress leads to the elevation of the cytosolic Ca^{2+} level inside *L. major* parasites, due the release from internal stores. This causes mitochondrial membrane potential depolarization and ATP loss resulting in ROS-dependent

release of cytochrome c and subsequent PS externalization, DNA fragmentation and cell shrinkage [46]. We hypothesize staurosporine to be such an ER stress inducer resulting in activation of this pathway. To investigate whether the ER stress-induced apoptotic pathway is involved in the apoptotic process after staurosporine treatment, the cytosolic Ca^{2+} level should be analyzed in the parasites. However, both mechanisms are ROS-dependent and mediated by the mitochondrion of the parasite. This supports our assumption that staurosporine induce a mitochondrial triggered apoptotic pathway which is ROS-dependent.

Another apoptosis inducer for *Leishmania* parasites is the anti-leishmanial drug miltefosine. Previous studies demonstrated miltefosine to induce cell death in *L. major* promastigotes showing PS externalization, cell rounding and finally DNA fragmentation [51, 83]. The exact mechanism of miltefosine induced apoptosis is unknown. However miltefosine is known to affect the parasite membrane composition via the induction of changes in the biosynthesis of phospholipids [104]. Using miltefosine we found a strong PS externalization in *L. major* parasites, which was higher and much faster than after staurosporine treatment. Moreover, we observed a significant lower induction of ROS as compared to staurosporine induced leishmanial apoptosis. Downstream of the inhibition of phosphatidylcholine biosynthesis which is important for the integrity of the cell membrane, miltefosine was additionally demonstrated to be responsible for the increase of cellular ceramide after apoptosis induction in mammalian cells [213]. Such a ceramide-mediated apoptotic pathway, which is independent from ROS would fit to our results and could be a possible mechanism for apoptosis induction in *L. major* after miltefosine treatment. Moreover ceramide induced cell death is independent of caspase functions [193]. Since *Leishmania* do not have apoptosis regulating caspases [8], this suggest miltefosine to have an effect on the parasite cell membrane biosynthesis [104] and subsequent trigger a ceramide-mediated ROS independent apoptotic pathway. To investigate whether ceramide is involved in the apoptotic machinery of *L. major*, the cytosolic ceramide level needs to be analyzed. Another example for ROS independent apoptosis was reported for *L. donovani* after the treatment with Aloe vera leaf exudate (AVL) as a potent anti-leishmanial agent [49]. Here AVL was demonstrated to mediate the loss of mitochondrial membrane potential, cytochrome c release into the cytosol, PS externalisation and chromatin condensation. However, they found no increase in cytosolic Ca^{2+} or generation of intracellular ROS, indicating a ROS independent apop-

tosis pathway for the parasites [49]. The fast and strong impact of miltefosine on the PS exposure of the treated parasites, combined with the delayed low ROS formation suggest this drug to induce apoptosis via a ROS independent apoptotic pathway in *L. major* [104]. This is further supported by the finding of such a ROS independent apoptotic pathway for another drug (AVL) [49].

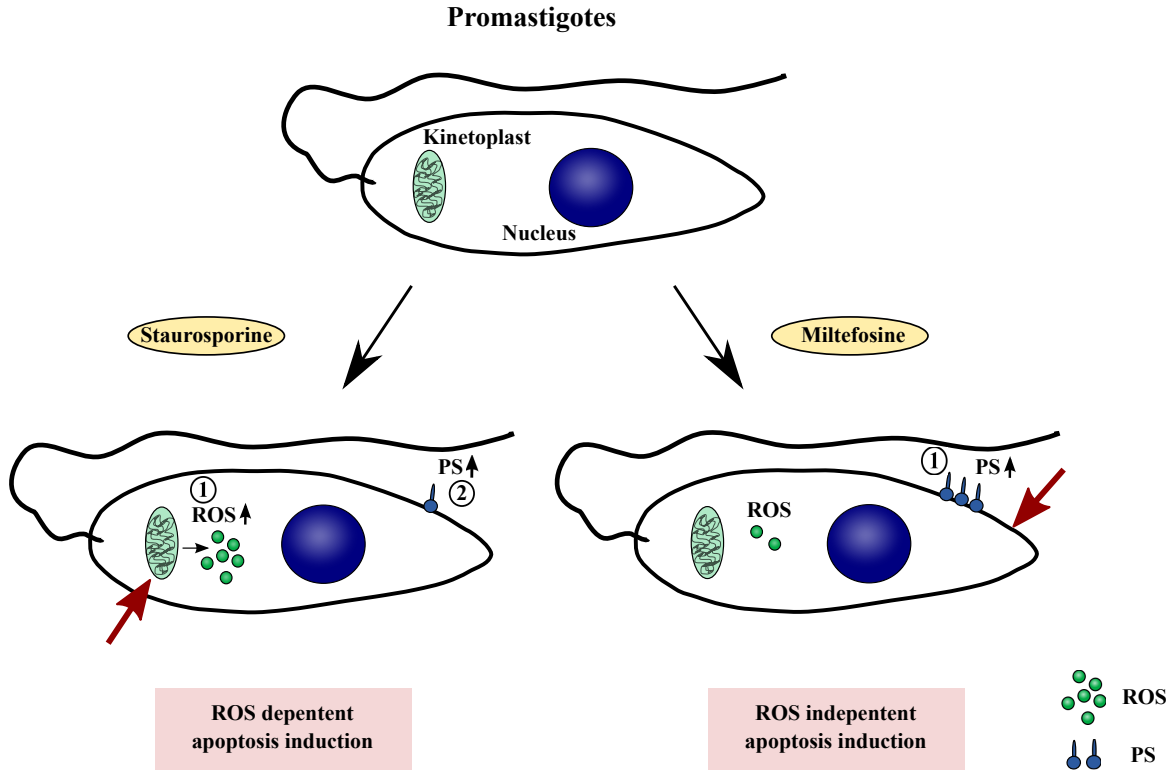

Figure 46: Overview of the different apoptotic mechanisms in *L. major* promastigotes. Viable *L. major* promastigotes show no phosphatidylserine (PS) externalization and no intracellular reactive oxygen species (ROS) formation. The induction of apoptosis with staurosporine and miltefosine results in two different apoptotic mechanisms. Staurosporine induces first an increase of intracellular ROS (1) and subsequently the externalization of PS (2), triggering a ROS dependent apoptotic pathway. Miltefosine treatment results only in the externalization of PS (1) without the involvement of ROS, leading to a ROS independent apoptotic pathway.

In contrast to *Leishmania* promastigotes, there is little known about apoptosis in the *Leishmania* amastigote life stage and the underlying mechanisms. Moreover nothing is known about *L. major* axenic amastigote apoptosis. The first reported apoptotic cell

death for axenic amastigotes was the nitric oxide (NO) induced cell death found by Lemesre et al. in several *Leishmania* species [99]. Further studies found *Leishmania* amastigotes to expose PS, induce ROS generation and show DNA fragmentation after apoptosis induction [70, 189]. As with promastigotes, the underlying mechanisms of the apoptotic pathway are still unclear. To investigate the characteristics of apoptosis in axenic *L. major* amastigotes, we first analyzed the viable parasites. Freshly isolated axenic *L. major* amastigotes were found to show in the viable and dividing constitution a high level of intracellular ROS in contrast to promastigotes. We suggest this high ROS level is due to the transformation of the parasites from the promastigote into the amastigote life stage. Besteiro et al. described the differentiation process for the different developmental stages in *Leishmania* to be associated with the autophagy machinery [20, 19]. They found several autophagy markers to be associated with the morphological transition between the developmental stages. In addition, the presence of ROS is shown to be essential for the autophagic process [169, 81]. These findings support our assumption that the high intracellular ROS concentration in the viable axenic amastigotes correlates with the stage differentiation of the parasites.

Apoptosis induction in axenic amastigotes using staurosporine resulted in a significant PS externalization of the parasites. Staurosporine was published to inhibit the growth of *L. donovani* axenic amastigotes [181]. However, our data are the first that demonstrate an apoptotic effect of staurosporine on *L. major* axenic amastigotes. Interestingly, we found staurosporine to down-regulate intracellular ROS in amastigotes, which was up-regulated in promastigotes. This data suggest staurosporine to induce a ROS dependent pathway in *L. major* amastigotes with a reversed role for ROS as compared to the promastigote life stage [181, 160].

Amastigote treatment with the anti-leishmanial drug miltefosine was demonstrated in previous studies to induce cell death in *L. donovani* axenic and intracellular amastigotes via DNA condensation and fragmentation [200, 201, 10]. We found miltefosine (50 μM) to result directly in an increased PS externalization without the involvement of ROS (data not shown). As mentioned above, miltefosine was reported to affect the parasite membrane composition [104] and subsequently to result in increased ceramide levels [213] leading to caspase independent cell death [193]. Together with these findings, our data suggests miltefosine to have an effect on the amastigote cell membrane biosynthesis and might subsequent trigger a ceramide-mediated ROS independent apoptotic

pathway as compared to the promastigote life stage.

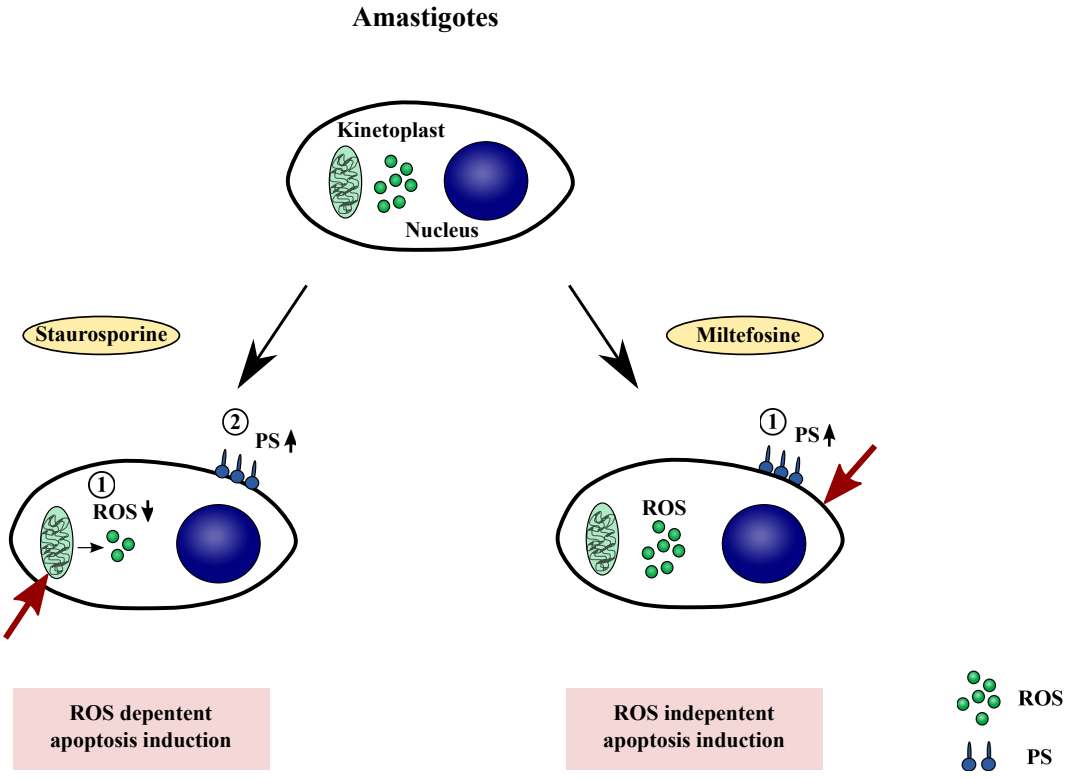

Figure 47: Overview of the different apoptotic mechanisms in *L. major* amastigotes. Viable *L. major* amastigotes show no phosphatidylserine (PS) externalization and a high intracellular reactive oxygen species (ROS) level due to stage differentiation. The induction of apoptosis with staurosporine and miltefosine results in two different apoptotic mechanisms. Staurosporine induces first a decrease of intracellular ROS (1) and subsequently the externalization of PS (2), triggering a ROS dependent apoptotic pathway. Miltefosine treatment results only in the externalization of PS (1) without the involvement of ROS, leading to a ROS independent apoptotic pathway.

Even though the exact biochemical mechanisms of the protozoan apoptotic machinery are poorly understood, there are a few proteins believed to be involved in apoptotic processes in *Leishmania*. For promastigotes it has been published that an activated nuclease similar to the endonuclease G (EndoG), migrates from the kinetoplast to the nucleus causing DNA degradation [157, 46]. Therefore *Leishmania* EndoG is suggested to be a pro-apoptotic protein. Another enzyme, the mitochondrial ascorbate peroxidase

(LmAPX) is known to inactivate ROS, which indicates this protein to inhibit a ROS-mediated cell death [47]. In order to elucidate the complex apoptotic machinery and identify the involved proteins, we generated lysates of *L. major* parasites after apoptosis induction and quantified a total of 707 proteins using mass spectrometry analysis (data not shown). We found several up- and down-regulated proteins upon apoptosis induction for both *L. major* life stages. These apoptosis dependent regulated proteins are potential candidates involved in the apoptotic machinery of *Leishmania*. Further analyses are under way to investigate their role in the course of apoptotic processes. The elucidation of the molecular pathways responsible for leishmanial apoptotic cell death might help to identify new target molecules for chemotherapeutic drug development and therapeutic intervention for cutaneous Leishmaniasis.

In conclusion, we found for the different parasite life stages of *L. major* two different pathways which could be involved in leishmanial apoptosis. One is ROS-mediated, which is induced by staurosporine and the second is independent from the formation of intracellular ROS, induced by miltefosine treatment. Furthermore, these mechanisms were found to be differently regulated between the two life stages of *L. major*.

Part 2

4.4 Interaction of *L. major* with human MF

Our aim was to investigate the interaction of *L. major* parasites with pro- and anti-inflammatory human MF in order to analyze which phenotype may be involved in disease propagation or healing. CD163, at typical marker for MF 2 was found to be down-regulated after treatment of MF II with LPS + INF gamma [126]. In addition, these reprogrammed MF II showed a higher antimicrobial activity compared to untreated MF II after the infection with *L. mexicana*. However, the adaption of the MF did not extend to all functions, such as the production of the cytokine IL-12 [126]. Another group demonstrated that the expression of CD163 is regulated by pro- and anti-inflammatory mediators like cytokines [30]. In monocytes CD163 expression was found to be strongly up-regulated by stimuli such as IL-6 and IL-10. On the other side LPS, INF gamma, and TNF alpha suppress the expression of CD163 [30]. These data suggest infected MF II to sort of change their phenotype towards the MF I phenotype after the infection with *L. major*. This was additionally supported by our findings of a down-regulation of CD163 on MF II after the infection with *L. major* parasites and a down-regulation of CD163 on mRNA level upon *L. major* promastigote infection.
Interestingly, uninfected MF I and MF II we found to show an equal expression of CD163 on the mRNA level, however we could not detect the CD163 receptor on the cell surface of MF I. A possible explanation could be a shedding of the receptor. Hintz and colleagues showed for monocytes pro-inflammatory stimuli like LPS to induce such a shedding of CD163 from the surface [69]. Therefore we suggest a swift extracellular shedding of CD163 to its soluble form, at the moment the protein reaches the cell membrane in MF I.

Upon infection, MF activation is needed for an effective immune response. In order to gain insights of possible MF activation, we analyzed the early intracellular activation state after the infection with *L. major* via the phosphorylation of mitogen-activated protein (MAP) kinases. We found in pro-inflammatory MF I the p38 MAP kinase to be activated after promastigote infection but down-regulated upon amastigote infection. On the other hand, preliminary data showed the ERK1/2 MAP kinases to

be down-regulated either after promastigote or amastigote infection. P38 activation is demonstrated to be involved in the induction of IL-12, while ERK1/2 MAP kinases (MAPK) suppress IL-12 transcription [52]. According to these findings, we detected the production of IL-12 only in MF I after the infection with *L. major* promastigotes. In contrast, the induction of IL-10 is shown to require the activation of both p38 and ERK1/2 MAPK [103]. Anti-inflammatory MF II were found to show such an activation of p38 and ERK1/2 MAPK upon the infection with either promastigotes or amastigotes. However, we detected only after promastigote infection the secretion of IL-10. This suggests the amastigote life stage of *L. major* to be able to inhibit the production of IL-10 despite the activation of p38 and ERK1/2. The underlying mechanisms of this phenomenon are still to be defined. However, our results showed that already after 15 min there are different activation patterns of p38 and ERK1/2 MAPK in the two phenotypes of MF after *L. major* infection. These data demonstrate that MF are able to respond in a very quick manner after parasite contact.

Furthermore, we wanted to study the consequences of a different susceptibility of both phenotypes of MF to *L. major* infection. As cytokine secretion is crucial for the development of an adaptive immune response, we investigate the cytokine profile and the underlying gene expression profile during *L. major* infection. In contrast to amastigote infection, promastigote infection induced an increase in TNF alpha in both MF I and II. In addition, we found the chemokines CCL3 and CCL4 to be up-regulated in MF I and II infected with promastigotes. These data demonstrate a specific MF activation occurring after promastigote uptake, whereas infection with amastigotes keeps the MF silenced and non-activated. The pro-inflammatory cytokine TNF alpha and the chemokines CCL3 and CCL4 are reported to be essential for the induction of local inflammatory responses [158]. Our results fit into the concept that the initial MF recruitment at the site of infection is mediated by TNF alpha and chemokines. However, the persistent infection and disease propagation is based on further transmission of the parasites to MF via the amastigote life stage inside the human host (reviewed by [79]). Therefore a silencing effect of amastigotes on MF would be more advantageous for disease propagation as previously found in mouse models [14, 209]. Thus, we suggest the amastigote life stage of *L. major* to be not involved in the initial TNF alpha mediated inflammatory response of infected MF.
As already reported, we also found the less susceptible MF I to produce the pro-

inflammatory cytokines TNF alpha and IL-12 [109, 202, 203]. These cytokines are also known to induce MF effector mechanism activation, leading to host defense against several pathogens including *Leishmania* [182, 56, 180, 3]. Moreover, IL-12 is a key cytokine driving the development of a protective Th-1 immune response in Leishmaniasis [156, 133]. Therefore we propose MF I to be the phenotype of MF involved in the initiation of a protective Th-1 mediated immune response, associated with parasite control and subsequent healing in human cutaneous Leishmaniasis.
Interestingly, anti-inflammatory MF II were found to secrete both anti-inflammatory IL-10 [202, 203, 88] as well as the pro-inflammatory TNF alpha upon *L. major* infection. This finding was first surprisingly. However as already mentioned, MF II are able to adapt their phenotype to pro-inflammatory MF I to a certain extent [126]. This might be the reason for pro-inflammatory cytokine expression of infected MF II. An explanation for the even higher TNF alpha secretion of MF II compared to MF I could be the fact that MF II manifest a higher infection rate. The cytokine production from a single MF II cell might be lower compared to MF I but the amount of cytokine producing cells is higher for MF II resulting in a higher combined TNF alpha secretion. In concordance with literature for the MF II adaption to the MF I phenotype [126], we found no IL-12 production from the altered MF II. These data additionally support our assumption of the ability of MF to adapt their phenotype upon the infection with *L. major*. Furthermore, MF II were found to secrete anti-inflammatory IL-10, which is reported to be the most common cytokine in Leishmaniasis patients [6]. In addition, IL-10 is demonstrated to decrease MF activation via down regulation of INF gamma and prevents effective parasite elimination [6, 7]. Together with the higher susceptibility of MF II to *L. major* parasites, these data indicate the MF II phenotype to be associated with a Th-2 mediated immune response, leading to parasite replication and disease propagation. To investigate this suggestion further studies are necessary, including the analyses of resulting T-cell activation and polarization after the infection with *L. major* parasites in the different phenotypes of human MF.

4.5 Clearance of *L. major* in human MF

Another aim was to investigate the degrading mechanisms of human MF that are responsible for the elimination of *L. major* parasites inside infected cells. We found MF I to clear *L. major* infection more efficiently as compared to MF II after 5 days of infection. This fit into our proposed concept of the pro-inflammatory MF I phenotype to be involved in protective immune response with subsequent healing. Furthermore, previous reports demonstrated in the murine system fully activated pro-inflammatory MF I to effectively eliminate intracellular *L. major* parasites, whereas "alternatively" activated MF (MF II) were demonstrated to have an induced arginase pathway [75, 65, 206]. Such activation of arginase was reported to be associated with an enhanced *L. major* parasite replication and persistence in MF [206]. Therefore we assumed a down-regulation of arginase in infected MF I, which would lead to a lower parasite replication or even more an inhibition of parasite survival. However, we did not find any significant differences neither for the arginase activity after infection nor the gene expression of arginase in MF I and II. This finding led to the assumption that there must be other mechanisms for parasite elimination in human MF.
An important killing mechanism in the mouse model of cutaneous Leishmaniasis is the inducible nitric oxide synthases (iNOS), which was shown to be involved in the clearance of *L. major* parasites [100]. There iNOS is responsible for the induction of nitric oxide (NO) radicals which are involved in the killing of the *Leishmania* parasites [100, 66]. However, for the human system the contribution of iNOS has been discussed controversy, as reviewed by Nussler et al. [132]. Since we were not able to detect iNOS activation in both MF I and II, we focused on the elucidation of other potential mechanisms that are involved in parasite clearance inside MF.

Interestingly we found a significant higher expression of cathelicidin (LL-37) in pro-inflammatory MF I as compared to anti-inflammatory MF II. LL-37 is a small antimicrobial peptide with a potent antimicrobial activity against a variety of pathogens [12, 48, 84]. The human CAP18 is processed into the active antimicrobial peptide LL-37 by the cleavage of its cathelicidin peptide domain with proteases like elastase or proteinase 3 [187]. The name of LL-37 is based on its two leucine residues in the beginning and its length of 37 amino acid residues [67]. The microbicidal activity of LL-37 re-

sults due to its binding to LPS residues and the subsequent disruption of the foreign cell membrane. Similar to defensins, LL-37 has also a chemotactic activity to neutrophils, monocytes and lymphocytes [29]. Originally LL-37 was found in neutrophils, but more recent studies showed LL-37 also present in many other cells including the (phago)lysosomes of MF [84], which makes LL-37 a potent candidate for *Leishmania* degradation. To investigate whether LL-37 has a microbicidal activity for *L. major*, we treated the parasites with recombinant human LL-37 (rhLL-37) and found indeed an efficient dose dependent killing effect for the promastigote life stage. Surprisingly, there was no degradation of the amastigote life stage by rhLL-37. Antimicrobial molecules such as LL-37 are cationic peptides and their charge is known to be an important mechanism for the binding to the attacked membrane [140, 221]. After binding to a foreign cell membrane, this membrane is subsequently disrupted leading to cell lysis and the elimination of the pathogen [221]. A possible explanation for the unaffected amastigotes could be a difference in their surface charge as compared to promastigotes. Such changes occurring in the surface charge during stage differentiation from promastigotes to amastigotes were demonstrated for *L. mexicana* [145]. Therefore we suggest that LL-37 is not able to bind to the amastigote cell membrane of *L. major*, causing the inefficiency of LL-37 for this life stage. Since cell-debris free and pure *L. major* amastigotes were not available in previous studies, there are no data concerning the charge of the cell membrane of *L. major* amastigotes. This should be investigated using our new *in vitro* culture method to generate axenic *L. major* amastigotes.

Since LL-37 is a potent killer of *L. major* promastigotes, we wanted to know whether LL-37 is able to eliminate intracellular parasites inside infected MF. Therefore a siRNA knockdown was established for LL-37 in primary human MF I and II. After the successful LL-37 knockdown, which was controlled by obtaining efficiency rates of not less than 85 %, the infection rates as well as the parasite survival was monitored. Anti-inflammatory MF II showed no differences in infection rates and parasite survival after *L. major* infection. As already mentioned LL-37 expression in MF II was strongly reduced compared to MF I, therefore we did not expect any measurable effects after a knockdown.

In contrast, we found a higher parasite survival in LL-37 knockdown of pro-inflammatory MF I compared to their corresponding nonsense controls, though we did not find any differences in the infection rates. This higher parasite survival was only detected in

L. major promastigote infected cells. Such a degradative influence of cathelicidin on *L. major* parasites was recently also reported in the mouse model, with the corresponding murine cathelicidin CAMP (or CRAMP) [89]. In mice the lack of CAMP expression was associated with higher levels of anti-inflammatory IL-10 and reduced production of pro-inflammatory IL-12 and IFN gamma. Furthermore, knockout mice for CAMP were reported to develop exacerbated lesions combined with a higher parasites distribution upon *L. major* infection as compared to wildtype mice [89]. These findings support the assumption that LL-37 is involved in *L. major* promastigote elimination in human MF I. In the knockdown MF I the intracellular LL-37 was strongly reduced, resulting in a lower parasite killing and subsequent higher parasite survival in the knockdown MF I. Moreover, we found a trend for higher parasite survival in knockdown MF I also after the infection with *L. major* amastigotes. This suggests intracellular amastigotes probably to be more sensitive towards LL-37 as compared to extracellular treatment. We hypothesize that the low pH-value inside phagolysosomes could have an effect on the amastigote surface and its charge leading to a more efficient LL-37 binding [221] and subsequent higher parasite elimination.

Interestingly, we did not find any up-regulation of the LL-37 gene expression upon *L. major* infection. However, we monitored the gene expression only 18 hours post infection. Therefore it would be interesting to analyze later time points. Furthermore, the induction of LL-37 could be a potent strategy to enhance the intracellular parasite elimination inside MF. An induction mechanism for LL-37 was demonstrated by Liu et al. via the pro-vitamin D_3 hormone [101]. The active form of vitamin D_3 (1,25-dihydroxyvitamin D_3) which is generated by the enzymatic conversion of the inactive pro-vitamin D_3, binds to the vitamin-D receptor leading to an induction of LL-37 production [101]. Moreover, the induction of this vitamin D-mediated up-regulation of LL-37 is stimulated by the binding of IL-15 to the IL-15 receptor on the MF surface [120]. Thus, further research is required to investigate whether such an induction of LL-37 either via the stimulation of the vitamin-D receptor or the IL-15 receptor influence the outcome of *L. major* infection in human MF.

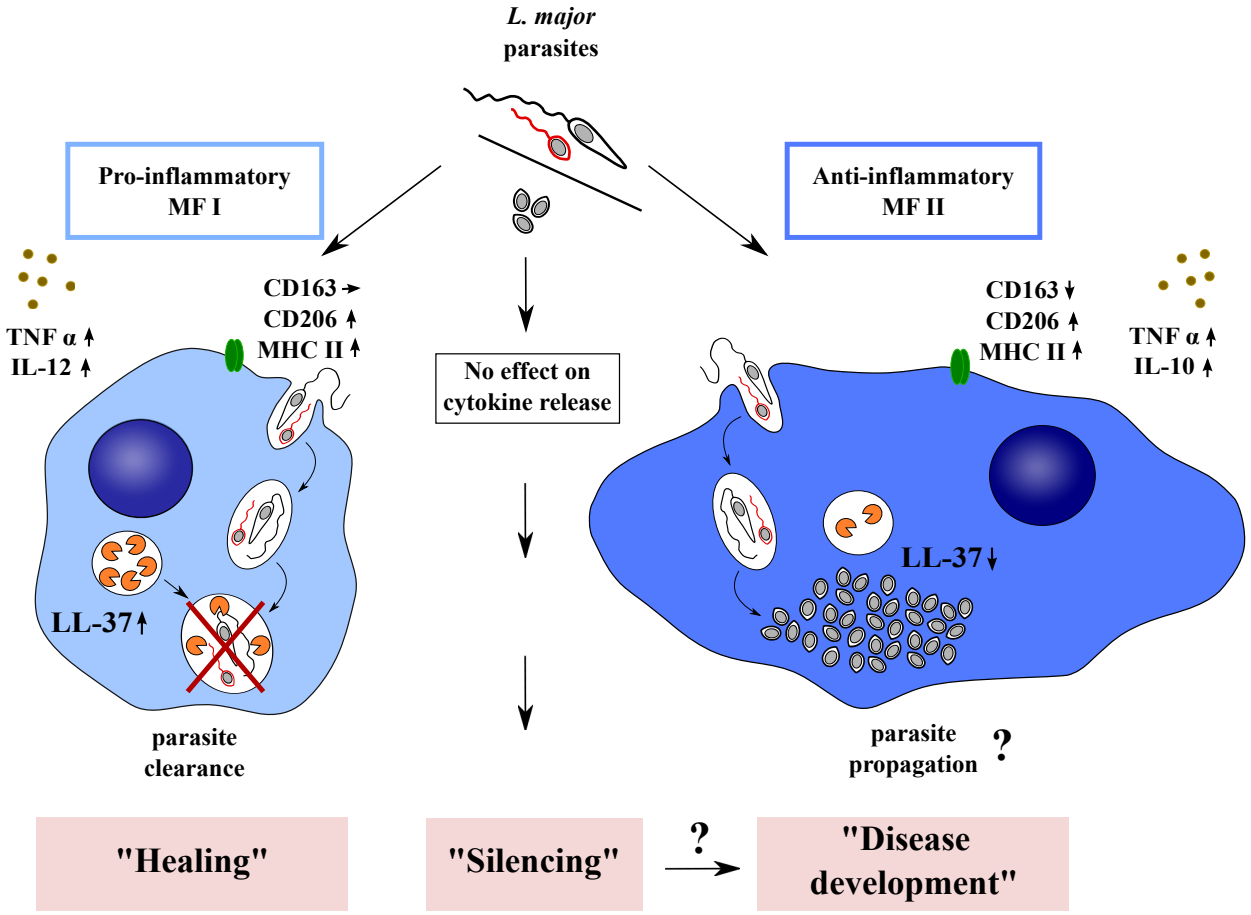

Figure 48: Overview of cell activation and *L. major* propagation in different phenotypes of human MF. *L. major* promastigotes and amastigotes are able to infect pro-inflammatory MF I and anti-inflammatory MF II. However, only the promastigotes result in cell response on activation markers and cytokine release. Amastigote infection leads to no effect in cytokine secretion in both phenotypes of MF, although they do show an up-regulation of surface activation markers (CD206 + MHC II). This suggests amastigotes to silence MF I and II resulting in parasite propagation. Upon promastigote infection, pro-inflammatory MF I respond in up-regulation of activation markers as well as the secretion of pro-inflammatory cytokines like TNF alpha and IL-12. Moreover, MF I express the antimicrobial cathelicidin (LL-37) which is able to degrade intracellular promastigotes. Therefore we suggest the MF I phenotype to be associated with disease healing. In contrast, anti-inflammatory MF II show cytokine production of anti-inflammatory IL-10 additional to the up-regulation of activation markers after promastigote infection. Furthermore, MF II express less LL-37, which is not sufficient to eliminate the promastigotes, leading to parasite propagation. Therefore we suggest the MF II phenotype might support disease development.

4.6 Concluding remarks

Taken together, the presented data demonstrates our axenic parasites to represent the multiplying amastigote life stage of *L. major*, which develops inside infected MF and is responsible for disease propagation. These parasites will be extremely useful for additional biological, biochemical and molecular studies on the intracellular stage of this parasite species itself as well as further investigations of the interaction with human host cells. Furthermore, the findings of this study and recent publications demonstrate *L. major* parasites to undergo apoptosis. In addition, we found at least two leishmanial cell death mechanisms, one dependent on ROS and one independent, which are differently regulated between the promastigote and amastigote life stages.

This study shows the pro- and anti-inflammatory phenotypes of human MF to respond differently upon the infection with *L. major* parasites. Disease inducing promastigotes result in pro-inflammatory MF I in the secretion of the pro-inflammatory cytokines TNF alpha and IL-12 combined with a lower susceptibility for infection. Therefore we suggest the MF I phenotype to be involved in the protective Th-1 mediated immune response and subsequent healing. In contrast, anti-inflammatory MF II produce anti-inflammatory IL-10 along with TNF alpha and show a higher susceptibility for *L. major* infection. Thus MF II are proposed to be associated with a disease propagating Th-2 mediated immune response, leading to disease establishment. Furthermore, we demonstrate the antimicrobial peptide LL-37 to efficiently kill axenic *L. major* promastigotes but not amastigotes in a dose dependent manner. Besides this, we found LL-37 to have an effect on the survival of intracellular *L. major* parasites in MF I.
Taken together we are the first to demonstrate LL-37 to have a leishmanicidal activity for *L. major* promastigotes in human primary MF. Further studies are required to investigate LL-37 as a potent candidate molecule for therapeutic intervention for cutaneous Leishmaniasis.

5 Summary

This study focused on the characterization of both life stages of *L. major* FEBNI parasites, promastigotes as well as amastigotes and their interaction with different phenotypes of human macrophages (MF). In this context, a novel *in vitro* method to generate *L. major* axenic amastigotes was applied and we found the *in vitro* generated *L. major* axenic amastigotes showed the same stage-specific gene expression as compared to MF-derived amastigotes. Moreover, we found the virulence factor GP63 to be stage-specific expressed and up-regulated in *L. major* axenic amastigotes. In addition, we successfully adapted the axenic culture system to generate axenic amastigotes from other *L. major* isolates such as Friedlin and 5ASKH. Interestingly we found this process to be dependent on isolate-specific temperature settings. Since there is only little know about apoptotic machinery of protozoan parasites we induced apoptosis in both promastigotes and amastigotes. We found two different apoptotic mechanisms in *L. major* parasites. One is dependent on reactive oxygen species (ROS) and one independent. These mechanisms were found to be regulated differentially in promastigotes and amastigotes.
In human disease it is still unclear which phenotype of MF is involved in disease development. Therefore we analyzed pro-inflammatory (MF I) and anti-inflammatory (MF II) MF. We found that *L. major* amastigotes infect both phenotypes of human MF better as compared to promastigotes. Furthermore, anti-inflammatory MF II are more susceptible to infection as compared to pro-inflammatory MF I. Analyzing possible "killing signaling", we found differential cytokine secretion in both phenotypes of MF. Interestingly, we found only after promastigote infection the release of cytokines. For MF I pro-inflammatory cytokines like TNF alpha and IL-12 were detected which are known to activate the cell and suggest MF I might clear parasite infection. In contrast, MF II secreted anti-inflammatory IL-10 upon infection indicating MF II to silence the cell and resulting in parasite propagation. Furthermore, we searched for intracellular

killing mechanisms of MF and found the antimicrobial peptide cathelicidin (LL-37) to be up-regulated in MF I as compared to MF II. LL-37 is located in lysosomes and is shown to be involved in the innate host defense against pathogens. Consistent with this, knockdown experiments for LL-37 demonstrated this peptide to be involved in the intracellular degradation of *L. major* promastigotes in human MF I.

In conclusion, this study suggests that pro-inflammatory MF I can eliminate *L. major* parasites via LL-37, whereas anti-inflammatory MF II might support disease development.

6 Zusammenfassung

Der Fokus dieser Arbeit lag auf der Charakterisierung beider Lebensstadien des Parasiten *L. major* FEBNI, der promastigoten und amastigoten Form, sowie deren Wechselwirkungen mit unterschiedlichen Phänotypen von humanen Makrophagen (MF). In diesem Zusammenhang wurde eine neue *in vitro* Methode zur Herstellung von *L. major* axenischen Amastigoten angewandt und dabei festgestellt, dass die *in vitro* generierten axenischen Amastigoten die gleiche stadium-spezifische Genexpression aufweisen wie Amastigote, die aus MF isoliert wurden. Des Weiteren konnte gezeigt werden, dass der Virulenzfaktor GP63 stadium-spezifisch exprimiert wird, wobei dieser in axenischen Amastigoten hochreguliert ist. Zusätzlich wurde die *in vitro* Kultivierungsmethode derart angepasst, sodass Amastigote auch aus anderen *L. major* Isolaten wie Friedlin und 5ASKH erfolgreich generiert werden konnten. Interessanterweise war dieser Prozess temperatursensitiv und abhängig von stamm-spezifischen Temperaturbedingungen. Da sehr wenig über das Apoptoseprogramm von einzelligen Parasiten bekannt ist, wurde sowohl in Promastigoten als auch in Amastigoten Apoptose induziert und dabei zwei verschiedene Mechanismen des programmierten Zelltods in *L. major* Parasiten gefunden. Der erste wird durch reaktive Sauerstoffspezies (ROS) vermittelt wohingegen der zweite unabhängig davon ist. Beide Mechanismen werden in Promastigoten und Amastigoten unterschiedlich reguliert.

In der humanen Leishmaniose ist bis heute nicht klar welcher Phänotyp von MF für die Krankheitsentstehung relevant ist. Deshalb haben wir sowohl pro-inflammatorische MF (MF I) als auch anti-inflammatorische MF (MF II) untersucht. Wir haben herausgefunden, dass *L. major* Amastigoten beide Phänotypen humaner MF besser infizieren als Promastigoten. Darüber hinaus sind anti-inflammatorische MF II viel anfälliger gegenüber einer Infektion verglichen mit pro-inflammatorische MF I. Die Analyse möglicher Signaltransduktionswege ergab Unterschiede in der Sekretion von Zytoki-

nen der beiden MF Phänotypen. Interessanterweise haben wir nur nach Infektion mit Promastigoten die Freisetzung von Zytokinen messen können. In MF I wurden pro-inflammatorische Zytokine wie TNF alpha und IL-12 nachgewiesen, die dafür bekannt sind MF zu aktivieren und darauf hinweisen, dass MF I die Infektion abwehren könnten. Im Gegensatz dazu sezernieren infizierte MF II anti-inflammatorisches IL-10 was darauf hindeutet, dass MF II in ihrer Immunreaktion gehemmt werden, was zur Vermehrung der Parasiten führen könnte. Darüber hinaus haben wir nach Abbaumechanismen von intrazellulären Parasiten in MF gesucht und haben gefunden, dass das antimikrobielle Peptid Cathelicidin (LL-37) in MF I im Vergleich zu MF II hochreguliert ist. LL-37 ist in Lysosomen zu finden und an der angeborenen Immunantwort im Kampf gegen Erreger beteiligt. Im Einklang dazu, haben unsere Knockdown Experimente für LL-37 gezeigt, dass LL-37 eine Rolle bei der intrazellulären Degradierung von *L. major* Promastigoten in MF I spielt.
Zusammenfassend legen die Ergebnisse dieser Dissertation nahe, dass pro-inflammatorische MF I *L. major* Parasiten mit Hilfe von LL-37 abtöten, wohingegen anti-inflammatorische MF II die Krankheitsentwicklung fördern könnten.

List of Figures

1 Life cycle of *Leishmania spp* 9
2 Distinct targets for apoptosis induction in *Leishmania* via different drugs 13
3 Overview of possible mechanisms for the clearance of *Leishmania* 18
4 Involved proteins during apoptosis in *L. major* parasites 20
5 Hypothesis for *L. major* parasite propagation in different phenotypes of human MF 21

6 RFLP analysis of the *Leishmania spp.* ITS1 marker 58
7 Morphology of log-phase *L. major* FEBNI promastigotes 59
8 Morphology of stat-phase *L. major* FEBNI promastigotes 60
9 Morphology of *L. major* FEBNI amastigotes 60
10 Annexin A5 staining of the different stages of *L. major* parasites 61
11 Stage-specific mRNA expression of SHERP and ABC-transporter homologue in *L. major* 62
12 Stage-specific mRNA expression of QDPR, alpha-tubulin, Cpb and GP63 in *L. major* 63
13 Stage-specific protein expression of LPG on the cell surface of *L. major* . 64
14 Stage-specific protein expression of LPG in *L. major* 65
15 Generation of *L. major* Friedlin axenic amastigotes 67
16 Phosphatidylserine externalisation after apoptosis induction in *L. major* FEBNI promastigotes 69
17 Formation of reactive oxygen species after apoptosis induction in *L. major* FEBNI promastigotes 70
18 Modulation of markers after apoptosis induction in *L. major* FEBNI promastigotes 71

19 Modulation of markers after apoptosis induction in *L. major* FEBNI amastigotes 72
20 Viable and apoptotic *L. major* FEBNI parasites in flow cytometry 73
21 Infected human MF with *L. major* parasites 76
22 Stage-specific interaction of *L. major* parasites with human MF 77
23 Characteristics of *L. major* FEBNI eGFP parasites 79
24 *L. major* eGFP parasite development in different types of human MF . . 80
25 Downregulation of CD163 on the cell surface in human MF II after infection with *L. major* parasites 82
26 Downregulation of CD163 on the cell surface and mRNA expression in human MF II after infection with *L. major* parasites 83
27 Up-regulation of CD206 on the cell surface in human MF after infection with *L. major* parasites 84
28 Up-regulation of MHC II on the cell surface in human MF after infection with *L. major* parasites 85
29 Up-regulation of CD86 on the cell surface in human MF after infection with *L. major* parasites 87
30 Different cytokine production of TNF alpha in human MF after infection with *L. major* parasites 88
31 Different cytokine production of IL-12 in human MF after infection with *L. major* parasites 90
32 Different cytokine mRNA expression of CCL3 and CCL4 in human MF after infection with *L. major* parasites 91
33 Different cytokine production of IL-10 in human MF after infection with *L. major* parasites 92
34 Different phosphorylation state of p38 and p44/42 (ERK1/2) MAP kinases (MAPK) in human type I MF after infection with *L. major* parasites 94
35 Different phosphorylation state of p38 MAP kinases (MAPK) in human MF after infection with *L. major* parasites 96
36 Different phosphorylation state of ERK1/2 MAP kinases (MAPK) in human MF after infection with *L. major* parasites 97
37 Infection rates after concanamycin A treatment and parasite location in human MF after *L. major* infection 99

38 Arginase activity and mRNA expression in human MF after infection with *L. major* parasites 101
39 Different cathelicidin (LL-37) mRNA expression in human MF 102
40 Crucifying effect of rhLL-37 on *L. major* promastigotes 103
41 Killing effect of rhLL-37 on *L. major* promastigotes 104
42 Morphology of rhLL-37 treated *L. major* promastigotes 105
43 No effect of rhLL-37 on *L. major* amastigotes 105
44 Parasite burden in LL-37 knockdown pro-inflammatory and anti-inflammatory human MF 107
45 Survival of *L. major* parasites in LL-37 knockdown pro-inflammatory and anti-inflammatory human MF 109

46 Overview of the different apoptotic mechanisms in *L. major* promastigotes 116
47 Overview of the different apoptotic mechanisms in *L. major* amastigotes 118
48 Overview of cell activation and *L. major* propagation in different phenotypes of human MF 126

Bibliography

[1] M. S. Alcouloumre, M. A. Ghannoum, A. S. Ibrahim, M. E. Selsted, and J. E. Edwards. Fungicidal properties of defensin np-1 and activity against cryptococcus neoformans in vitro. *Antimicrob Agents Chemother*, 37(12):2628–2632, Dec 1993.

[2] J. Alexander, A. R. Satoskar, and D. G. Russell. Leishmania species: models of intracellular parasitism. *J Cell Sci*, 112 Pt 18:2993–3002, Sep 1999.

[3] Cindy Allenbach, Pascal Launois, Christoph Mueller, and Fabienne Tacchini-Cottier. An essential role for transmembrane tnf in the resolution of the inflammatory lesion induced by leishmania major infection. *Eur J Immunol*, 38(3):720–731, Mar 2008.

[4] Jorge Alvar, Sergio Yactayo, and Caryn Bern. Leishmaniasis and poverty. *Trends Parasitol*, 22(12):552–557, Dec 2006.

[5] J. F. Alzate, A. Alvarez-Barrientos, V. M. González, and A. Jiménez-Ruiz. Heat-induced programmed cell death in leishmania infantum is reverted by bcl-x(l) expression. *Apoptosis*, 11(2):161–171, Feb 2006.

[6] Charles F Anderson, Susana Mendez, and David L Sacks. Nonhealing infection despite th1 polarization produced by a strain of leishmania major in c57bl/6 mice. *J Immunol*, 174(5):2934–2941, Mar 2005.

[7] Charles F Anderson, Mohammed Oukka, Vijay J Kuchroo, and David Sacks. Cd4(+)cd25(-)foxp3(-) th1 cells are the source of il-10-mediated immune suppression in chronic cutaneous leishmaniasis. *J Exp Med*, 204(2):285–297, Feb 2007.

[8] L. Aravind, V. M. Dixit, and E. V. Koonin. Apoptotic molecular machinery: vastly increased complexity in vertebrates revealed by genome comparisons. *Science*, 291(5507):1279–1284, Feb 2001.

[9] D. Arnoult, K. Akarid, A. Grodet, P. X. Petit, and J. Estaquier sand J. C. Ameisen. On the evolution of programmed cell death: apoptosis of the unicellular eukaryote leishmania major involves cysteine proteinase activation and mitochondrion permeabilization. *Cell Death Differ*, 9(1):65–81, Jan 2002.

[10] Samira Azzouz, Mimoun Maache, Ramon Gil Garcia, and Antonio Osuna. Leishmanicidal activity of edelfosine, miltefosine and ilmofosine. *Basic Clin Pharmacol Toxicol*, 96(1):60–65, Jan 2005.

[11] V. Bahr, Y. D. Stierhof, T. Ilg, M. Demar, M. Quinten, and P. Overath. Expression of lipophosphoglycan, high-molecular weight phosphoglycan and glycoprotein 63 in promastigotes and amastigotes of leishmania mexicana. *Mol Biochem Parasitol*, 58(1):107–121, Mar 1993.

[12] R. Bals, X. Wang, M. Zasloff, and J. M. Wilson. The peptide antibiotic ll-37/hcap-18 is expressed in epithelia of the human lung where it has broad antimicrobial activity at the airway surface. *Proc Natl Acad Sci U S A*, 95(16):9541–9546, Aug 1998.

[13] S. Becker and C. L. Jaffe. Effect of protein kinase inhibitors on the growth, morphology, and infectivity of leishmania promastigotes. *Parasitol Res*, 83(3):273–280, 1997.

[14] Y. Belkaid, B. Butcher, and D. L. Sacks. Analysis of cytokine production by inflammatory mouse macrophages at the single-cell level: selective impairment of il-12 induction in leishmania-infected cells. *Eur J Immunol*, 28(4):1389–1400, Apr 1998.

[15] Rym Ben-Othman, Koussay Dellagi, and Lamia Guizani-Tabbane. Leishmania major parasites induced macrophage tolerance: implication of mapk and nf-kappab pathways. *Mol Immunol*, 46(16):3438–3444, Oct 2009.

[16] Rym Ben-Othman, Lamia Guizani-Tabbane, and Koussay Dellagi. Leishmania initially activates but subsequently down-regulates intracellular mitogen-activated

protein kinases and nuclear factor-kappab signaling in macrophages. *Mol Immunol*, 45(11):3222–3229, Jun 2008.

[17] J. D. Berman. Human leishmaniasis: clinical, diagnostic, and chemotherapeutic developments in the last 10 years. *Clin Infect Dis*, 24(4):684–703, Apr 1997.

[18] J. D. Berman and F. A. Neva. Effect of temperature on multiplication of leishmania amastigotes within human monocyte-derived macrophages in vitro. *Am J Trop Med Hyg*, 30(2):318–321, Mar 1981.

[19] Sébastien Besteiro, Roderick A M Williams, Graham H Coombs, and Jeremy C Mottram. Protein turnover and differentiation in leishmania. *Int J Parasitol*, 37(10):1063–1075, Aug 2007.

[20] Sébastien Besteiro, Roderick A M Williams, Lesley S Morrison, Graham H Coombs, and Jeremy C Mottram. Endosome sorting and autophagy are essential for differentiation and virulence of leishmania major. *J Biol Chem*, 281(16):11384–11396, Apr 2006.

[21] D. Biegel, G. Topper, and M. Rabinovitch. Leishmania mexicana: temperature sensitivity of isolated amastigotes and of amastigotes infecting macrophages in culture. *Exp Parasitol*, 56(3):289–297, Dec 1983.

[22] C. Bogdan and M. Röllinghoff. The immune response to leishmania: mechanisms of parasite control and evasion. *Int J Parasitol*, 28(1):121–134, Jan 1998.

[23] C. Bogdan, Y. Vodovotz, and C. Nathan. Macrophage deactivation by interleukin 10. *J Exp Med*, 174(6):1549–1555, Dec 1991.

[24] Glória Bomfim, Bruno B Andrade, Silvane Santos, Jorge Clarêncio, Manoel Barral-Netto, and Aldina Barral. Cellular analysis of cutaneous leishmaniasis lymphadenopathy: insights into the early phases of human disease. *Am J Trop Med Hyg*, 77(5):854–859, Nov 2007.

[25] Eliane Bourreau, Jacques Gardon, Roger Pradinaud, Hervé Pascalis, Ghislaine Prévot-Linguet, Amina Kariminia, and Launois Pascal. Th2 responses predominate during the early phases of infection in patients with localized cutaneous leish-

maniasis and precede the development of th1 responses. *Infect Immun*, 71(4):2244–2246, Apr 2003.

[26] Barry J Bowman and Emma Jean Bowman. Mutations in subunit c of the vacuolar atpase confer resistance to bafilomycin and identify a conserved antibiotic binding site. *J Biol Chem*, 277(6):3965–3972, Feb 2002.

[27] A. Brittingham, C. J. Morrison, W. R. McMaster, B. S. McGwire, K. P. Chang, and D. M. Mosser. Role of the leishmania surface protease gp63 in complement fixation, cell adhesion, and resistance to complement-mediated lysis. *J Immunol*, 155(6):3102–3111, Sep 1995.

[28] F. M. Brodsky, L. Lem, A. Solache, and E. M. Bennett. Human pathogen subversion of antigen presentation. *Immunol Rev*, 168:199–215, Apr 1999.

[29] Kelly L Brown and Robert E W Hancock. Cationic host defense (antimicrobial) peptides. *Curr Opin Immunol*, 18(1):24–30, Feb 2006.

[30] C. Buechler, M. Ritter, E. Orsó, T. Langmann, J. Klucken, and G. Schmitz. Regulation of scavenger receptor cd163 expression in human monocytes and macrophages by pro- and antiinflammatory stimuli. *J Leukoc Biol*, 67(1):97–103, Jan 2000.

[31] E. Buentke, A. Zargari, L. C. Heffler, J. Avila-Cariño, J. Savolainen, and A. Scheynius. Uptake of the yeast malassezia furfur and its allergenic components by human immature cd1a+ dendritic cells. *Clin Exp Allergy*, 30(12):1759–1770, Dec 2000.

[32] C. Buser and P. Walther. Freeze-substitution: the addition of water to polar solvents enhances the retention of structure and acts at temperatures around -60 degrees c. *J Microsc*, 230(Pt 2):268–277, May 2008.

[33] L. L. Button, D. G. Russell, H. L. Klein, E. Medina-Acosta, R. E. Karess, and W. R. McMaster. Genes encoding the major surface glycoprotein in leishmania are tandemly linked at a single chromosomal locus and are constitutively transcribed. *Mol Biochem Parasitol*, 32(2-3):271–283, Jan 1989.

[34] L. L. Button, G. Wilson, C. R. Astell, and W. R. McMaster. Recombinant leishmania surface glycoprotein gp63 is secreted in the baculovirus expression system as a latent metalloproteinase. *Gene*, 134(1):75–81, Nov 1993.

[35] M. H. Cobb and E. J. Goldsmith. How map kinases are regulated. *J Biol Chem*, 270(25):14843–14846, Jun 1995.

[36] Gabriela Cohen-Freue, Timothy R Holzer, James D Forney, and W. Robert McMaster. Global gene expression in leishmania. *Int J Parasitol*, 37(10):1077–1086, Aug 2007.

[37] G. H. Coombs and J. Baxter. Inhibition of leishmania amastigote growth by antipain and leupeptin. *Ann Trop Med Parasitol*, 78(1):21–24, Feb 1984.

[38] S. L. Croft, D. Snowdon, and V. Yardley. The activities of four anticancer alkyllysophospholipids against leishmania donovani, trypanosoma cruzi and trypanosoma brucei. *J Antimicrob Chemother*, 38(6):1041–1047, Dec 1996.

[39] Anna C Cunningham. Parasitic adaptive mechanisms in infection by leishmania. *Exp Mol Pathol*, 72(2):132–141, Apr 2002.

[40] M. L. Cunningham, R. G. Titus, S. J. Turco, and S. M. Beverley. Regulation of differentiation to the infective stage of the protozoan parasite leishmania major by tetrahydrobiopterin. *Science*, 292(5515):285–287, Apr 2001.

[41] K. A. Daher, M. E. Selsted, and R. I. Lehrer. Direct inactivation of viruses by human granulocyte defensins. *J Virol*, 60(3):1068–1074, Dec 1986.

[42] M. Das, S. B. Mukherjee, and C. Shaha. Hydrogen peroxide induces apoptosis-like death in leishmania donovani promastigotes. *J Cell Sci*, 114(Pt 13):2461–2469, Jul 2001.

[43] Alain Debrabant, Nancy Lee, Sylvie Bertholet, Robert Duncan, and Hira L Nakhasi. Programmed cell death in trypanosomatids and other unicellular organisms. *Int J Parasitol*, 33(3):257–267, Mar 2003.

[44] Marcel Deponte and Katja Becker. Plasmodium falciparum–do killers commit suicide? *Trends Parasitol*, 20(4):165–169, Apr 2004.

[45] L. Ding, P. S. Linsley, L. Y. Huang, R. N. Germain, and E. M. Shevach. Il-10 inhibits macrophage costimulatory activity by selectively inhibiting the up-regulation of b7 expression. *J Immunol*, 151(3):1224–1234, Aug 1993.

[46] Subhankar Dolai, Swati Pal, Rajesh K Yadav, and Subrata Adak. Endoplasmic reticulum stress-induced apoptosis in leishmania through ca2+-dependent and caspase-independent mechanism. *J Biol Chem*, 286(15):13638–13646, Apr 2011.

[47] Subhankar Dolai, Rajesh K Yadav, Swati Pal, and Subrata Adak. Overexpression of mitochondrial leishmania major ascorbate peroxidase enhances tolerance to oxidative stress-induced programmed cell death and protein damage. *Eukaryot Cell*, 8(11):1721–1731, Nov 2009.

[48] R. A. Dorschner, V. K. Pestonjamasp, S. Tamakuwala, T. Ohtake, J. Rudisill, V. Nizet, B. Agerberth, G. H. Gudmundsson, and R. L. Gallo. Cutaneous injury induces the release of cathelicidin anti-microbial peptides active against group a streptococcus. *J Invest Dermatol*, 117(1):91–97, Jul 2001.

[49] Avijit Dutta, Suman Bandyopadhyay, Chitra Mandal, and Mitali Chatterjee. Aloe vera leaf exudate induces a caspase-independent cell death in leishmania donovani promastigotes. *J Med Microbiol*, 56(Pt 5):629–636, May 2007.

[50] S. Ehrt, D. Schnappinger, S. Bekiranov, J. Drenkow, S. Shi, T. R. Gingeras, T. Gaasterland, G. Schoolnik, and C. Nathan. Reprogramming of the macrophage transcriptome in response to interferon-gamma and mycobacterium tuberculosis: signaling roles of nitric oxide synthase-2 and phagocyte oxidase. *J Exp Med*, 194(8):1123–1140, Oct 2001.

[51] Patricia Escobar, Sangeeta Matu, Cláudia Marques, and Simon L Croft. Sensitivities of leishmania species to hexadecylphosphocholine (miltefosine), et-18-och(3) (edelfosine) and amphotericin b. *Acta Trop*, 81(2):151–157, Feb 2002.

[52] G. J. Feng, H. S. Goodridge, M. M. Harnett, X. Q. Wei, A. V. Nikolaev, A. P. Higson, and F. Y. Liew. Extracellular signal-related kinase (erk) and p38 mitogen-activated protein (map) kinases differentially regulate the lipopolysaccharide-mediated induction of inducible nitric oxide synthase and il-12 in macrophages:

Leishmania phosphoglycans subvert macrophage il-12 production by targeting erk map kinase. *J Immunol*, 163(12):6403–6412, Dec 1999.

[53] K. F. Ferri and G. Kroemer. Mitochondria–the suicide organelles. *Bioessays*, 23(2):111–115, Feb 2001.

[54] Y. Le Fichoux, D. Rousseau, B. Ferrua, S. Ruette, A. Leliévre, D. Grousson, and J. Kubar. Short- and long-term efficacy of hexadecylphosphocholine against established leishmania infantum infection in balb/c mice. *Antimicrob Agents Chemother*, 42(3):654–658, Mar 1998.

[55] D. F. Fiorentino, A. Zlotnik, T. R. Mosmann, M. Howard, and A. O'Garra. Il-10 inhibits cytokine production by activated macrophages. *J Immunol*, 147(11):3815–3822, Dec 1991.

[56] J. L. Flynn, M. M. Goldstein, K. J. Triebold, J. Sypek, S. Wolf, and B. R. Bloom. Il-12 increases resistance of balb/c mice to mycobacterium tuberculosis infection. *J Immunol*, 155(5):2515–2524, Sep 1995.

[57] Michael Forgac. Vacuolar atpases: rotary proton pumps in physiology and pathophysiology. *Nat Rev Mol Cell Biol*, 8(11):917–929, Nov 2007.

[58] R. L. Gallo, K. J. Kim, M. Bernfield, C. A. Kozak, M. Zanetti, L. Merluzzi, and R. Gennaro. Identification of cramp, a cathelin-related antimicrobial peptide expressed in the embryonic and adult mouse. *J Biol Chem*, 272(20):13088–13093, May 1997.

[59] T. Ganz, M. E. Selsted, D. Szklarek, S. S. Harwig, K. Daher, D. F. Bainton, and R. I. Lehrer. Defensins. natural peptide antibiotics of human neutrophils. *J Clin Invest*, 76(4):1427–1435, Oct 1985.

[60] R. T. Gazzinelli, I. P. Oswald, S. L. James, and A. Sher. Il-10 inhibits parasite killing and nitrogen oxide production by ifn-gamma-activated macrophages. *J Immunol*, 148(6):1792–1796, Mar 1992.

[61] R. Gennaro and M. Zanetti. Structural features and biological activities of the cathelicidin-derived antimicrobial peptides. *Biopolymers*, 55(1):31–49, 2000.

[62] M. S. Giannini. Effects of promastigote growth phase, frequency of subculture, and host age on promastigote-initiated infections with leishmania donovani in the golden hamster. *J Protozool*, 21(4):521–527, Oct 1974.

[63] T. A. Glaser, S. F. Moody, E. Handman, A. Bacic, and T. W. Spithill. An antigenically distinct lipophosphoglycan on amastigotes of leishmania major. *Mol Biochem Parasitol*, 45(2):337–344, Apr 1991.

[64] Y. Jerold Gordon, Ling C Huang, Eric G Romanowski, Kathleen A Yates, Rita J Proske, and Alison M McDermott. Human cathelicidin (ll-37), a multifunctional peptide, is expressed by ocular surface epithelia and has potent antibacterial and antiviral activity. *Curr Eye Res*, 30(5):385–394, May 2005.

[65] S. J. Green, S. Mellouk, S. L. Hoffman, M. S. Meltzer, and C. A. Nacy. Cellular mechanisms of nonspecific immunity to intracellular infection: cytokine-induced synthesis of toxic nitrogen oxides from l-arginine by macrophages and hepatocytes. *Immunol Lett*, 25(1-3):15–19, Aug 1990.

[66] S. J. Green, C. A. Nacy, and M. S. Meltzer. Cytokine-induced synthesis of nitrogen oxides in macrophages: a protective host response to leishmania and other intracellular pathogens. *J Leukoc Biol*, 50(1):93–103, Jul 1991.

[67] G. H. Gudmundsson, B. Agerberth, J. Odeberg, T. Bergman, B. Olsson, and R. Salcedo. The human gene fall39 and processing of the cathelin precursor to the antibacterial peptide ll-37 in granulocytes. *Eur J Biochem*, 238(2):325–332, Jun 1996.

[68] C. F. Higgins. Abc transporters: from microorganisms to man. *Annu Rev Cell Biol*, 8:67–113, 1992.

[69] Katharine A Hintz, Athos J Rassias, Kathleen Wardwell, Marcia L Moss, Peter M Morganelli, Patricia A Pioli, Alice L Givan, Paul K Wallace, Mark P Yeager, and Paul M Guyre. Endotoxin induces rapid metalloproteinase-mediated shedding followed by up-regulation of the monocyte hemoglobin scavenger receptor cd163. *J Leukoc Biol*, 72(4):711–717, Oct 2002.

[70] Philippe Holzmuller, Denis Sereno, Mireille Cavaleyra, Isabelle Mangot, Sylvie Daulouede, Philippe Vincendeau, and Jean-Loup Lemesre. Nitric oxide-mediated

proteasome-dependent oligonucleosomal dna fragmentation in leishmania amazonensis amastigotes. *Infect Immun*, 70(7):3727–3735, Jul 2002.

[71] Michael D Howell, James F Jones, Kevin O Kisich, Joanne E Streib, Richard L Gallo, and Donald Y M Leung. Selective killing of vaccinia virus by ll-37: implications for eczema vaccinatum. *J Immunol*, 172(3):1763–1767, Feb 2004.

[72] Y. H. Hsiang, R. Hertzberg, S. Hecht, and L. F. Liu. Camptothecin induces protein-linked dna breaks via mammalian dna topoisomerase i. *J Biol Chem*, 260(27):14873–14878, Nov 1985.

[73] C. S. Hsieh, S. E. Macatonia, C. S. Tripp, S. F. Wolf, A. O'Garra, and K. M. Murphy. Development of th1 cd4+ t cells through il-12 produced by listeria-induced macrophages. *Science*, 260(5107):547–549, Apr 1993.

[74] Markus Huss, Gudrun Ingenhorst, Simone König, Michael Gassel, Stefan Dröse, Axel Zeeck, Karlheinz Altendorf, and Helmut Wieczorek. Concanamycin a, the specific inhibitor of v-atpases, binds to the v(o) subunit c. *J Biol Chem*, 277(43):40544–40548, Oct 2002.

[75] Virginia Iniesta, Jesualdo Carcelén, Isabel Molano, Pablo M V Peixoto, Eloy Redondo, Pilar Parra, Marina Mangas, Isabel Monroy, Maria Luisa Campo, Carlos Gómez Nieto, and Inés Corraliza. Arginase i induction during leishmania major infection mediates the development of disease. *Infect Immun*, 73(9):6085–6090, Sep 2005.

[76] Alasdair C Ivens, Christopher S Peacock, Elizabeth A Worthey, Lee Murphy, Gautam Aggarwal, Matthew Berriman, Ellen Sisk, Marie-Adele Rajandream, Ellen Adlem, Rita Aert, Atashi Anupama, Zina Apostolou, Philip Attipoe, Nathalie Bason, Christopher Bauser, Alfred Beck, Stephen M Beverley, Gabriella Bianchettin, Katja Borzym, Gordana Bothe, Carlo V Bruschi, Matt Collins, Eithon Cadag, Laura Ciarloni, Christine Clayton, Richard M R Coulson, Ann Cronin, Angela K Cruz, Robert M Davies, Javier De Gaudenzi, Deborah E Dobson, Andreas Duesterhoeft, Gholam Fazelina, Nigel Fosker, Alberto Carlos Frasch, Audrey Fraser, Monika Fuchs, Claudia Gabel, Arlette Goble, André Goffeau, David Harris, Christiane Hertz-Fowler, Helmut Hilbert, David Horn, Yiting Huang, Sven

Klages, Andrew Knights, Michael Kube, Natasha Larke, Lyudmila Litvin, Angela Lord, Tin Louie, Marco Marra, David Masuy, Keith Matthews, Shulamit Michaeli, Jeremy C Mottram, Silke Müller-Auer, Heather Munden, Siri Nelson, Halina Norbertczak, Karen Oliver, Susan O'neil, Martin Pentony, Thomas M Pohl, Claire Price, Bénédicte Purnelle, Michael A Quail, Ester Rabbinowitsch, Richard Reinhardt, Michael Rieger, Joel Rinta, Johan Robben, Laura Robertson, Jeronimo C Ruiz, Simon Rutter, David Saunders, Melanie Schäfer, Jacquie Schein, David C Schwartz, Kathy Seeger, Amber Seyler, Sarah Sharp, Heesun Shin, Dhileep Sivam, Rob Squares, Steve Squares, Valentina Tosato, Christy Vogt, Guido Volckaert, Rolf Wambutt, Tim Warren, Holger Wedler, John Woodward, Shiguo Zhou, Wolfgang Zimmermann, Deborah F Smith, Jenefer M Blackwell, Kenneth D Stuart, Bart Barrell, and Peter J Myler. The genome of the kinetoplastid parasite, leishmania major. *Science*, 309(5733):436–442, Jul 2005.

[77] Muthoni Junghae and John G Raynes. Activation of p38 mitogen-activated protein kinase attenuates leishmania donovani infection in macrophages. *Infect Immun*, 70(9):5026–5035, Sep 2002.

[78] B. L. Kagan, M. E. Selsted, T. Ganz, and R. I. Lehrer. Antimicrobial defensin peptides form voltage-dependent ion-permeable channels in planar lipid bilayer membranes. *Proc Natl Acad Sci U S A*, 87(1):210–214, Jan 1990.

[79] M. M. Kane and D. M. Mosser. Leishmania parasites and their ploys to disrupt macrophage activation. *Curr Opin Hematol*, 7(1):26–31, Jan 2000.

[80] Mazen W Karaman, Sanna Herrgard, Daniel K Treiber, Paul Gallant, Corey E Atteridge, Brian T Campbell, Katrina W Chan, Pietro Ciceri, Mindy I Davis, Philip T Edeen, Raffaella Faraoni, Mark Floyd, Jeremy P Hunt, Daniel J Lockhart, Zdravko V Milanov, Michael J Morrison, Gabriel Pallares, Hitesh K Patel, Stephanie Pritchard, Lisa M Wodicka, and Patrick P Zarrinkar. A quantitative analysis of kinase inhibitor selectivity. *Nat Biotechnol*, 26(1):127–132, Jan 2008.

[81] Prasanthi Karna, Susu Zughaier, Vaishali Pannu, Robert Simmons, Satya Narayan, and Ritu Aneja. Induction of reactive oxygen species-mediated autophagy by a novel microtubule-modulating agent. *J Biol Chem*, 285(24):18737–18748, Jun 2010.

[82] J. F. Kerr, A. H. Wyllie, and A. R. Currie. Apoptosis: a basic biological phenomenon with wide-ranging implications in tissue kinetics. *Br J Cancer*, 26(4):239–257, Aug 1972.

[83] Shahram Khademvatan, Mohammad Javad Gharavi, Fakher Rahim, and Jasem Saki. Miltefosine-induced apoptotic cell death on leishmania major and l. tropica strains. *Korean J Parasitol*, 49(1):17–23, Mar 2011.

[84] Mary E Klotman and Theresa L Chang. Defensins in innate antiviral immunity. *Nat Rev Immunol*, 6(6):447–456, Jun 2006.

[85] R. M. Kluck, E. Bossy-Wetzel, D. R. Green, and D. D. Newmeyer. The release of cytochrome c from mitochondria: a primary site for bcl-2 regulation of apoptosis. *Science*, 275(5303):1132–1136, Feb 1997.

[86] E. Knuepfer, Y. D. Stierhof, P. G. McKean, and D. F. Smith. Characterization of a differentially expressed protein that shows an unusual localization to intracellular membranes in leishmania major. *Biochem J*, 356(Pt 2):335–344, Jun 2001.

[87] M. Kobayashi, L. Fitz, M. Ryan, R. M. Hewick, S. C. Clark, S. Chan, R. Loudon, F. Sherman, B. Perussia, and G. Trinchieri. Identification and purification of natural killer cell stimulatory factor (nksf), a cytokine with multiple biologic effects on human lymphocytes. *J Exp Med*, 170(3):827–845, Sep 1989.

[88] Stephan R Krutzik, Belinda Tan, Huiying Li, Maria Teresa Ochoa, Philip T Liu, Sarah E Sharfstein, Thomas G Graeber, Peter A Sieling, Yong-Jun Liu, Thomas H Rea, Barry R Bloom, and Robert L Modlin. Tlr activation triggers the rapid differentiation of monocytes into macrophages and dendritic cells. *Nat Med*, 11(6):653–660, Jun 2005.

[89] Manjusha M Kulkarni, Joseph Barbi, W. Robert McMaster, Richard L Gallo, Abhay R Satoskar, and Bradford S McGwire. Mammalian antimicrobial peptide influences control of cutaneous leishmania infection. *Cell Microbiol*, 13(6):913–923, Jun 2011.

[90] Promod Kumar, Kalpana Pai, Haushila P Pandey, and Shyam Sundar. Nadh-oxidase, nadph-oxidase and myeloperoxidase activity of visceral leishmaniasis patients. *J Med Microbiol*, 51(10):832–836, Oct 2002.

[91] R. Lainson. Ecological interactions in the transmission of the leishmaniases. *Philos Trans R Soc Lond B Biol Sci*, 321(1207):389–404, Oct 1988.

[92] J. W. Larrick, M. Hirata, R. F. Balint, J. Lee, J. Zhong, and S. C. Wright. Human cap18: a novel antimicrobial lipopolysaccharide-binding protein. *Infect Immun*, 63(4):1291–1297, Apr 1995.

[93] J. W. Larrick, J. Lee, S. Ma, X. Li, U. Francke, S. C. Wright, and R. F. Balint. Structural, functional analysis and localization of the human cap18 gene. *FEBS Lett*, 398(1):74–80, Nov 1996.

[94] Tamás Laskay, Ger van Zandbergen, and Werner Solbach. Neutrophil granulocytes–trojan horses for leishmania major and other intracellular microbes? *Trends Microbiol*, 11(5):210–214, May 2003.

[95] Carsten Gk Lüder, Jenny Campos-Salinas, Elena Gonzalez-Rey, and Ger van Zandbergen. Impact of protozoan cell death on parasite-host interactions and pathogenesis. *Parasit Vectors*, 3:116, 2010.

[96] N. Lee, S. Bertholet, A. Debrabant, J. Muller, R. Duncan, and H. L. Nakhasi. Programmed cell death in the unicellular protozoan parasite leishmania. *Cell Death Differ*, 9(1):53–64, Jan 2002.

[97] R. I. Lehrer and T. Ganz. Antimicrobial peptides in mammalian and insect host defence. *Curr Opin Immunol*, 11(1):23–27, Feb 1999.

[98] Kirk Leifso, Gabriela Cohen-Freue, Nisha Dogra, Angus Murray, and W. Robert McMaster. Genomic and proteomic expression analysis of leishmania promastigote and amastigote life stages: the leishmania genome is constitutively expressed. *Mol Biochem Parasitol*, 152(1):35–46, Mar 2007.

[99] J. L. Lemesre, D. Sereno, S. Daulouède, B. Veyret, N. Brajon, and P. Vincendeau. Leishmania spp.: nitric oxide-mediated metabolic inhibition of promastigote and axenically grown amastigote forms. *Exp Parasitol*, 86(1):58–68, May 1997.

[100] F. Y. Liew, S. Millott, C. Parkinson, R. M. Palmer, and S. Moncada. Macrophage killing of leishmania parasite in vivo is mediated by nitric oxide from l-arginine. *J Immunol*, 144(12):4794–4797, Jun 1990.

[101] Philip T Liu, Steffen Stenger, Huiying Li, Linda Wenzel, Belinda H Tan, Stephan R Krutzik, Maria Teresa Ochoa, Jürgen Schauber, Kent Wu, Christoph Meinken, Diane L Kamen, Manfred Wagner, Robert Bals, Andreas Steinmeyer, Ulrich Zügel, Richard L Gallo, David Eisenberg, Martin Hewison, Bruce W Hollis, John S Adams, Barry R Bloom, and Robert L Modlin. Toll-like receptor triggering of a vitamin d-mediated human antimicrobial response. *Science*, 311(5768):1770–1773, Mar 2006.

[102] P. J. Lohuis, M. M. Lipovsky, A. I. Hoepelman, G. J. Hordijk, and E. H. Huizing. Leishmania braziliensis presenting as a granulomatous lesion of the nasal septum mucosa. *J Laryngol Otol*, 111(10):973–975, Oct 1997.

[103] Mark Lucas, Xia Zhang, Vikram Prasanna, and David M Mosser. Erk activation following macrophage fcgammar ligation leads to chromatin modifications at the il-10 locus. *J Immunol*, 175(1):469–477, Jul 2005.

[104] H. Lux, N. Heise, T. Klenner, D. Hart, and F. R. Opperdoes. Ether–lipid (alkyl-phospholipid) metabolism and the mechanism of action of ether–lipid analogues in leishmania. *Mol Biochem Parasitol*, 111(1):1–14, Nov 2000.

[105] Lon-Fye Lye, Mark L Cunningham, and Stephen M Beverley. Characterization of quinonoid-dihydropteridine reductase (qdpr) from the lower eukaryote leishmania major. *J Biol Chem*, 277(41):38245–38253, Oct 2002.

[106] Miriam A Lynn and W. Robert McMaster. Leishmania: conserved evolution–diverse diseases. *Trends Parasitol*, 24(3):103–105, Mar 2008.

[107] R. Manetti, P. Parronchi, M. G. Giudizi, M. P. Piccinni, E. Maggi, G. Trinchieri, and S. Romagnani. Natural killer cell stimulatory factor (interleukin 12 [il-12]) induces t helper type 1 (th1)-specific immune responses and inhibits the development of il-4-producing th cells. *J Exp Med*, 177(4):1199–1204, Apr 1993.

[108] S. P. Manickasingham, S. M. Anderton, C. Burkhart, and D. C. Wraith. Qualitative and quantitative effects of cd28/b7-mediated costimulation on naive t cells in vitro. *J Immunol*, 161(8):3827–3835, Oct 1998.

[109] Alberto Mantovani, Antonio Sica, Silvano Sozzani, Paola Allavena, Annunciata Vecchi, and Massimo Locati. The chemokine system in diverse forms of

macrophage activation and polarization. *Trends Immunol*, 25(12):677–686, Dec 2004.

[110] S. J. Martin, C. P. Reutelingsperger, A. J. McGahon, J. A. Rader, R. C. van Schie, D. M. LaFace, and D. R. Green. Early redistribution of plasma membrane phosphatidylserine is a general feature of apoptosis regardless of the initiating stimulus: inhibition by overexpression of bcl-2 and abl. *J Exp Med*, 182(5):1545–1556, Nov 1995.

[111] M. Maurer and E. von Stebut. Macrophage inflammatory protein-1. *Int J Biochem Cell Biol*, 36(10):1882–1886, Oct 2004.

[112] M. J. McConville and J. M. Blackwell. Developmental changes in the glycosylated phosphatidylinositols of leishmania donovani. characterization of the promastigote and amastigote glycolipids. *J Biol Chem*, 266(23):15170–15179, Aug 1991.

[113] M. J. McConville, S. J. Turco, M. A. Ferguson, and D. L. Sacks. Developmental modification of lipophosphoglycan during the differentiation of leishmania major promastigotes to an infectious stage. *EMBO J*, 11(10):3593–3600, Oct 1992.

[114] J. H. McKerrow, E. Sun, P. J. Rosenthal, and J. Bouvier. The proteases and pathogenicity of parasitic protozoa. *Annu Rev Microbiol*, 47:821–853, 1993.

[115] E. Medina-Acosta, R. E. Karess, and D. G. Russell. Structurally distinct genes for the surface protease of leishmania mexicana are developmentally regulated. *Mol Biochem Parasitol*, 57(1):31–45, Jan 1993.

[116] E. Medina-Acosta, R. E. Karess, H. Schwartz, and D. G. Russell. The promastigote surface protease (gp63) of leishmania is expressed but differentially processed and localized in the amastigote stage. *Mol Biochem Parasitol*, 37(2):263–273, Dec 1989.

[117] Ashish Mehta and Chandrima Shaha. Apoptotic death in leishmania donovani promastigotes in response to respiratory chain inhibition: complex ii inhibition results in increased pentamidine cytotoxicity. *J Biol Chem*, 279(12):11798–11813, Mar 2004.

[118] A. Misslitz, J. C. Mottram, P. Overath, and T. Aebischer. Targeted integration into a rrna locus results in uniform and high level expression of transgenes in leishmania amastigotes. *Mol Biochem Parasitol*, 107(2):251–261, Apr 2000.

[119] Søren K Moestrup and Holger J Møller. Cd163: a regulated hemoglobin scavenger receptor with a role in the anti-inflammatory response. *Ann Med*, 36(5):347–354, 2004.

[120] Dennis Montoya, Daniel Cruz, Rosane M B Teles, Delphine J Lee, Maria Teresa Ochoa, Stephan R Krutzik, Rene Chun, Mirjam Schenk, Xiaoran Zhang, Benjamin G Ferguson, Anne E Burdick, Euzenir N Sarno, Thomas H Rea, Martin Hewison, John S Adams, Genhong Cheng, and Robert L Modlin. Divergence of macrophage phagocytic and antimicrobial programs in leprosy. *Cell Host Microbe*, 6(4):343–353, Oct 2009.

[121] S. F. Moody, E. Handman, M. J. McConville, and A. Bacic. The structure of leishmania major amastigote lipophosphoglycan. *J Biol Chem*, 268(25):18457–18466, Sep 1993.

[122] K. J. Moore, S. Labrecque, and G. Matlashewski. Alteration of leishmania donovani infection levels by selective impairment of macrophage signal transduction. *J Immunol*, 150(10):4457–4465, May 1993.

[123] J. C. Mottram, A. E. Souza, J. E. Hutchison, R. Carter, M. J. Frame, and G. H. Coombs. Evidence from disruption of the lmcpb gene array of leishmania mexicana that cysteine proteinases are virulence factors. *Proc Natl Acad Sci U S A*, 93(12):6008–6013, Jun 1996.

[124] E. E. Murphy, G. Terres, S. E. Macatonia, C. S. Hsieh, J. Mattson, L. Lanier, M. Wysocka, G. Trinchieri, K. Murphy, and A. O'Garra. B7 and interleukin 12 cooperate for proliferation and interferon gamma production by mouse t helper clones that are unresponsive to b7 costimulation. *J Exp Med*, 180(1):223–231, Jul 1994.

[125] P. J. Myler, S. M. Beverley, A. K. Cruz, D. E. Dobson, A. C. Ivens, P. D. McDonagh, R. Madhubala, S. Martinez-Calvillo, J. C. Ruiz, A. Saxena, E. Sisk, S. M. Sunkin, E. Worthey, S. Yan, and K. D. Stuart. The leishmania genome project:

new insights into gene organization and function. *Med Microbiol Immunol*, 190(1-2):9–12, Nov 2001.

[126] Katie J Mylonas, Meera G Nair, Lidia Prieto-Lafuente, Daniel Paape, and Judith E Allen. Alternatively activated macrophages elicited by helminth infection can be reprogrammed to enable microbial killing. *J Immunol*, 182(5):3084–3094, Mar 2009.

[127] S. Nagata. Apoptosis by death factor. *Cell*, 88(3):355–365, Feb 1997.

[128] B. Nare, L. W. Hardy, and S. M. Beverley. The roles of pteridine reductase 1 and dihydrofolate reductase-thymidylate synthase in pteridine metabolism in the protozoan parasite leishmania major. *J Biol Chem*, 272(21):13883–13891, May 1997.

[129] Abedelmajeed Nasereddin, Carola Schweynoch, Gabriele Schonian, and Charles L Jaffe. Characterization of leishmania (leishmania) tropica axenic amastigotes. *Acta Trop*, 113(1):72–79, Jan 2010.

[130] Paul A Nguewa, Miguel A Fuertes, Victoria Cepeda, Salvador Iborra, Javier Carrión, Basilio Valladares, Carlos Alonso, and José M Pérez. Pentamidine is an antiparasitic and apoptotic drug that selectively modifies ubiquitin. *Chem Biodivers*, 2(10):1387–1400, Oct 2005.

[131] Paul A Nguewa, Miguel A Fuertes, Basilio Valladares, Carlos Alonso, and José M Pérez. Programmed cell death in trypanosomatids: a way to maximize their biological fitness? *Trends Parasitol*, 20(8):375–380, Aug 2004.

[132] A. K. Nussler, L. Rénia, V. Pasquetto, F. Miltgen, H. Matile, and D. Mazier. In vivo induction of the nitric oxide pathway in hepatocytes after injection with irradiated malaria sporozoites, malaria blood parasites or adjuvants. *Eur J Immunol*, 23(4):882–887, Apr 1993.

[133] A. O'Garra. Cytokines induce the development of functionally heterogeneous t helper cell subsets. *Immunity*, 8(3):275–283, Mar 1998.

[134] M. Olivier, R. W. Brownsey, and N. E. Reiner. Defective stimulus-response coupling in human monocytes infected with leishmania donovani is associated with

altered activation and translocation of protein kinase c. *Proc Natl Acad Sci U S A*, 89(16):7481–7485, Aug 1992.

[135] Gabriela Onofre, Martina Kolácková, Karolina Jankovicová, and Jan Krejsek. Scavenger receptor cd163 and its biological functions. *Acta Medica (Hradec Kralove)*, 52(2):57–61, 2009.

[136] Bastian Opitz, Anja Püschel, Wiebke Beermann, Andreas C Hocke, Stefanie Förster, Bernd Schmeck, Vincent van Laak, Trinad Chakraborty, Norbert Suttorp, and Stefan Hippenstiel. Listeria monocytogenes activated p38 mapk and induced il-8 secretion in a nucleotide-binding oligomerization domain 1-dependent manner in endothelial cells. *J Immunol*, 176(1):484–490, Jan 2006.

[137] Mary O'Riordan, Caroline H Yi, Ramona Gonzales, Kyung-Dall Lee, and Daniel A Portnoy. Innate recognition of bacteria by a macrophage cytosolic surveillance pathway. *Proc Natl Acad Sci U S A*, 99(21):13861–13866, Oct 2002.

[138] I. P. Oswald, R. T. Gazzinelli, A. Sher, and S. L. James. Il-10 synergizes with il-4 and transforming growth factor-beta to inhibit macrophage cytotoxic activity. *J Immunol*, 148(11):3578–3582, Jun 1992.

[139] Meriam Ouakad, Narges Bahi-Jaber, Mehdi Chenik, Koussay Dellagi, and Hechmi Louzir. Selection of endogenous reference genes for gene expression analysis in leishmania major developmental stages. *Parasitol Res*, 101(2):473–477, Jul 2007.

[140] Emilios Andrew Papanastasiou, Quyen Hua, Aline Sandouk, U. Hyon Son, Andrew James Christenson, Monique Louise Van Hoek, and Barney Michael Bishop. Role of acetylation and charge in antimicrobial peptides based on human beta-defensin-3. *APMIS*, 117(7):492–499, Jul 2009.

[141] A. Paul, S. Wilson, C. M. Belham, C. J. Robinson, P. H. Scott, G. W. Gould, and R. Plevin. Stress-activated protein kinases: activation, regulation and function. *Cell Signal*, 9(6):403–410, Sep 1997.

[142] G. Pearson, F. Robinson, T. Beers Gibson, B. E. Xu, M. Karandikar, K. Berman, and M. H. Cobb. Mitogen-activated protein (map) kinase pathways: regulation and physiological functions. *Endocr Rev*, 22(2):153–183, Apr 2001.

[143] R. D. Pearson and A. Q. Sousa. Clinical spectrum of leishmaniasis. *Clin Infect Dis*, 22(1):1–13, Jan 1996.

[144] R. D. Pearson, D. A. Wheeler, L. H. Harrison, and H. D. Kay. The immunobiology of leishmaniasis. *Rev Infect Dis*, 5(5):907–927, 1983.

[145] P. F. Pimenta and W. de Souza. Leishmania mexicana amazonensis: surface charge of amastigote and promastigote forms. *Exp Parasitol*, 56(2):194–206, Oct 1983.

[146] P. F. Pimenta, E. M. Saraiva, and D. L. Sacks. The comparative fine structure and surface glycoconjugate expression of three life stages of leishmania major. *Exp Parasitol*, 72(2):191–204, Feb 1991.

[147] P. F. Pimenta, S. J. Turco, M. J. McConville, P. G. Lawyer, P. V. Perkins, and D. L. Sacks. Stage-specific adhesion of leishmania promastigotes to the sandfly midgut. *Science*, 256(5065):1812–1815, Jun 1992.

[148] E. Prina, J. C. Antoine, B. Wiederanders, and H. Kirschke. Localization and activity of various lysosomal proteases in leishmania amazonensis-infected macrophages. *Infect Immun*, 58(6):1730–1737, Jun 1990.

[149] S. M. Puentes, R. P. Da Silva, D. L. Sacks, C. H. Hammer, and K. A. Joiner. Serum resistance of metacyclic stage leishmania major promastigotes is due to release of c5b-9. *J Immunol*, 145(12):4311–4316, Dec 1990.

[150] J. Raingeaud, S. Gupta, J. S. Rogers, M. Dickens, J. Han, R. J. Ulevitch, and R. J. Davis. Pro-inflammatory cytokines and environmental stress cause p38 mitogen-activated protein kinase activation by dual phosphorylation on tyrosine and threonine. *J Biol Chem*, 270(13):7420–7426, Mar 1995.

[151] P. Ralph, I. Nakoinz, A. Sampson-Johannes, S. Fong, D. Lowe, H. Y. Min, and L. Lin. Il-10, t lymphocyte inhibitor of human blood cell production of il-1 and tumor necrosis factor. *J Immunol*, 148(3):808–814, Feb 1992.

[152] L. Ramachandra, R. Song, and C. V. Harding. Phagosomes are fully competent antigen-processing organelles that mediate the formation of peptide:class ii mhc complexes. *J Immunol*, 162(6):3263–3272, Mar 1999.

[153] R. Ramamoorthy, J. E. Donelson, K. E. Paetz, M. Maybodi, S. C. Roberts, and M. E. Wilson. Three distinct rnas for the surface protease gp63 are differentially expressed during development of leishmania donovani chagasi promastigotes to an infectious form. *J Biol Chem*, 267(3):1888–1895, Jan 1992.

[154] Neil D Rawlings, Fraser R Morton, and Alan J Barrett. Merops: the peptidase database. *Nucleic Acids Res*, 34(Database issue):D270–D272, Jan 2006.

[155] M. R. Redinbo, L. Stewart, P. Kuhn, J. J. Champoux, and W. G. Hol. Crystal structures of human topoisomerase i in covalent and noncovalent complexes with dna. *Science*, 279(5356):1504–1513, Mar 1998.

[156] S. L. Reiner and R. M. Locksley. The regulation of immunity to leishmania major. *Annu Rev Immunol*, 13:151–177, 1995.

[157] Eva Rico, Juan Fernando Alzate, Andrés Augusto Arias, David Moreno, Joachim Clos, Federico Gago, Inmaculada Moreno, Mercedes Domínguez, and Antonio Jiménez-Ruiz. Leishmania infantum expresses a mitochondrial nuclease homologous to endog that migrates to the nucleus in response to an apoptotic stimulus. *Mol Biochem Parasitol*, 163(1):28–38, Jan 2009.

[158] Uwe Ritter and Heinrich Körner. Divergent expression of inflammatory dermal chemokines in cutaneous leishmaniasis. *Parasite Immunol*, 24(6):295–301, Jun 2002.

[159] M. E. Rogers, M. L. Chance, and P. A. Bates. The role of promastigote secretory gel in the origin and transmission of the infective stage of leishmania mexicana by the sandfly lutzomyia longipalpis. *Parasitology*, 124(Pt 5):495–507, May 2002.

[160] Amit Roy, Agneyo Ganguly, Somdeb BoseDasgupta, Benu Brata Das, Churala Pal, Parasuraman Jaisankar, and Hemanta K Majumder. Mitochondria-dependent reactive oxygen species-mediated programmed cell death induced by 3,3'-diindolylmethane through inhibition of f0f1-atp synthase in unicellular protozoan parasite leishmania donovani. *Mol Pharmacol*, 74(5):1292–1307, Nov 2008.

[161] D. G. Russell. Immunoelectron microscopy of endosomal trafficking in macrophages infected with microbial pathogens. *Methods Cell Biol*, 45:277–288, 1994.

[162] D. L. Sacks, A. Barral, and F. A. Neva. Thermosensitivity patterns of old vs. new world cutaneous strains of leishmania growing within mouse peritoneal macrophages in vitro. *Am J Trop Med Hyg*, 32(2):300–304, Mar 1983.

[163] D. L. Sacks, T. N. Brodin, and S. J. Turco. Developmental modification of the lipophosphoglycan from leishmania major promastigotes during metacyclogenesis. *Mol Biochem Parasitol*, 42(2):225–233, 1990.

[164] D. L. Sacks and P. V. Perkins. Identification of an infective stage of leishmania promastigotes. *Science*, 223(4643):1417–1419, Mar 1984.

[165] D. L. Sacks and P. V. Perkins. Development of infective stage leishmania promastigotes within phlebotomine sand flies. *Am J Trop Med Hyg*, 34(3):456–459, May 1985.

[166] David Sacks and Nancy Noben-Trauth. The immunology of susceptibility and resistance to leishmania major in mice. *Nat Rev Immunol*, 2(11):845–858, Nov 2002.

[167] F. Sallusto, M. Cella, C. Danieli, and A. Lanzavecchia. Dendritic cells use macropinocytosis and the mannose receptor to concentrate macromolecules in the major histocompatibility complex class ii compartment: downregulation by cytokines and bacterial products. *J Exp Med*, 182(2):389–400, Aug 1995.

[168] Nigel D L Savage, Tjitske de Boer, Kimberley V Walburg, Simone A Joosten, Krista van Meijgaarden, Annemiek Geluk, and Tom H M Ottenhoff. Human anti-inflammatory macrophages induce foxp3+ gitr+ cd25+ regulatory t cells, which suppress via membrane-bound tgfbeta-1. *J Immunol*, 181(3):2220–2226, Aug 2008.

[169] Ruth Scherz-Shouval, Elena Shvets, Ephraim Fass, Hagai Shorer, Lidor Gil, and Zvulun Elazar. Reactive oxygen species are essential for autophagy and specifically regulate the activity of atg4. *EMBO J*, 26(7):1749–1760, Apr 2007.

[170] P. Schneider, J. P. Rosat, J. Bouvier, J. Louis, and C. Bordier. Leishmania major: differential regulation of the surface metalloprotease in amastigote and promastigote stages. *Exp Parasitol*, 75(2):196–206, Sep 1992.

[171] P. Schneider, J. P. Rosat, A. Ransijn, M. A. Ferguson, and M. J. McConville. Characterization of glycoinositol phospholipids in the amastigote stage of the protozoan parasite leishmania major. *Biochem J*, 295 (Pt 2):555–564, Oct 1993.

[172] Gabriele Schönian, Abedelmajeed Nasereddin, Nicole Dinse, Carola Schweynoch, Henk D F H Schallig, Wolfgang Presber, and Charles L Jaffe. Pcr diagnosis and characterization of leishmania in local and imported clinical samples. *Diagn Microbiol Infect Dis*, 47(1):349–358, Sep 2003.

[173] K. Schulze-Osthoff, R. Beyaert, V. Vandevoorde, G. Haegeman, and W. Fiers. Depletion of the mitochondrial electron transport abrogates the cytotoxic and gene-inductive effects of tnf. *EMBO J*, 12(8):3095–3104, Aug 1993.

[174] J. C. Schwartz, X. Zhang, A. A. Fedorov, S. G. Nathenson, and S. C. Almo. Structural basis for co-stimulation by the human ctla-4/b7-2 complex. *Nature*, 410(6828):604–608, Mar 2001.

[175] Jovana Sádlová, Helen P Price, Barbara A Smith, Jan Vot?pka, Petr Volf, and Deborah F Smith. The stage-regulated haspb and sherp proteins are essential for differentiation of the protozoan parasite leishmania major in its sand fly vector, phlebotomus papatasi. *Cell Microbiol*, 12(12):1765–1779, Dec 2010.

[176] N. Sen, B. B. Das, A. Ganguly, T. Mukherjee, G. Tripathi, S. Bandyopadhyay, S. Rakshit, T. Sen, and H. K. Majumder. Camptothecin induced mitochondrial dysfunction leading to programmed cell death in unicellular hemoflagellate leishmania donovani. *Cell Death Differ*, 11(8):924–936, Aug 2004.

[177] Md Shadab and Nahid Ali. Evasion of host defence by leishmania donovani: Subversion of signaling pathways. *Mol Biol Int*, 2011:343961, 2011.

[178] Umakant Sharma and Sarman Singh. Insect vectors of leishmania: distribution, physiology and their control. *J Vector Borne Dis*, 45(4):255–272, Dec 2008.

[179] Arlene H Sharpe and Gordon J Freeman. The b7-cd28 superfamily. *Nat Rev Immunol*, 2(2):116–126, Feb 2002.

[180] Lee M Shaughnessy and Joel A Swanson. The role of the activated macrophage in clearing listeria monocytogenes infection. *Front Biosci*, 12:2683–2692, 2007.

[181] Orly Shimony and Charles L Jaffe. Rapid fluorescent assay for screening drugs on leishmania amastigotes. *J Microbiol Methods*, 75(2):196–200, Oct 2008.

[182] J. S. Silva, G. N. Vespa, M. A. Cardoso, J. C. Aliberti, and F. Q. Cunha. Tumor necrosis factor alpha mediates resistance to trypanosoma cruzi infection in mice by inducing nitric oxide production in infected gamma interferon-activated macrophages. *Infect Immun*, 63(12):4862–4867, Dec 1995.

[183] R. P. Da Silva, B. F. Hall, K. A. Joiner, and D. L. Sacks. Cr1, the c3b receptor, mediates binding of infective leishmania major metacyclic promastigotes to human macrophages. *J Immunol*, 143(2):617–622, Jul 1989.

[184] W. Smith, M. Feldmann, and M. Londei. Human macrophages induced in vitro by macrophage colony-stimulating factor are deficient in il-12 production. *Eur J Immunol*, 28(8):2498–2507, Aug 1998.

[185] Gerald F Späth, L. A. Garraway, Salvatore J Turco, and Stephen M Beverley. The role(s) of lipophosphoglycan (lpg) in the establishment of leishmania major infections in mammalian hosts. *Proc Natl Acad Sci U S A*, 100(16):9536–9541, Aug 2003.

[186] Meike Sörensen, Christoph Lippuner, Toralf Kaiser, Ana Misslitz, Toni Aebischer, and Dirk Bumann. Rapidly maturing red fluorescent protein variants with strongly enhanced brightness in bacteria. *FEBS Lett*, 552(2-3):110–114, Sep 2003.

[187] O. E. Sørensen, P. Follin, A. H. Johnsen, J. Calafat, G. S. Tjabringa, P. S. Hiemstra, and N. Borregaard. Human cathelicidin, hcap-18, is processed to the antimicrobial peptide ll-37 by extracellular cleavage with proteinase 3. *Blood*, 97(12):3951–3959, Jun 2001.

[188] A. Strasser, L. O'Connor, and V. M. Dixit. Apoptosis signaling. *Annu Rev Biochem*, 69:217–245, 2000.

[189] G. Sudhandiran and Chandrima Shaha. Antimonial-induced increase in intracellular ca2+ through non-selective cation channels in the host and the parasite is responsible for apoptosis of intracellular leishmania donovani amastigotes. *J Biol Chem*, 278(27):25120–25132, Jul 2003.

[190] M. Tafani, D. A. Minchenko, A. Serroni, and J. L. Farber. Induction of the mitochondrial permeability transition mediates the killing of hela cells by staurosporine. *Cancer Res*, 61(6):2459–2466, Mar 2001.

[191] Marco Tafani, Joshua A Cohn, Natalie O Karpinich, Ronald J Rothman, Matteo A Russo, and John L Farber. Regulation of intracellular ph mediates bax activation in hela cells treated with staurosporine or tumor necrosis factor-alpha. *J Biol Chem*, 277(51):49569–49576, Dec 2002.

[192] M. C. Tan, A. M. Mommaas, J. W. Drijfhout, R. Jordens, J. J. Onderwater, D. Verwoerd, A. A. Mulder, A. N. van der Heiden, D. Scheidegger, L. C. Oomen, T. H. Ottenhoff, A. Tulp, J. J. Neefjes, and F. Koning. Mannose receptor-mediated uptake of antigens strongly enhances hla class ii-restricted antigen presentation by cultured dendritic cells. *Eur J Immunol*, 27(9):2426–2435, Sep 1997.

[193] Lutz Thon, Heike Möhlig, Sabine Mathieu, Arne Lange, Elena Bulanova, Supandi Winoto-Morbach, Stefan Schütze, Silvia Bulfone-Paus, and Dieter Adam. Ceramide mediates caspase-independent programmed cell death. *FASEB J*, 19(14):1945–1956, Dec 2005.

[194] S. J. Turco and D. L. Sacks. Expression of a stage-specific lipophosphoglycan in leishmania major amastigotes. *Mol Biochem Parasitol*, 45(1):91–99, Mar 1991.

[195] Boris Turk and Veronika Stoka. Protease signalling in cell death: caspases versus cysteine cathepsins. *FEBS Lett*, 581(15):2761–2767, Jun 2007.

[196] V. Turk, B. Turk, and D. Turk. Lysosomal cysteine proteases: facts and opportunities. *EMBO J*, 20(17):4629–4633, Sep 2001.

[197] G. van Zandbergen, N. Hermann, H. Laufs, W. Solbach, and T. Laskay. Leishmania promastigotes release a granulocyte chemotactic factor and induce interleukin-8 release but inhibit gamma interferon-inducible protein 10 production by neutrophil granulocytes. *Infect Immun*, 70(8):4177–4184, Aug 2002.

[198] Ger van Zandbergen, Annalena Bollinger, Alexander Wenzel, Shaden Kamhawi, Reinhard Voll, Matthias Klinger, Antje Müller, Christoph Hölscher, Martin Herrmann, David Sacks, Werner Solbach, and Tamás Laskay. Leishmania disease

development depends on the presence of apoptotic promastigotes in the virulent inoculum. *Proc Natl Acad Sci U S A*, 103(37):13837–13842, Sep 2006.

[199] Ger van Zandbergen, Carsten G K Lüder, Volker Heussler, and Michael Duszenko. Programmed cell death in unicellular parasites: a prerequisite for sustained infection? *Trends Parasitol*, 26(10):477–483, Oct 2010.

[200] Navin K Verma and Chinmoy S Dey. Possible mechanism of miltefosine-mediated death of leishmania donovani. *Antimicrob Agents Chemother*, 48(8):3010–3015, Aug 2004.

[201] Marieke Vermeersch, Raquel Inocêncio da Luz, Kim Toté, Jean-Pierre Timmermans, Paul Cos, and Louis Maes. In vitro susceptibilities of leishmania donovani promastigote and amastigote stages to antileishmanial reference drugs: practical relevance of stage-specific differences. *Antimicrob Agents Chemother*, 53(9):3855–3859, Sep 2009.

[202] Frank A W Verreck, Tjitske de Boer, Dennis M L Langenberg, Marieke A Hoeve, Matthijs Kramer, Elena Vaisberg, Robert Kastelein, Arend Kolk, René de Waal-Malefyt, and Tom H M Ottenhoff. Human il-23-producing type 1 macrophages promote but il-10-producing type 2 macrophages subvert immunity to (myco)bacteria. *Proc Natl Acad Sci U S A*, 101(13):4560–4565, Mar 2004.

[203] Frank A W Verreck, Tjitske de Boer, Dennis M L Langenberg, Linda van der Zanden, and Tom H M Ottenhoff. Phenotypic and functional profiling of human proinflammatory type-1 and anti-inflammatory type-2 macrophages in response to microbial antigens and ifn-gamma- and cd40l-mediated costimulation. *J Leukoc Biol*, 79(2):285–293, Feb 2006.

[204] B. R. Voth, B. L. Kelly, P. B. Joshi, A. C. Ivens, and W. R. McMaster. Differentially expressed leishmania major gp63 genes encode cell surface leishmanolysin with distinct signals for glycosylphosphatidylinositol attachment. *Mol Biochem Parasitol*, 93(1):31–41, May 1998.

[205] P. Walther and A. Ziegler. Freeze substitution of high-pressure frozen samples: the visibility of biological membranes is improved when the substitution medium contains water. *J Microsc*, 208(Pt 1):3–10, Oct 2002.

[206] Nanchaya Wanasen and Lynn Soong. L-arginine metabolism and its impact on host immunity against leishmania infection. *Immunol Res*, 41(1):15–25, 2008.

[207] João Luiz Mendes Wanderley, Lucia Helena Pinto da Silva, Poliana Deolindo, Lynn Soong, Valéria Matos Borges, Deboraci Brito Prates, Ana Paula Almeida de Souza, Aldina Barral, José Mario de Freitas Balanco, Michelle Tanny Cunha do Nascimento, Elvira Maria Saraiva, and Marcello André Barcinski. Cooperation between apoptotic and viable metacyclics enhances the pathogenesis of leishmaniasis. *PLoS One*, 4(5):e5733, 2009.

[208] J. R. Webb, L. L. Button, and W. R. McMaster. Heterogeneity of the genes encoding the major surface glycoprotein of leishmania donovani. *Mol Biochem Parasitol*, 48(2):173–184, Oct 1991.

[209] N. Weinheber, M. Wolfram, D. Harbecke, and T. Aebischer. Phagocytosis of leishmania mexicana amastigotes by macrophages leads to a sustained suppression of il-12 production. *Eur J Immunol*, 28(8):2467–2477, Aug 1998.

[210] Alexander Wenzel and Ger Van Zandbergen. Lipoxin a4 receptor dependent leishmania infection. *Autoimmunity*, 42(4):331–333, May 2009.

[211] Ulf Alexander Wenzel. *Stage specific interactions of Leishmania major with human phagocytes*. PhD thesis, Technology and Sciences of the University of Lübeck, 2009.

[212] Ulf Alexander Wenzel, Elena Bank, Christian Florian, Sabine Förster, Nicole Zimara, Jochen Steinacker, Matthias Klinger, Norbert Reiling, Uwe Ritter, and Ger van Zandbergen. Leishmania major parasite stage-dependent host cell invasion and immune evasion. *FASEB J*, 26(1):29–39, Jan 2012.

[213] T. Wieder, C. E. Orfanos, and C. C. Geilen. Induction of ceramide-mediated apoptosis by the anticancer phospholipid analog, hexadecylphosphocholine. *J Biol Chem*, 273(18):11025–11031, May 1998.

[214] M. E. Wilson and R. D. Pearson. Roles of cr3 and mannose receptors in the attachment and ingestion of leishmania donovani by human mononuclear phagocytes. *Infect Immun*, 56(2):363–369, Feb 1988.

[215] World health organisation (WHO) `http://www.who.int/leishmaniasis/en/`, accessed on 06/03/2012.

[216] A. H. Wyllie. Glucocorticoid-induced thymocyte apoptosis is associated with endogenous endonuclease activation. *Nature*, 284(5756):555–556, Apr 1980.

[217] Wei Xu, Anja Roos, Nicole Schlagwein, Andrea M Woltman, Mohamed R Daha, and Cees van Kooten. Il-10-producing macrophages preferentially clear early apoptotic cells. *Blood*, 107(12):4930–4937, Jun 2006.

[218] Wei Xu, Nicole Schlagwein, Anja Roos, Timo K van den Berg, Mohamed R Daha, and Cees van Kooten. Human peritoneal macrophages show functional characteristics of m-csf-driven anti-inflammatory type 2 macrophages. *Eur J Immunol*, 37(6):1594–1599, Jun 2007.

[219] Z. W. Yang and F. Y. Yang. Sensitivity of ca2+ transport of mitochondria to reactive oxygen species. *Biosci Rep*, 17(6):557–567, Dec 1997.

[220] G. S. Yap, T. Scharton-Kersten, H. Charest, and A. Sher. Decreased resistance of tnf receptor p55- and p75-deficient mice to chronic toxoplasmosis despite normal activation of inducible nitric oxide synthase in vivo. *J Immunol*, 160(3):1340–1345, Feb 1998.

[221] Lois M Yin, Michelle A Edwards, Jessica Li, Christopher M Yip, and Charles M Deber. Roles of hydrophobicity and charge distribution of cationic antimicrobial peptides in peptide-membrane interactions. *J Biol Chem*, 287(10):7738–7745, Mar 2012.

[222] R. Zeledon. Effecto de la temperature de la piel en la leishmaniasis cutanea experimental. *Rev. Soc. Brasil. Med.*, 25:121–138, 1971.

[223] C. Zhao, T. Nguyen, L. M. Boo, T. Hong, C. Espiritu, D. Orlov, W. Wang, A. Waring, and R. I. Lehrer. Rl-37, an alpha-helical antimicrobial peptide of the rhesus monkey. *Antimicrob Agents Chemother*, 45(10):2695–2702, Oct 2001.

[224] D. Zilberstein and M. Shapira. The role of ph and temperature in the development of leishmania parasites. *Annu Rev Microbiol*, 48:449–470, 1994.

Abbreviations

A. bidest	aqua bidestillata
AAM	alex aastigote medium
Ab	antibody
ama	amastigotes
AnxA5	Annexin-A5
bp	base pair
cDNA	complementary DNA
DNA	desoxyribonucleic acid
EM	transmission electron microscopy
FACS	fluorescence activated cell sorting
g	gramm or gravity
h	hour
HRP	horseradish peroxidase
kb	kilobase pairs
kDa	kilodalton
l	liter
M	mol
m	milli or meter

MFI	Mean fluorescence of intensity
min	minute
mRNA	messenger RNA
n	nano
p	pico
PCR	polymerase chain reaction
PI	post infection
pro	promastigotes
PS	phosphatidylserin
RNA	ribonucleic acid
ROS	reactive oxigen species
rpm	rounds per minute
rRNA	ribosomal RNA
RT	roomtemperature or reverse transkriptase
sec	second
siRNA	small interfering RNA
Temp.	temperature
WB	westernblot

Declaration of Authorship:

I herewith declare that I have completed the present thesis independently making use only of the specified literature and aids. Sentences or parts of sentences quoted literally are marked as quotations; identification of other references with regard to the statement and scope of the work is quoted. The thesis in this form or in any other form has not been submitted to an examination body.

Elena Bank

Mainz, June 11. 2012

Acknowledgements

I would like to express my sincere gratitude to my supervisor for providing me with the opportunity to carry out this work at the Paul-Ehrlich-Institute in Langen as well as for his exemplary guidance and thoughtful supervision. His encouragement, his constructive criticism, my discussions with him, and his insightful advice have helped me to mature and develop my own scientific concepts.

I also thank my second dissertation advisor for his willingness to supervise my doctoral research in behalf of the Faculty of Biology at the Johannes-Gutenberg University of Mainz.

My warm thanks to Karin and Sabrina for their support, help, our funny coffee breaks and the warm atmosphere in the lab.

I especially thank Peter for many productive discussions and his constructive criticism during the preparation of this thesis. I am grateful for his great support and help during difficult moments. Thanks for our "Frühstücks-Pause" and being a friend in and outside the lab.

I am gratefully indebted to Steffi for her immense encouragement, her friendly support and lots of wise words.

During this work I have collaborated with many colleagues for whom I have great regard, and I wish to extend my warmest thanks to all present and former members of the lab: Alex, Lisa, Cordula, Sebastian, Florian, Jochen, Stefan, Susi, Vanessa, Sabine, Meike and Stephan for their support, technical assistance, stimulating discussions and the

friendly cooperation.

My warm and sincere thanks to Norbert from the Division of Microbial Interface Biology at the Research Center Borstel, who performed parts of the quantitative real-time PCR analyses and gave valuable advice and constructive comments.

For friendly cooperation I want to acknowledge the whole group from the Department of Electron Microscopy at the University of Ulm for introducing me in the electron microscopy, their friendly help and the opportunity to use the electron microscope facility.

I would like to extent my regards to our "former Institute" the Institute for Medical Microbiology and Hygiene at the University Hospital of Ulm.

I am deeply grateful to all my friends for their moral support and continuous help throughout my work.

However, the greatest thank is owed to my husband Mathias and my family for their enormous support, love and untiring help during the whole time. Without their encouragement and understanding it would have been impossible for me to finish this work.